

Interactions of the adaptor proteins AP2 and 14-3-3 with the presynaptic scaffolding protein Bassoon

Dissertation

zur Erlangung des akademischen Grades

doctor rerum naturalium

(Dr. rer. nat.)

genehmigt durch die Fakultät für
Naturwissenschaften der Otto-von-Guericke-
Universität Magdeburg

von Diplom-Biochemiker Markus Schröder

geb. am 24.02.1981 in Hamburg

Gutachter: Prof. Dr. Eckart D. Gundelfinger
Prof. Dr. Christian Rosenmund

eingereicht am 28.04.2014
verteidigt am 08.05.2015

Summary

Chemical synapses of the central nervous system (CNS) are highly specialized signalling connections for neuronal communication. They consist of a presynaptic terminal belonging to the signal emitting neuron and a postsynaptic terminal from the signal receiving neuron. Signal transmission is triggered by an incoming action potential initiating the release of neurotransmitter from the presynaptic terminal into the synaptic cleft which separates the two boutons. The signal is then transferred to the postsynaptic neuron by detection of transmitter molecules by appropriate receptors located in the postsynaptic membrane. Exocytosis of neurotransmitter filled synaptic vesicles (SVs) is tightly controlled and regulated by constituents of a protein network called cytomatrix at the active zone (CAZ). The scaffolding protein Bassoon is an essential component of this network and is involved in structural organisation and functional regulation of neurotransmitter release sites. Currently, very little is known about the molecular mechanisms by which it influences neuronal signalling.

This work contains the description of interactions of AP2 μ 1 and 14-3-3 η with Bassoon. The common aim of the two interconnected projects was to shed light on the way adaptor proteins can influence the role of Bassoon at the presynaptic active zone. Adaptor proteins generally exert their function by modulation of protein-protein interactions or regulation of protein complex formation mediated by their set of specific binding domains. AP complexes play an important role in clathrin-mediated endocytosis (CME) and are involved in the recycling of SVs at the presynapse. 14-3-3 adaptors are multifaceted regulators of protein interactions and mediators of intracellular signalling. They were also shown to interact with several other key players of the neurotransmitter release machinery. Analysis of the observed interactions therefore promised to gain a deeper understanding of the complex mechanisms of presynaptic function. The two interactions were initially found in a yeast two-hybrid (Y2H) screening for binding partners of Bassoon. Verification of the interactions in mammalian cells as well as identification of the amino acid (aa) motifs responsible for the binding was for both projects successfully achieved by a combination of biochemical and cell based interaction assays.

Due to the role of AP complexes in SV retrieval and recycling the working hypothesis of the AP2 project was focussed on examination of an influence of the interaction on clathrin-mediated endocytosis and the SV cycle. In the end transferrin and synaptotagmin uptake assays used to functionally test this hypothesis could not reveal any influence of the interaction on vesicle cycling. AP complexes are also involved in vesicular protein sorting and trafficking while synaptic Bassoon targeting during early development is known to depend on association with special Piccolo-Bassoon transport vesicles (PTVs). Therefore it seems conceivable that functionally the interaction with AP2 μ 1 may rather be connected to the targeting of Bassoon than to its presynaptic function.

The interaction of Bassoon with 14-3-3s was shown to depend on phosphorylation of Serine-2845 of Bassoon. It was further demonstrated that this phosphorylation can be mediated by protein kinases from the RSK family. Functionally, disruption of the 14-3-3 binding motif of Bassoon by site directed mutation led to decreased exchange rates of synaptic Bassoon in FRAP experiments. This fits to the working hypothesis of 14-3-3s regulating association and attachment of Bassoon to the CAZ. It appears likely that molecular remodelling of such complex protein network requires loosening of intermolecular interactions of its components. The proposed mechanism of phosphorylation induced and 14-3-3 mediated regulation of CAZ attachment might finally not only apply to Bassoon but eventually also to other 14-3-3 interacting CAZ components like RIM1, CAST or liprin- α .

Zusammenfassung

Chemische Synapsen des zentralen Nervensystems sind hoch spezialisierte Zellkontakte für neuronale Kommunikation. Sie bestehen aus einer zum signalgebenden Neuron gehörenden präsynaptischen Endigung und einer postsynaptischen Endigung des signalempfangenden Neurons. Signalübermittlung wird durch ein eintreffendes Aktionspotenzial ausgelöst, welches die Freisetzung von Neurotransmitter von der präsynaptischen Endigung in den synaptischen Spalt einleitet, der die beiden Endigungen trennt. Das Signal wird an das postsynaptische Neuron übermittelt indem Neurotransmitter an geeignete Rezeptoren in der postsynaptischen Membran binden. Die Exozytose von mit Neurotransmitter gefüllten synaptischen Vesikeln wird durch die Bestandteile eines Proteinnetzwerkes mit Namen Zytomatrix an der aktiven Zone streng reguliert. Das Gerüstprotein Bassoon ist ein zentraler Bestandteil dieses Netzwerks und ist in die strukturelle Organisation und funktionelle Regulation der Ausschüttung von Neurotransmittern eingebunden. Gleichzeitig sind die molekularen Mechanismen durch die es neuronale Signalgebung beeinflusst unbekannt.

Diese Arbeit beinhaltet die Beschreibung von Interaktionen der Proteine AP2 μ 1 und 14-3-3 η mit Bassoon. Das gemeinsame Ziel dieser beiden Teilprojekte war es zu erfahren wie Adaptorproteine die Aufgabe von Bassoon an der präsynaptischen aktiven Zone beeinflussen können. Generell üben Adaptorproteine ihre Funktion durch die Modulation von Protein-Protein Interaktionen oder die Regulation von der Bildung von Proteinkomplexen durch ihre spezifischen Bindungsdomänen aus. AP-Komplexe spielen eine wichtige Rolle bei Clathrin vermittelter Endozytose und sind an der Wiederverwertung von synaptischen Vesikeln beteiligt. 14-3-3 Adaptoren sind bekannte Regulatoren von Protein Wechselwirkungen und Vermittler von intrazellulärer Signalweiterleitung. Sie wurden ebenfalls bereits als Bindungspartner anderer für die Neurotransmitterfreisetzung essentieller Proteine beschrieben. Die Untersuchung der beobachteten Interaktionen versprach daher einen tieferen Einblick in die komplexen Mechanismen der präsynaptischen Funktion zu gewähren. Beide Interaktionen wurden ursprünglich durch ein Hefe-zwei-Hybrid-Selektionsverfahren für Bindungspartner von Bassoon entdeckt. Bestätigung der Interaktion in Säugetierzellen und Identifikation der Aminosäuresequenz-Motive die für die Bindung verantwortlich sind, wurde in beiden Projekten erfolgreich durch eine Kombination aus biochemischen und zellbasierten Methoden erreicht.

Aufgrund der Rolle von AP-Komplexen in der Wiederverwertung von synaptischen Vesikeln war die Arbeitshypothese des AP2-Projektes auf die Untersuchung des Einflusses der Bindung auf Clathrin-vermittelte Endozytose und den synaptischen Vesikelzyklus ausgerichtet. Schlussendlich konnte durch die Methoden der Transferrin- und Synaptotagminaufnahme, die angewandt wurden um diese Hypothese zu überprüfen, kein Einfluss der Bindung auf den Vesikelkreislauf festgestellt werden. AP Komplexe sind ebenfalls an der vesikulären Zielsteuerung synaptischer Proteine beteiligt und es ist bekannt, dass die synaptische Zielsteuerung von Bassoon in frühen Entwicklungsstadien von seiner Assoziation mit speziellen Piccolo-Bassoon-Transportvesikeln abhängt. Daher scheint es vorstellbar, dass die Interaktion mit AP2 μ 1 funktionell eher mit der Zielsteuerung Bassoons als mit seiner präsynaptischen Funktion zusammenhängt.

Es wurde gezeigt, dass die Interaktion von Bassoon mit 14-3-3 von der Phosphorylierung Bassoons am Serinrest 2845 abhängt. Es wurde weiterhin nachgewiesen, dass diese Phosphorylierung von Mitgliedern der Familie der RSK-Proteinkinasen vermittelt werden kann. Funktionsbezogen reduziert die Störung der Interaktion durch gezielte Mutation der Bindungsstelle die synaptische Austauschrate von Bassoon in so genannten FRAP-Experimenten. Dies unterstützt die Arbeitshypothese einer durch 14-3-3 vermittelten Regulation der Assoziation von Bassoon mit der Zytomatrix an der aktiven Zone. Es ist

wahrscheinlich, dass die molekulare Umstrukturierung eines solch komplexen Netzwerkes die Lockerung von Bindungen seiner Komponenten erfordert. Der hier vorgeschlagene Mechanismus einer phosphorylierungsabhängigen und 14-3-3 vermittelten Regulation der Verbindung mit der Zytomatrix könnte schlussendlich nicht nur für Bassoon zutreffen, sondern ebenfalls für andere Zytomatrixkomponenten wie RIM1, CAST oder liprin- α gelten.

Acknowledgements

First I would like to cordially thank Eckart Gundelfinger for his trust in me, for his mindful and foresighted advice, for his empathy and subtle guidance and most of all for promoting me in every possible way while always respecting every facet of my character. I would also like to thank Anna Fejtova for her constant supervision, for teaching me all the cutting edge sophisticated techniques, for always intense discussions and especially for her honest and productive criticism.

Great thanks also go to Anne Stellmacher for the good teamwork, to Carolina Montenegro, Renato Frischknecht, Stefano Romorini, Martin Heine and Karl-Heinz Smalla for always being ready to discuss problems or to provide some good advice.

I want to thank all friends and members from the department for Neurochemistry & Molecular Biology for the great working atmosphere. Claudia, Stefano, Franzi, Barbara, Romy, Gilbert, Renato, Vesna, Dascha, Dani, Maria, Anil, Anika, Arthur, Stefan, Rodrigo, Juliane, Jeet, Jose, Juancarlos without you, work and also the time after work and my whole time in Magdeburg would not have been half as much fun.

Further I would like to thank Janina Juhle, Heidi Wickborn and Sabine Opitz for excellent technical work and help I could always rely on.

Big thanks also to the supervisors Eckart Gundelfinger and Michael Naumann and also to the members of the GRK1167. It was always a pleasure and we learned a lot.

Last but not least I want to thank Philippa and my family and friends from Hamburg for their love and all the support and motivation through all these years. I don't know what I would do without you.

Contents

Summary	2
Zusammenfassung.....	3
Acknowledgements.....	5
Contents.....	6
Figures and tables.....	8
Figures	8
Tables	9
Abbreviations.....	10
1 Introduction.....	11
1.1 Chemical synapses	11
1.2 The Cytomatrix at the Active Zone	12
1.3 Bassoon and Piccolo	15
1.4 Adaptor Proteins	17
1.4.1 Heterotetrameric Adaptor Proteins	18
1.4.2 14-3-3 Proteins.....	21
1.5 Ribosomal S6 kinases	23
1.6 Aims.....	26
2 Material and Methods	27
2.1 Materials	27
2.1.1 Chemicals.....	27
2.1.2 Kits, enzymes and molecular biology reagents.....	27
2.1.3 Molecular weight markers	27
2.1.4 Bacteria and Yeast stems	27
2.1.5 Media and reagents for bacterial and yeast culture.....	27
2.1.6 Buffers for Yeast experiments	28
2.1.7 Mammalian cell lines	28
2.1.8 Media and reagents for mammalian cell line culture.....	28
2.1.9 Buffers and reagents for biochemistry and molecular biology.....	28
2.1.10 Antibodies	29
2.1.11 Animals	29
2.2 Methods.....	29
2.2.1 Molecular biological methods.....	29
2.2.2 Yeast experiments	32

2.2.3	Biochemical methods.....	33
2.2.4	Cell culture techniques.....	37
2.2.5	Immunocytochemistry, microscopy and image analysis	40
2.2.6	Transferrin uptake and fluorescence activated cell sorting (FACS).....	43
2.2.7	Statistical data analysis	43
3	Results	44
3.1	Interaction of Bassoon with Adaptor Protein Complexes.....	44
3.1.1	The AP2 μ subunit and Bassoon interact in yeast	44
3.1.2	The AP2 μ subunit and Bassoon interact in mammalian cells	47
3.1.3	Bassoon does not influence clathrin-mediated endocytosis of the transferrin Receptor	52
3.1.4	AP binding-deficient Bassoon can rescue KO-induced SV recycling phenotype	55
3.2	Interaction of Bassoon with 14-3-3.....	57
3.2.1	Bassoon interacts directly with 14-3-3 proteins in a phosphorylation-dependent manner.....	57
3.2.2	14-3-3 interacts with Bassoon in mammalian cells	61
3.2.3	Generation of a phosphorylation-specific antibody for pS2845 of Bassoon	65
3.2.4	The 14-3-3 binding site on Bassoon can be phosphorylated by RSK kinases.....	66
3.2.5	Mutation of the 14-3-3 binding site influences molecular dynamics of synaptic Bassoon.....	69
4	Discussion.....	75
4.1	AP Complexes	76
4.2	14-3-3 Proteins.....	81
4.3	Conclusions and Outlook.....	87
5	Declaration.....	88
6	Literature.....	89

Figures and tables

Figures

Fig. 1: Schematic and electron microscopic illustration of a chemical synapse.	11
Fig. 2: Schematic illustration of the cytomatrix at the active zone.	13
Fig. 3: AP complexes mediate cellular membrane protein sorting and targeting.	20
Fig. 4: Structure and function of 14-3-3.	22
Fig. 5: Activation and effectors of RSK signalling.	24
Fig. 6: Scheme of constructs used in the Y2H Assay for AP2 interaction.	45
Fig. 7: AP2 μ 1 is co-recruited to Bassoon clusters in COS-7 cells.	48
Fig. 8: Co-IP of myc-tagged c-terminal constructs of AP μ subunits with GFP tagged Bassoon wt and mutant constructs.	50
Fig. 9: Bassoon and AP complexes co-localise in neurons.	51
Fig. 10: Transferrin uptake mechanism.	52
Fig. 11: Intracellular distribution patterns of the Bassoon constructs used for FACS analysis.	54
Fig. 12: Expression of Bassoon constructs does not influence CME of fluorescently labeled transferrin in HEK293T cells.	55
Fig. 13: AP binding-deficient Bassoon rescues Bassoon KO phenotype of reduced synaptotagmin uptake.	56
Fig. 14: Bassoon contains a 14-3-3 interaction interface.	58
Fig. 15: Direct binding of Bassoon to 14-3-3 depends on phosphorylation of Serine-2845.	60
Fig. 16: Bassoon interacts with 14-3-3 in HEK293T cells.	62
Fig. 17: Bassoon recruits 14-3-3 in neurons.	64
Fig. 18: Characterisation of the antibody against phosphorylated S2845 of Bassoon.	66
Fig. 19: RSK inhibition prevents Okadaic acid induced phosphorylation of S2845 of Bassoon.	67
Fig. 20: Protein kinases of the RSK family phosphorylate Bassoon S2845 in vitro.	69
Fig. 21: Co-localisation of GFP-Bsn and GFP-Bsn ^{S2845A} with synaptic markers.	70
Fig. 22: Analysis of molecular dynamics of GFP-Bsn and GFP-BsnS2845A by FRAP.	71
Fig. 23: Expression analysis of GFP-Bsn and GFP-BsnS2845A in the FRAP videos.	72
Fig. 24: Analysis of Bassoon transport characteristics.	73
Fig. 25: Hypothetical settings for interaction of Bassoon with AP complexes.	78
Fig. 26: Proposed mechanism of the Bassoon-14-3-3 interaction.	84

Tables

Tab. 1: List of used kits, enzymes and molecular biology reagents.....	27
Tab. 2: List of used molecular weight markers	27
Tab. 3: List of used bacterial stems	27
Tab. 4: Used yeast stem.....	27
Tab. 5: List of media and reagents for bacterial and yeast culture.....	28
Tab. 6: Buffers and reagents for Yeast experiments	28
Tab. 7: List of used mammalian cell lines	28
Tab. 8: List of media and reagents for mammalian cell line culture.....	28
Tab. 9: List of buffers and reagents for biochemistry and molecular biology	28
Tab. 10: List of used primary antibodies.....	29
Tab. 11: Animal lines	29
Tab. 12: Primer sequences for genotyping PCRs.....	30
Tab. 13: PCR programs for genotyping PCRs	30
Tab. 14: PCR program for cDNA fragment amplification.....	31
Tab. 15: Buffers for plasmid isolation	32
Tab. 16: Solutions for amidoblack assay	33
Tab. 17: List of Buffers for TRIS-Glycine SDS-PAGE.....	34
Tab. 18: List of solutions for Coomassie staining of SDS-PAGE gels.....	34
Tab. 19: Buffers for affinity purification	36
Tab. 20: Media and reagents for eukaryotic cell culture.....	37
Tab. 21: Intensities of Y2H interaction of Bassoon bait with AP2 μ 1 prey constructs.	46
Tab. 22: Intensities of Y2H interaction of Ap2 μ 1 prey constructs with Bassoon bait constructs containing mutated Yxx ϕ motifs.....	47

Abbreviations

α	Anti
aa	Amino acid
AP	Adaptor protein complex
Bsn	Bassoon
CAZ	Cytomatrix at the active zone
CC	Coiled coil domain
CCV	Clathrin coated vesicle
CLS	Coffin-Lowry syndrome
CME	Clathrin mediated endocytosis
CNS	Central nervous system
DIV	Days in vitro
E	Embryonic day
EGFP	Enhanced green fluorescent protein
ELM	The Eukaryotic Linear Motif resource for Functional Sites in Proteins
Fig.	Figure
FRAP	Fluorescence recovery after photobleaching
g	Goat
gp	Guinea pig
GST	Glutathion S-transferase
H	Homogenate
HBSS	Hanks balances salt solution
IP	Immunoprecipitation
kDa	Kilo Dalton
KO	Knockout
m	Mouse
MAPK	Mitogen activated protein kinase
mRFP	Monomeric red fluorescent protein
OA	Okadaic acid
P	Postnatal day
PAGE	Polyacrylamide gelelectrophoresis
PCR	Polymerase chain reaction
PHB	Piccolo/Bassoon homology domain
PRS	Proline rich sequence
pS	Phosphorylated serine
PSD	Postsynaptic density
PTV	Piccolo/Bassoon transport vesicle
rb	Rabbit
SEM	Standard error of the mean
SDS	Sodium dodecyl sulfate
SPM	Synaptic plasma membrane
SV	Synaptic vesicle
SVC	Synaptic vesicle cycle
Tab.	Table
TfR	Transferrin receptor
TGN	Trans Golgi network
wt	Wild type
Y2H	Y2H

1 Introduction

1.1 Chemical synapses

In the CNS, chemical synapses are sites of cell-cell-communication between neurons. These synapses are composed of a presynaptic and a postsynaptic terminal, which are divided by a ~20 nm wide synaptic cleft (Fig. 1.). Activation of the synapse by an incoming action potential leads to influx of calcium ions into the presynaptic bouton through voltage-dependent calcium channels. Elevated levels of bivalent Ca^{2+} ions then induce exocytosis of neurotransmitter-filled SVs. The release of SVs is restricted to a specialised and spatially defined membrane area, the presynaptic active zone (Landis et al., 1988). In the synaptic cleft, neurotransmitters diffuse and bind to appropriate receptors located in the postsynaptic membrane area opposing the active zone. Activation of the receptors leads to propagation of the signal to the receiving cell resulting in excitation or inhibition depending on the released neurotransmitter. In neurons, like in other secretory cells, regular exocytosis of vesicles at the site of secretion is balanced by retrieval and recycling of membrane and proteins via compensatory endocytosis. This ensures maintenance of the secretive function as well as shape and structure of the cell.

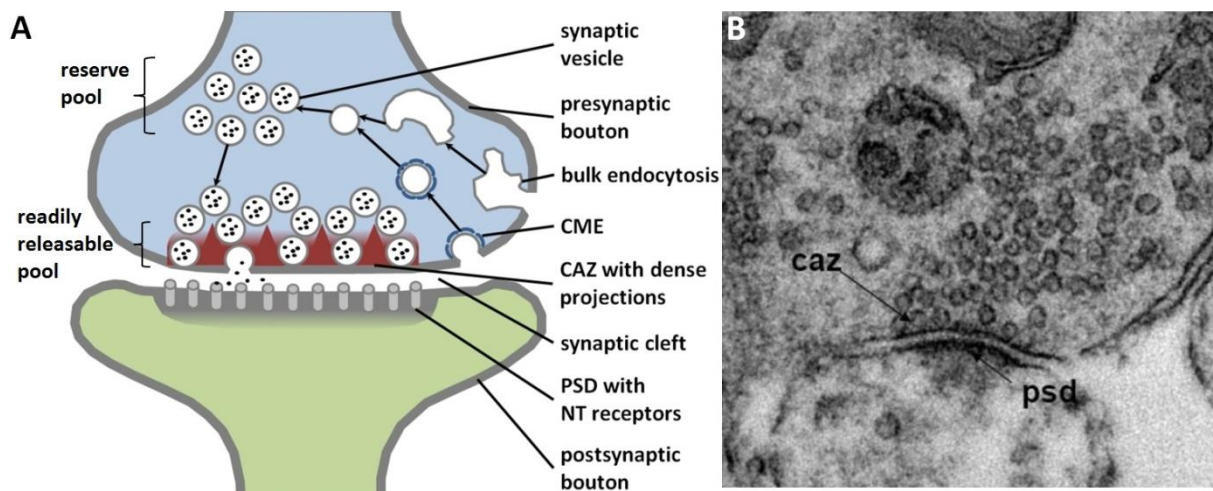


Fig. 1: Schematic and electron microscopic illustration of a chemical synapse.

(A) Schematic drawing of a synapse with essential steps of the synaptic vesicle cycle at the presynaptic bouton. CME: Clathrin-mediated endocytosis, CAZ: Cytomatrix at the active zone, PSD: Postsynaptic density NT: Neurotransmitter receptor. **(B)** Electron microscopic picture of a CNS synapse with well visible SVs, synaptic cleft, CAZ and PSD. Electron microscopic picture from (Lazarevic, 2010).

At chemical synapses the coordinated membrane trafficking events including exo- and endocytosis in connection with the release of neurotransmitter and the recycling of vesicles is

summarised in the term SVC (Takei et al., 1996; Betz and Angleson, 1998; Sudhof, 2004). This procedure can be divided into two parts. The first, in which SVs are prepared and processed to undergo exocytosis and the second, in which the components essential for the first part are retrieved, recycled and reassembled to form new vesicles available for exocytosis. These two parts can further be subdivided into single temporally and spatially controlled steps (Gundelfinger et al., 2003). For exocytosis the vesicles are docked to the membrane and processed by a series of priming steps. The ATP-dependent priming process prepares them for the final fusion step in which neurotransmitters are released. An alternative to the complete fusion of vesicles with the plasma membrane is the so-called “kiss-and-run” mechanism. In this variant the transmitter release is accomplished by a temporally restricted opening of a fusion pore under subsequent preservation of the intact vesicle (Ceccarelli et al., 1973). Membrane and protein components of the vesicles completely inserted into the plasma membrane are retrieved by endocytosis in the vicinity of the active zone. The best described endocytic mechanism for SV recycling is CME (Saheki and De Camilli, 2012). This mechanism provides the possibility of vesicle reformation from clathrin-coated pits (see also 1.4.1). In this case Adaptor Protein complexes (APs) ensure sorting of vesicular content into the budding membrane pit by linking it to the assembling clathrin coat. Finally the developing clathrin-coated vesicle (CCV) is pinched from the plasma membrane in a scission procedure mediated by the large GTPase Dynamin (Ferguson and De Camilli, 2012). After removal of the clathrin cage from the internalised vesicle, termed uncoating, the endocytosis process is complete. The new vesicles can subsequently be refilled with neurotransmitter to directly regain SV properties. Another variant called bulk endocytosis does not require AP complexes or clathrin and is triggered by intense synaptic activity (Clayton et al., 2008; Wenzel et al., 2012). It causes the internalisation of larger membranous structures, which results in the formation of endocytic intermediates. Indirect recycling of SVs from these structures can in turn take place by utilisation of clathrin and AP complexes in comparable manner as for the budding of vesicles from the plasma membrane (Cheung and Cousin, 2012).

1.2 The Cytomatrix at the Active Zone

Spatial and temporal coordination of the SVC is believed to be mediated by components of a complex protein network associated with the active zone and extending into the cytosol of the presynaptic terminal (Hida and Ohtsuka, 2010; Gundelfinger and Fejtova, 2012; Sudhof, 2012). This network is called CAZ; it can be detected as an area of high electron density in electron

micrographs (Fig. 1B, (Dresbach et al., 2001)). It is further considered as the presynaptic counterpart of the postsynaptic density (PSD) and was proposed to be involved in the docking of SVs, anchoring of channels and structural linkage of components involved in exocytosis (Harlow et al., 2001; Siksou et al., 2007). Although the exact composition of the CAZ is not completely defined, several protein families including liprins- α , UNC-13/Munc13 proteins, RIMs (Rab3-interacting molecules), ELKS (ERC/CAST), and Bassoon as well as Piccolo/Aczonin were shown to be essential components of this network (Fig. 2, (Fejtova and Gundelfinger, 2006; Schoch and Gundelfinger, 2006)).

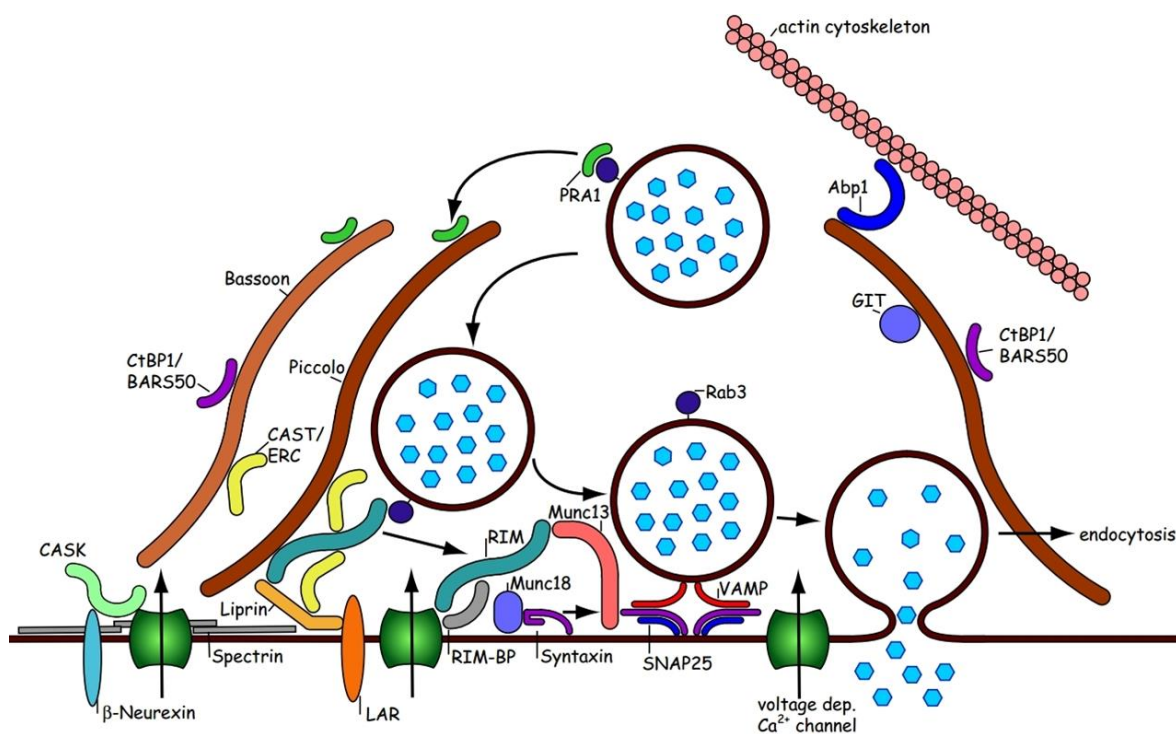


Fig. 2: Schematic illustration of the cytomatrix at the active zone.

Proteins of the CAZ are forming a complex network to build a scaffold for the key players of exo- and endocytosis at the active zone of SV release. Bassoon and Piccolo, RIM, CAST, liprin- α , and Munc13 are the core components of this network (Fejtova and Gundelfinger, 2006).

The relevance of an intact CAZ for proper synaptic development and function is mirrored in multiple examples of interference with its basic building blocks. In mice deficient for the CAZ protein RIM1 α , hippocampal mossy fiber synapses (Castillo et al., 2002) and synaptic contacts of cerebellar granule cells with Purkinje neurons (Lonart et al., 2003), showed disrupted presynaptic long-term potentiation (LTP). Additionally short-term plasticity and SV release were altered in neurons from RIM1 α ^{-/-} animals (Schoch et al., 2002; Calakos et al., 2004). On the behavioural level these mice further displayed severely impaired learning and memory performance (Powell et al., 2004). *Drosophila* and *C. Elegans* orthologues of liprin- α were

found to be involved in differentiation and morphogenesis of presynaptic terminals as well as in regular synaptic transmission (Zhen and Jin, 1999; Kaufmann et al., 2002). In liprin- α mutants of *C. Elegans* several presynaptic proteins including ELKS-1 were not synaptically enriched but diffusely expressed (Patel et al., 2006). Furthermore it was shown recently that liprin- α is important for presynaptic RIM recruitment and turnover in rat hippocampal neurons (Spangler et al., 2013). Proteins from the CAST/ELKS family are also part of the CAZ scaffold and are able to interact with liprin- α (Ko et al., 2003), Munc13 (Wang et al., 2009), and Piccolo as well as Bassoon (Takao-Rikitsu et al., 2004). They can also bind to RIM1 and are like liprin- α supposed to play a role in RIM recruitment to the active zone (Ohtsuka et al., 2002). On the one hand, microinjection of the RIM1 binding domain of CAST or the CAST binding domain of RIM1 into superior cervical ganglion neurons significantly impaired neurotransmission by disruption of proper RIM recruitment (Takao-Rikitsu et al., 2004). On the other hand, deletion of CAST in mutant mice did not show any significant phenotype in excitatory synapses but instead boosted inhibitory neurotransmitter release (Kaeser et al., 2009). The CAZ protein Munc13 is known as an important priming factor (Betz et al., 2001) and can bind to RIM, CAST and Bassoon as well as Piccolo (Wang et al., 2009). It was published that *Drosophila*, *C. elegans* and mouse mutants lacking UNC13/Munc13 showed disturbed or abolished SV release (Aravamudan et al., 1999; Augustin et al., 1999; Richmond et al., 1999; Varoqueaux et al., 2002). It was also found that Munc13-1 is a mediator of presynaptic LTP and that this function depends on its interaction with RIM1 α (Yang and Calakos, 2011). Further, STP was reported to rely on Munc13 in connection with the Ca²⁺ sensor Calmodulin (Junge et al., 2004; Lipstein et al., 2013). Absence of Piccolo, a protein with significant homology to Bassoon, was demonstrated to promote SV exocytosis. Probably this is achieved through enhancement of SV translocation from the vesicular reserve pool to the readily-releasable pool. It was suggested that this effect on SV release probability was based on a resulting change of the dynamic properties of the SV protein synapsin I a (Leal-Ortiz et al., 2008). Last but not least, mutant mice lacking exons 4 and 5 of Bassoon display a phenotype, in which synapses appear ultra-structurally normal but show a reduction of 30-50 % of overall synaptic strength. This is based on an increase in functionally mute presynaptic terminals in neurons of these mice (Altrock et al., 2003). Additionally it was demonstrated that in cerebellar mossy fiber to granule cell synapses of Bassoon KO mice the vesicle reloading rate is halved under conditions of high-frequency stimulation. This impairment of the SVC leads to enhanced short-term depression in mice lacking Bassoon (Hallermann et al., 2010).

Based on the presented scientific background it becomes evident, that integrity of the CAZ network and its components is essential for controlled release of neurotransmitter from presynaptic terminals. Further it demonstrates that interconnectivity of CAZ proteins is complex and that their targeting as well as their recruitment and function are strongly interdependent. Knowledge about the mechanisms by which single proteins may exert their influence on the SVC is more and more emerging. By virtue of this it becomes increasingly worthwhile to focus on the way they collectively work together to achieve precise synaptic signalling and rapid adaption to variations in physiological requirements. Since critical SVC steps like priming, docking, reloading or release probability are influenced by CAZ components, the alteration of these parameters can probably be mediated by modification or reorganisation of the network. First steps to answer this question have already been taken. As a model for homeostatic plasticity the pharmacological silencing of neuronal cultures led to an increase of synaptic strength. This effect is not only reflected in elevated release probabilities but also in enlargements of the active zone as detected by electron microscopy (Murthy et al., 2001). Interestingly similar enlargements of the active zones were observed in flies, worms and mice lacking orthologues of the CAZ proteins liprin- α , Munc13 and Bassoon/Piccolo (Zhen and Jin, 1999; Kaufmann et al., 2002; Varoqueaux et al., 2002; Mukherjee et al., 2010). These findings were further linked together by demonstration of changes in the synaptic expression levels of CAZ proteins also induced by pharmacological silencing or electrophysiological strengthening of synapses (Lazarevic et al., 2011; Weyhersmuller et al., 2011). Together these publications indicate, that plasticity related changes in presynaptic strength are mediated by ultra-structural and biochemical alterations of the CAZ network and its components. Comparable observations were previously also made for the postsynaptic compartment (Ehlers, 2003).

1.3 Bassoon and Piccolo

Bassoon and Piccolo are two large CAZ proteins of 420 and 530 kDa, respectively. They are structurally related and localised in both excitatory and inhibitory presynapses in all regions of the brain (tom Dieck et al., 1998; Richter et al., 1999). Several regions of high sequence similarity, called Piccolo-Bassoon homology (PHB) domains, are shared by the two proteins. These PHB domains include two zinc fingers and three coiled coil (CC) domains. The C-terminus of Piccolo, which is not conserved in Bassoon contains a PDZ and two C2 domains. Additionally, both proteins also have proline-rich sequences (PRS), which may act as SH3

domain binding sites for proteins involved in endo- and exocytosis (Fenster et al., 2000). Bassoon can get post-translationally modified by N-myristoylation, acting as a membrane anchor (Dresbach et al., 2003). Extremely harsh detergent conditions, which are necessary to solubilise the two proteins from synaptosomes, are pointing towards a strong association with the presynaptic cytoskeleton (Cases-Langhoff et al., 1996; tom Dieck et al., 1998). Their resistance against solubilisation, the large size and their multi-domain structure indicate that the molecules may act as major scaffolding proteins of the CAZ. This notion was also confirmed by studies of synapses from retinal photoreceptor cells and inner hair cells of the cochlea. These types of neurons possess presynaptic structures called synaptic ribbons, which are considered as a specialised form of the CAZ (Zhai and Bellen, 2004; tom Dieck et al., 2005). In neurons of Bassoon-mutant mice these ribbons were found to be detached from the active zones (Dick et al., 2003; Khimich et al., 2005), implicating that Bassoon acts as a molecular anchor structurally connecting them with the active zone.

Bassoon was shown to be among the earliest proteins incorporated into developing synapses suggesting a role in assembly and organisation of the early AZ (Zhai et al., 2000). It was reported that both Piccolo and Bassoon are transported along axons to synapses in association with distinct trans-Golgi Network (TGN) derived vesicles named PTVs (Zhai et al., 2001; Dresbach et al., 2006). PTVs are assumed to carry complexes of pre-assembled active zone material which may substantially contribute to the process of synaptogenesis (Ahmari et al., 2000; Shapira et al., 2003; Tao-Cheng, 2007). While the synaptic transport of CAST seems to be exclusively dependent on PTVs, other CAZ proteins can also reach their destination by different mechanisms. The failure of CAST to localise to synapses if Bassoon and Piccolo are missing further indicates that at least one of both proteins is necessary for the generation of intact PTVs at the TGN (Maas et al., 2012). Axonal transport of PTVs along the microtubular cytoskeleton is mediated by dynein and kinesin motor complexes (Cai et al., 2007; Fejtova et al., 2009). While the long distance transport of Bassoon and Piccolo from TGN to synapses by PTVs is relatively well described, short distance redistribution of the proteins is yet poorly understood. Although the half-life time of Bassoon at individual synapses is long compared to other proteins, it was found to exchange between different presynaptic boutons in a similar way as synapsin (Tsuruel et al., 2006; Tsuruel et al., 2009). In how far vesicular transport is necessary for this exchange is unclear since stepwise but also fast monotonous recovery were observed in the regarding FRAP experiments.

To study the role of Bassoon in the organisation of various steps of the SVC and in the assembly of the presynaptic apparatus, a mouse mutant (Bsn Δ Ex4/5) of the protein was generated (Altrock et al., 2003). This mutant is lacking the central exons 4 and 5 of the Bassoon gene coding the aa 505-2889 of the protein. Bassoon-mutant mice suffer from spontaneous seizures, indicating a general imbalance of the excitatory and inhibitory network at a systemic level. Partial enlargement of various brain structures was assumed to result from increased levels of brain-derived neurotrophic factor (BDNF) and a dysregulation of neurogenesis and apoptosis (Heyden et al., 2011). The mice are further characterised by a reduction in the normal synaptic transmission. Accordingly, a subset of excitatory synapses was found to be ultra-structurally normal but functionally inactive (Altrock et al., 2003). Although the reason for this inactivity is unclear it is possible that this phenotype is connected with a defect in the regulation of the SVC. As mentioned above the phenotype of Bassoon-mutant mice was supported by studies of Bassoon KO mice lacking the entire protein. These mice showed halved vesicle reloading rates in cerebellar mossy fiber to granule cell synapses under conditions of high frequency stimulation. This confirms an impairment of the SVC and leads to enhanced short-term depression in these mice (Hallermann et al., 2010).

1.4 Adaptor Proteins

Adaptor proteins are characterised by their ability to bind at least two different proteins at the same time. To achieve this they often harbour two or more functional protein-protein interaction domains like PDZ, SH2, SH3 or others. They normally do not exhibit any enzymatic activity and are mostly unable to directly change the physical composition or constitution of their targets (Flynn, 2001). Instead they influence single proteins or functional protein complexes by establishing or inhibiting specific interactions to achieve recruitment, disassembly or conformational changes of their binding partners. In regard to this, they show a strong similarity to scaffolding molecules and mainly differ in terms of mobility, size and cellular distribution. In their function they can often be regarded as effectors or integrators of signalling cascades. Many of them are able to detect signalling initiated posttranslational modifications or are modified themselves and mediate or promote the effects as biological switches.

Two examples for postsynaptically relevant adaptor proteins are GRIP1 and Gephyrin, which play roles in the clustering and targeting of Glycin-, GABA- and AMPA-receptors at the PSD of excitatory and inhibitory synapses (Dong et al., 1997; Kneussel et al., 1999; Setou et al., 2002; Sola et al., 2004; Maas et al., 2006). At the presynaptic compartment, the vesicle transport

adaptors FEZ1 and Nesca are involved in targeting of the SNARE protein Syntaxin1 and its fusion relevant binding partner Munc18 (Chua et al., 2012; MacDonald et al., 2012). Also indispensable for the SVC is the arsenal of adaptors responsible for endocytosis. The most important and best-known candidates are the heterotetrameric adaptor protein complexes (APs), the monomeric AP180 as well as Stonin2 and Epsin. Together they facilitate the sorting and recycling of SV proteins like SV2, neurotransmitter transporters, synaptobrevin or synaptotagmin (Haucke and De Camilli, 1999; Traub, 2003; Diril et al., 2006; Dittman and Kaplan, 2006; Jakobsson et al., 2008). An example for the influence of adaptor proteins on synaptic development is reflected in the importance of the adaptor DAB1 from the Reelin signalling pathway involved in neurogenesis and synaptic plasticity (Niu et al., 2004; Trotter et al., 2013). The adaptor syntenin1 is a binding partner of CAST1 and links the CAZ network to its interaction partner β -Neurexin, a presynaptic cell adhesion molecule critical for synaptogenesis (Ko et al., 2006). Last but not least several other adaptors have been shown to mediate different aspects of presynaptic function like release probability or plasticity. Proteins of the Mint family regulate SV release (Ho et al., 2006), which is assumed to be based on their interaction with the fusion protein Munc18 (Okamoto and Sudhof, 1997). Cbl-b an adaptor originally best known for its role in T-cell receptor signalling was not only introduced as a candidate for neuronal apoptosis control (Sproul et al., 2009), but also as regulator of long-term memory retention and short-term synaptic plasticity (Tan et al., 2006). Members of the family of 14-3-3 adaptor proteins are influencing opening properties and surface expression of voltage-dependent calcium channels (Beguin et al., 2006; Li et al., 2006). Additionally, their interaction with the CAZ protein RIM1 was reported to be necessary for presynaptic LTP in cultured cerebellar neurons (see 1.4.2).

Although adaptor proteins are not counted as exclusive components of the CAZ, they are present at the presynaptic compartment and can participate in the regulation of synaptic development, structure, function and plasticity. They are therefore interesting targets in the search for CAZ regulatory mechanisms.

1.4.1 Heterotetrameric Adaptor Proteins

The protein family of heterotetrameric APs is involved in sorting and trafficking processes of proteins and membranes between different cellular membrane compartments. The complexes can bind directly to phosphatidylinositol phosphates of membranes, to cargo proteins associated with the membranes and to the scaffolding protein clathrin. By these interactions they establish

links between cargo proteins and the coat of clathrin-coated pits (Fig. 3A). This finally leads to the sorting of a defined set of protein content into an emerging clathrin-coated vesicle. The complexes AP1, AP2, AP3, AP4 and their appropriate tissue-specific subtypes can be found to varying extents in all nucleated cells from yeast to human (Kirchhausen, 1999). Each AP subtype has a molecular weight of about 300 kDa and consists of two different large, one medium and one small subunit (Fig. 3B). The subunits have molecular weights of about 110 kDa, 50 kDa and 20 kDa, respectively. The small (σ_1 , σ_2 , σ_3 , σ_4), the medium (AP1 μ_1 , AP2 μ_1 , AP3 μ_1 for AP3A, AP3 μ_2 for AP3B, AP4 μ_1) and one type of the large subunits (β_1 , β_2 , β_3 , β_4) show 50-80 % similarity in the aa sequences between each corresponding homologue among all APs. The second large chain (γ for AP1, α for AP2, δ for AP3, ϵ for AP4), although functionally clearly related, differs between the complexes with a similarity of only about 25% (Kirchhausen, 1999).

Although the structure of the AP complexes is comparable to each other and although their function depends on the same mechanisms, the different subtypes are specialised to act in distinct subcellular membrane compartments (Fig. 3C). AP2 is the best-known member of the AP family. It is important for CME at the plasma membrane and the sorting of cargo to endosomal compartments (Owen et al., 2004). It is also a major AP complex for SV recycling from the presynaptic plasma membrane since knock down of AP2 severely impairs SV recycling kinetics (Kim and Ryan, 2009). Interestingly it was shown in the same publication that AP1 can partly compensate for the lack of AP2 in SV recycling. Although still controversially discussed the AP1 complex is normally thought to mediate clathrin-dependent sorting of cargo proteins from the TGN to endosomal structures (Ohno, 2006). For the AP3 complex two different forms are distinguished, first the ubiquitously expressed AP3A and second the neuronal specific subtype AP3B. Generally the AP3A complex is supposed to be involved in sorting of cargo from TGN to the lysosomal compartment or lysosome related organelles like melanosomes (Nakatsu and Ohno, 2003). Neuronal AP3B was shown to play a role in the formation of SVs from endosomal structures at the presynaptic bouton (Blumstein et al., 2001). Little is yet known about AP4 the last member of the AP family. Unlike the other complexes AP4 was found only in mammals and plants and does not associate with clathrin. It is assumed that AP4 is sorting cargo from the TGN to lysosomes and/or late endosomes possibly interacting with a non-clathrin coat. Although there are several examples for the involvement of individual APs in different sorting pathways this field is still under intense investigation. (Nakatsu and Ohno, 2003)

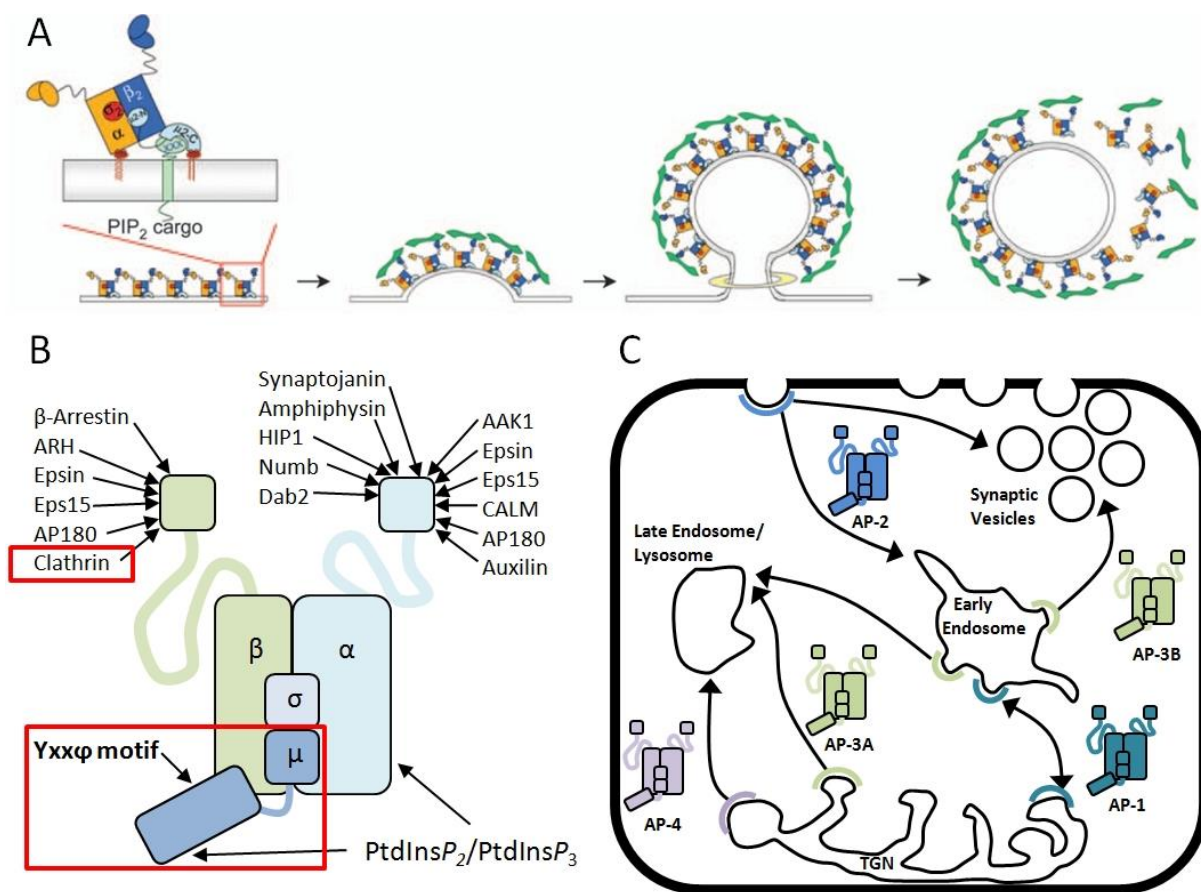


Fig. 3: AP complexes mediate cellular membrane protein sorting and targeting.

(A) Steps of Clathrin mediated endocytosis. First: binding of AP complexes to cargo and membrane. Second: formation of a clathrin coated pit. Third: Dynamin mediated fission of the budding vesicle. Fourth: uncoating of the clathrin coated vesicle (Jung and Haucke, 2007). **(B)** Functional scheme of a heterotetrameric AP complex with its subunits and binding sites of interaction partners (Ohno, 2006). **(C)** Functional specialisation of AP complexes in sorting and targeting between the different cellular membranous compartments (Ohno, 2006).

AP complexes can bind to their target proteins by interaction with different binding motifs on the cargo. The most common and at the same time best understood way is the interaction of AP μ subunits with tyrosine based binding motifs of the target proteins. This binding site is typically called Yxx ϕ motif. The only prerequisites for the functionality of the motif are a tyrosine and a bulky hydrophobic aa residue, divided by two arbitrary aa (Owen et al., 2004). Although it was shown that the residues adjacent to the motif can contribute to the specificity for binding of certain AP subtypes, the recognition of this type of motif is generally strongly overlapping between different members of the AP family (Ohno et al., 1998). It was reported that the Binding of AP2 to its target can be regulated by phosphorylation of the tyrosine residues in the Yxx ϕ motifs of some cargo proteins, probably facilitating the regulation of their internalisation (Shiratori et al., 1997; Schaefer et al., 2002; Zhang et al., 2008).

1.4.2 14-3-3 Proteins

The 14-3-3 proteins are a family of highly conserved acidic proteins of about 30 kDa ubiquitously expressed in invertebrates and vertebrates. In mammals the 14-3-3 family contains seven isoforms: β , γ , ϵ , ζ , η , θ and σ (Wang and Shakes, 1996). They share a high aa sequence identity and are able to form homo- or heterodimers (Jones et al., 1995). The tissue with the highest expression of 14-3-3s is the CNS but they can also be detected in almost every other tissue of the body (Boston et al., 1982). The sigma isoform is the only 14-3-3 subtype which shows only very weak expression in the brain in relation to the whole organism (Thorrez et al., 2008). Dimeric 14-3-3 functional units (Fig. 4A) can bind to two types of phosphorylation dependent 14-3-3 consensus binding motifs identified among a variety of 14-3-3 binding partners. Both mode1 (RSXpSXP) and mode2 (RXXXpSXP; R: arginine, S: serine, pS: phosphorylated serine, P: proline, X: any aa) motifs contain arginine and proline at the edges and a phosphorylated serine or threonine in the centre of the motif (Yaffe et al., 1997; Rittinger et al., 1999; Bridges and Moorhead, 2004). In rare cases also phosphorylation independent interactions have been reported (Petosa et al., 1998; Masters et al., 1999). Generally there are three possible modes (Fig. 4B) by which 14-3-3s can exert their function on target proteins (Bridges and Moorhead, 2004). First is the so-called “clamping”, by which the conformation of the interacting protein is changed due to the binding of 14-3-3. Often this is mediated by the binding of a 14-3-3 dimer to two distinct interaction sites on the same target protein. The second mode works by sterically occupying or “masking” a binding site for a competing third protein by 14-3-3. The third possibility is called “scaffolding”. In this mode a 14-3-3 dimer interacts with two different binding partners, bringing them into close proximity. While the character of the interaction of 14-3-3s with their binding partners is well understood, the physiological effects of these interactions show a huge variability. This is due to the adaptor nature of 14-3-3 proteins, not having a direct active function, but rather influencing the function of their interaction partners by binding to them. The three different modes of action of 14-3-3 can thereby lead to different effects on the target protein. This can include changes in enzymatic activity, positive or negative influence on protein-protein complex formation, recruitment of the target to certain cellular compartments or changes in protein solubility (Mackintosh, 2004; Morrison, 2009). The function of 14-3-3 binding is conclusively rather based on the attributes

of the interacting target protein and the circumstances of the interaction than on intrinsic features of 14-3-3 itself.

The huge number of more than 200 interaction partners of 14-3-3, mostly identified by proteomic studies, are involved in a wide range of different cellular activities, such as transcription, protein synthesis, metabolic pathways, cell cycle, cell signalling, cytoskeletal organisation, cellular trafficking and many more (Dougherty and Morrison, 2004; Jin et al., 2004; Shikano et al., 2006). One important way, by which 14-3-3 proteins can regulate cellular processes, is by influencing the subcellular localisation of target proteins. In many cases this is achieved by masking protein interaction sites such as localisation sequences of the interaction partner (Muslin and Xing, 2000).

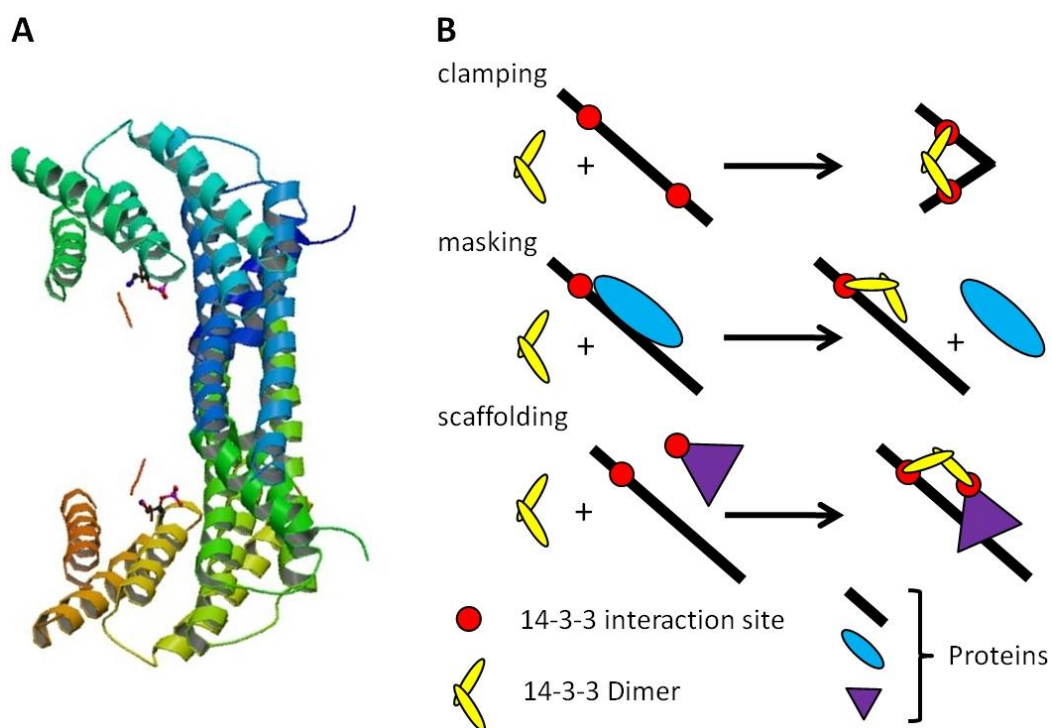


Fig. 4: Structure and function of 14-3-3.

(A) 3D ribbon representation of a 14-3-3 ζ dimer in complex with Raf peptides (Petosa et al., 1998). **(B)** Schematic illustration of the three 14-3-3 modes of action. Clamping induces conformational changes of the target protein. Masking sterically competes with other binding partners of the target. Scaffolding links two proteins together.

Regarding their function in the Brain, 14-3-3s are connected to several neurological disorders including Alzheimer's Disease (Layfield et al., 1996), Parkinson's Disease (Kawamoto et al., 2002; Ubl et al., 2002), Spinocerebellar ataxia type 1 (Chen et al., 2003; Emamian et al., 2003) and the Miller-Dieker syndrome (Cardoso et al., 2003; Toyooka et al., 2003). Further it was demonstrated that in *Drosophila* the 14-3-3 orthologue Leonardo is important for synaptic

transmission properties and regulation of SV dynamics (Broadie et al., 1997). Influence of 14-3-3 on presynaptic LTP in mouse cerebellar neurons by interaction with the CAZ protein RIM1 α was reported but shows inconsistencies between *in vitro* and *in vivo* studies (Simsek-Duran et al., 2004; Kaeser et al., 2008). Furthermore the two CAZ proteins ERC/CAST and liprin- α were found in proteomic screenings for 14-3-3 interaction partners (Jin et al., 2004; Angrand et al., 2006). Maybe the most interesting finding in regard to presynaptic function was the observation, that 14-3-3 binding to the voltage dependent calcium channel Ca_v2.2 regulates its inactivation properties and thereby possibly influences short term plasticity (Li et al., 2006). Taken together 14-3-3 interacts with different components of the CAZ and other proteins important for the function of the presynapse. On the one hand, 14-3-3 could function as scaffold, cross-linking different CAZ components to each other. On the other hand, looking at the existing 14-3-3 literature, it seems likely that 14-3-3 binding could also instead loosen the tight association between the CAZ components by masking their interaction sites.

1.5 Ribosomal S6 kinases

The family of ribosomal S6 Kinases (RSKs) comprises four family members in mouse and human. They are serine/threonine kinases and contain two independent functional kinase domains (Anjum and Blenis, 2008). RSKs are ubiquitously expressed in cell lines and tissues and can be found from mollusca to insects and mammals but not in yeasts or plants (Moller et al., 1994; Carriere et al., 2008). Usually they are directly activated by the mitogen activated protein kinase (MAPK) ERK1/2 in response to growth factors, hormones, neurotransmitters, chemokines or other stimuli triggering the MAPK signalling pathway (Blenis, 1993). Subsequently full activation of RSKs is achieved through additional phosphorylation by the protein kinase PDK1 (Frodin et al., 2002). Moreover it was reported that they can also be activated via the stress-related p38 MAPK pathway (Zaru et al., 2007).

Functionally RSKs were found to phosphorylate nuclear as well as cytosolic proteins (Romeo et al., 2012). Phosphorylation of RSK targets can influence cell survival, cell growth and cell proliferation (Fig. 5) by the inactivation of apoptotic factors and the regulation of gene transcription and mRNA translation (Bonni et al., 1999; Frodin and Gammeltoft, 1999). Little is known about functional redundancy of the four isoforms, but differences in spatial and temporal expression patterns suggest certain isoform specificities (Carriere et al., 2008).

From the perspective of temporal mRNA expression it is assumed that RSK1 is more important for earlier developmental stages while RSK3 takes over in later development. A conclusive interpretation is that RSK1 is needed preferentially for proliferation while RSK3 is more involved in differentiation related processes. This is supported by the observation that in late development RSK1 is mostly expressed in continuously proliferating tissues like liver, thymus and gut epithelia. While RSK2 mRNA levels stay relatively low during development, RSK4 mRNA is very abundant in fetal and adult tissues especially in the brain (Carriere et al., 2008).

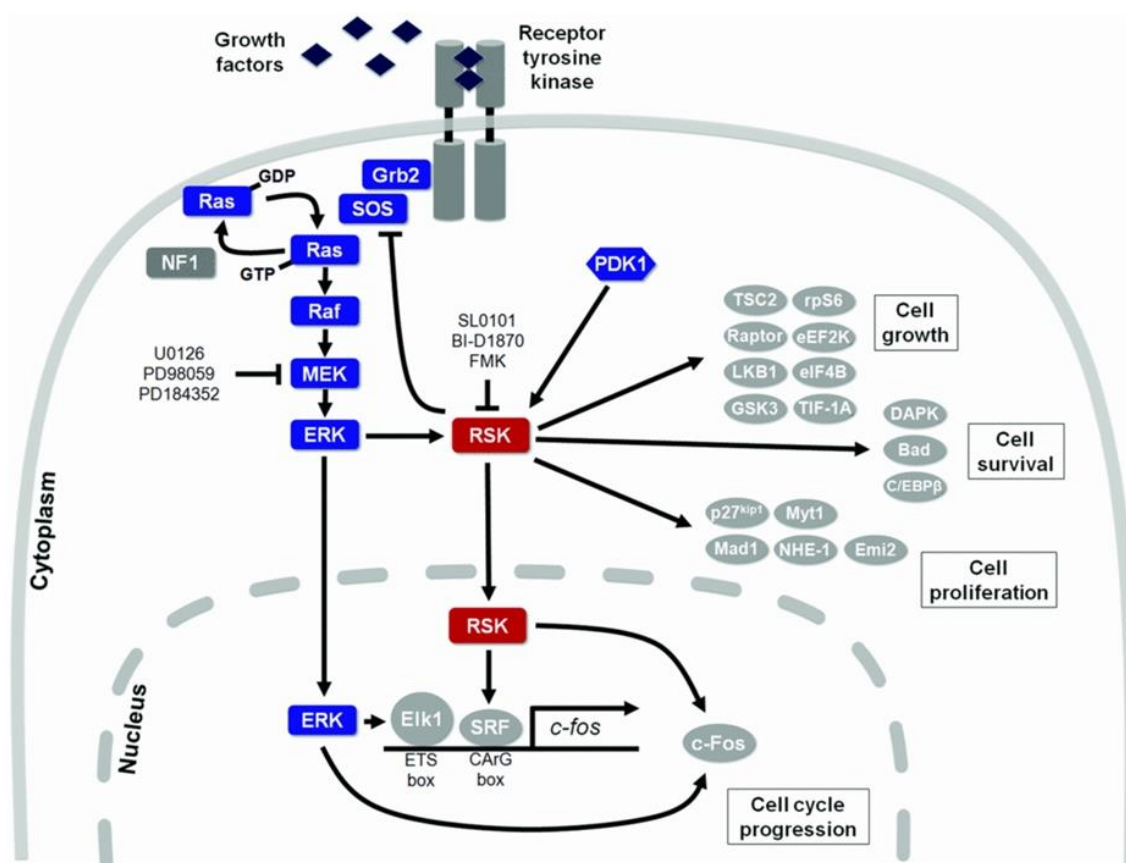


Fig. 5: Activation and effectors of RSK signalling.

Binding of growth factors to receptor tyrosine kinases activates the MAPK signalling pathway, which leads to the phosphorylation of RSK by ERK1/2. Full activation of RSK is achieved through subsequent phosphorylation by PDK1. Activated RSK can phosphorylate different cytosolic targets implicated in growth, survival and proliferation. It can also translocate to the nucleus and influence transcription and cell cycle progression. Known pharmacological inhibitors of RSKs comprise SL0101, BI-D187 and FMK (Romeo et al., 2012).

Regarding spatial distribution in the adult mouse brain, RSK1 is only present in the granule cell layer of the cerebellum, while RSK3 is highly expressed in many brain regions important for cognition, like the cerebral cortex, the dentate gyrus and the amygdala. RSK2 expression is enriched in regions of high synaptic activity as the hippocampus, the neocortex and in Purkinje

cells, which are also important for cognition and memory formation. RSK4 expression is abundant in the whole adult brain. (Zeniou et al., 2002)

Mutations in the human RSK2 gene are known to cause Coffin-Lowry Syndrome (CLS), an X-chromosome related genetic disorder leading to heavy mental retardation and bone malformation (Trivier et al., 1996). In consistency with the mental retardation of CLS patients, RSK2 KO mice show abnormalities in learning, cognition and coordination (Poirier et al., 2007). The malfunctions in these mice are probably based on the various neuronal tasks of the kinase. RSK2 was shown to be involved in neuronal proliferation (Dugani et al., 2010), axonal growth (Wong et al., 1996; Fischer et al., 2009c) and BDNF-mediated neuronal survival (Kharebava et al., 2008). In *Drosophila* it was also shown to influence learning (Putz et al., 2004) and to regulate the number of presynaptic boutons at the neuromuscular junction (Fischer et al., 2009b). Furthermore it was connected to PLD induced calcium dependent vesicle release in PC12 and chromaffine cells (Zeniou-Meyer et al., 2008). Last but not least, RSK2 KO mice suffer from impaired spatial learning and memory and have blocked LTP in the amygdala (Zeniou-Meyer et al., 2010). The spatiotemporal distribution pattern of RSK3 suggests that this isoform could also represent an interesting candidate for the cause of CNS disorders like mental retardation. Although KO mice of RSK1 and RSK3 as well as RSK1/RSK2/RSK3 triple knockouts were reported to be viable, no information about characteristics or phenotypes of these mice is available until now (Dumont et al., 2005).

In context with the presented data it is interesting to mention that RSKs were previously reported to phosphorylate 14-3-3 interaction sites and thereby regulate complex formation, changes in localisation or function of target proteins. The translocation of the glucose transporter GLUT4 from intracellular vesicles to the cell surface was demonstrated to depend on the interaction between the Rab-GAP AS160 and 14-3-3 (Ramm et al., 2006). RSKs were shortly after found to mediate PMA induced phosphorylation of the 14-3-3 binding site on AS160 (Geraghty et al., 2007). Another example is the cyclin-dependent kinase inhibitor p27^{Kip1}, which is translocated from the nucleus to the cytosol upon RSK mediated 14-3-3 interaction (Fujita et al., 2003). Also the function of the Na⁺/H⁺ exchanger NHE1 (Takahashi et al., 1999; Lehoux et al., 2001) and cytosolic retention of the pro-apoptotic protein BAD (Bonni et al., 1999; Shimamura et al., 2000; Rapp et al., 2007) are regulated by RSK induced 14-3-3 binding.

1.6 Aims

In this work the interactions of two different ubiquitous adaptor proteins with the neuron-specific presynaptic scaffold protein Bassoon have been investigated. The analysed adaptor proteins are the μ subunit of AP complexes known to be essential for CME and the multifunctional small adaptor protein 14-3-3. The main aim was to elucidate in which way these adaptors acting as protein-protein interaction hubs can influence the role of Bassoon at the presynaptic active zone.

- 1) AP complexes are key players in synaptic CME and massively influence SV recycling at the presynaptic compartment. Bassoon is a major scaffolding protein of the CAZ network believed to organise and orchestrate the SVC. At the same time it is a paralogue of Piccolo, the only CAZ protein, which was linked to both exocytosis and endocytosis to date. The aims of this project were therefore to answer the following questions:
 - Is the interaction of Bassoon with AP complexes influencing CME in general?
 - If yes, does the interaction play a role for CME dependent SV recycling at the presynaptic bouton?
 - In how far is the interaction involved in the coupling of exo- and endocytosis, or the processing of the SVC?

- 2) 14-3-3 adaptors are well known regulators of protein-protein interactions and complexes. Binding to their targets usually depends on signalling controlled phosphorylation of interaction motifs. As major scaffolding protein of the CAZ Bassoon is a member of a complex and tightly interconnected but at the same time structurally dynamic protein network. Moreover it was reported to be one of the most intensely phosphorylated synaptic proteins. The aims of this part were therefore to answer:
 - Is the interaction of Bassoon with 14-3-3 classically phosphorylation dependent?
 - If yes which signalling pathway is involved in the regulation?
 - How far does the interaction with 14-3-3 influence the behaviour of Bassoon as a CAZ scaffold?

2 Material and Methods

2.1 Materials

2.1.1 Chemicals

Kits and chemicals that were used in this work were purchased from the described companies. The quality of the reagents was of analytical grade.

2.1.2 Kits, enzymes and molecular biology reagents

Tab. 1: List of used kits, enzymes and molecular biology reagents

Item	Company
Endonucleases (Restriction enzymes)	New England Biolabs; Fermentas
Taq DNA polymerase	Qiagen
Phusion® DNA Polymerase	Finnzymes
Alkaline Phosphatase from calf intestine (CIAP)	Fermentas
Deoxynucleoside Triphosphate Set (dNTPs)	Fermentas
T4 DNA ligase	Fermentas
T4 Polynucleotide Kinase (PNK)	Fermentas
Oligonucleotides (Primer)	Invitrogen

2.1.3 Molecular weight markers

Tab. 2: List of used molecular weight markers

Item	Company
Smart Ladder DNA marker	Eurogentec
Precision Plus Protein TM Standards	BIO-RAD

2.1.4 Bacteria and Yeast stems

Tab. 3: List of used bacterial stems

Bacteria	Company
E.coli BL21-CodonPlus@(DE3)-RIPL	Stratagene
E.coli XL10 Gold Bacteria	Stratagene

Tab. 4: Used yeast stem

Yeast	Genotype	Company
<i>S. cerevisiae</i> AH 109	MAT a, trp 1-901, leu2-3, 112, ura-3-52, his3-200, gal4Δ, gal80Δ, LYS2::GAL1uasGAL1TATA-HIS3, GAL2UASGAL2TATA-ADE2, URA3::MEL1UAS-MEL1TATA-lacZ	Clontech

2.1.5 Media and reagents for bacterial and yeast culture

All media were autoclavated at 121°C for 15 minutes. The additives were filtered with a 0.2 µm filter-unit (Schleicher & Schuell) and stored at -20°C.

Tab. 5: List of media and reagents for bacterial and yeast culture

Bacterial medium	Composition
LB-medium	20 g LB Broth Base (Invitrogen) / 1000 ml H ₂ O
SOC-medium	20 g/l peptone 140 (Gibco); 5 g/l yeast extract (Gibco); 10 mM NaCl; 2,5mM KCl; mM Glucose 10 mM MgSO ₄ ; 20 mM Glucose
LB-Agar	15 g Select Agar (Invitrogen) / 1000 ml LB-medium
Yeast medium	Composition
YPDA medium	50 g Broth (Gibco) / 1000 ml H ₂ O; plus 10 ml 0,3% Adeninehemisulfate
Minimal-SD-medium	20 g Glucose; 1,7 g Yeast-Nitrogen Base (Gibco), 5 g (NH ₄) ₂ SO ₄ / 1000 ml H ₂ O; pH 7,0
-LW-medium	0,64 g -Leu/-Trp DO Supplement (Clontech) pro 1 l MinimalSD-Medium
-ALWH-medium	0,60 g -Ade/-Leu/-Trp/-His DO Supplement (Clontech) pro 1 l Minimal-SD-medium; 1 mM 3-amino-1,2,4-triazole

2.1.6 Buffers for Yeast experiments

Tab. 6: Buffers and reagents for Yeast experiments

Buffer	Composition
10x LiAc	1 M LiAc in H ₂ O, pH 7,5
10x TE	0.1 M Tris-HCl, 10 mM EDTA, pH 7,5
PEG	50 % (v/v) polyethylenteglycol 4000 (PEG) in H ₂ O
PEG/TE/LiAc	8 ml PE; 1 ml 10x TE; 1 ml 10x LiAc

2.1.7 Mammalian cell lines

Tab. 7: List of used mammalian cell lines

Cell line	Company
Kidney Fibroblast Cells from African green monkey (COS-7 cells)	Clontech
Human Embryonic Kidney Cells (HEK293-T)	ATCC

2.1.8 Media and reagents for mammalian cell line culture

Tab. 8: List of media and reagents for mammalian cell line culture

Item	Composition
COS-7 and HEK293-T cell culture medium	DMEM (Invitrogen), 10% fetal calf serum, 2 mM L-glutamine, 100 U/ml penicillin, 100 µg/ml streptomycin
Trypsin	0,5% Stock solution, diluted 1:10 in HBSS (Invitrogen)
Poly-D-lysin	100 mg/l poly-D-lysin in 100 mM boric acid, pH 8,5, sterile filtered
HBSS	Hank's balanced salt solution, Ca ²⁺ and Mg ²⁺ free (Invitrogen)

2.1.9 Buffers and reagents for biochemistry and molecular biology

Tab. 9: List of buffers and reagents for biochemistry and molecular biology

Buffer	Composition
PBS	2,7 mM KCl, 1,5 mM KH ₂ PO ₄ , 137 mM NaCl, 8 mM Na ₂ HPO ₄ , pH 7,4
PBST	2,7 mM KCl, 1,5 mM KH ₂ PO ₄ , 137 mM NaCl, 8 mM Na ₂ HPO ₄ , pH 7,4, 0,1% Tween 20
6x DNA sample buffer	30% (v/v) Glycerine, 50 mM EDTA, 0,25% Bromophenolblue, 0,25% Xylene Cyanol
Cell lysis buffer	10 mM Hepes (pH 7.5), 100 mM NaCl, 0.5% Triton-X100, protease inhibitors Complete mini (Roche) 1 Tbl per 10 ml

2.1.10 Antibodies

Tab. 10: List of used primary antibodies

Primary Antibody	Species	Antigen	WB dilution	ICC dilution	Company / Origin
α -pan 14-3-3; sc-629	rb	general 14-3-3	1:500		Santa Cruz
α -14-3-3 η ; AB9736	rb	14-3-3 η	1:3000		Milipore-Chemicon
α -sap7f	rb	Bassoon	1:2000	1:1000	(tom Dieck et al., 1998)
α -GFP; ab 6556	rb	GFP	1:5000	1:1000	Abcam
α -Bsn C-term	ms	Bassoon C-term	1:5000		Synaptic Systems
α -Bsn m7f	ms	Bassoon	1:1000		Enzo Lifescience
α -GST	ms	GST-tag	1:10000		Covance
α -His	ms	His-tag	1:1000		Cell Signaling Inc.
α -RSK	ms	RSK1,2,3	1:1000		Cell Signaling Inc.
α -Bsn gp	gp	aa 2613-2774 of rat Bassoon	1:1000		From Anna Fejtova
α -pS2845 Bsn	rb	KHL-coupled peptide CLQRSL-pS-DPK	1:500		BioGenes GmbH
α - α -Adaptin; 610501	ms	α -Adaptin		1:1000	BD Transduction
α - γ -Adaptin; 610385	ms	γ -Adaptin		1:1000	BD Transduction
α -Synaptotagmin1; 105 311C3	ms	Synaptotagmin1 luminal domain		1:200	Synaptic Systems
α -Homer	rt	Homer1a		1:2000	Acris
α -Synaptophysin	gp	Synaptophysin 1		1:1000	Synaptic Systems

Species: mouse (ms); rabbit (rb); guinea pig (gp); rat (rt). Alexa Fluor 488-, Cy3-, Cy5 (1:2000), and peroxidase-coupled (1:20000) secondary antibodies were purchased from Jackson Immuno Research Laboratories.

2.1.11 Animals

Animal lines used for organ harvesting are listed in Tab. 11. Animals were bred in the animal facility of the Leibniz Institute for Neurobiology, Magdeburg and in the ZENIT, Magdeburg.

Tab. 11: Animal lines

Animal line	Notes	Origin
C57Bl6 J cre	<i>Mus musculus</i> (wild type)	Charles River Labs
SV129EMSJ	<i>Mus musculus</i> (wild type)	Jackson Laboratories
Bassoon mutant mice (Bsn Δ Ex4/5)	Genetic background: 50% C57Bl J cre and 50% SV129EMSJ	Altrock et al., 2003
BGT KO	Omnibank clone 486029; Gene trapping vector VICTR 48; mixed genetic background	Lexicon pharmaceuticals
Wistar rats	<i>Rattus norvegicus familiaris</i>	Leibniz Institute for Neurobiology

2.2 Methods

2.2.1 Molecular biological methods

The molecular biological methods used in this work were mostly carried out according to standard protocols. A brief overview will be described in the following chapter. For further

information please consult the specific literature "Molecular Cloning" (Sambrook et al., 1989) and "Current Protocols in Molecular Biology" (Ausubel et al., 1990).

2.2.1.1 Genotyping of mutant mice

Newborn pups were labeled and tailcut samples were taken for DNA extraction. The tailcut samples were incubated together with 500 µl lysis buffer including freshly added Proteinase K at 55°C for 20 min under shaking. Inactivation of the enzyme followed by incubation for 10 minutes at 98°C. The samples were now ready for PCR. One tube without tailcut sample was used as a negative control. Subsequently a genotyping PCR was conducted. The PCR was performed using 21 µl of master mix for WT and KO PCR with freshly added Taq Polymerase and 4 µl of DNA extract for genotyping. The final concentrations of the PCR reagents were: 1 pM forward primer, 1 pM reverse primer (see Tab. 12 for sequences), 2,5 mM MgCl₂, 0.1 units/µl Taq-polymerase, 0.2 mM dNTPs in Q-solution (Qiagen, 5x) and PCR buffer (Qiagen, 10x). For reagents used see Tab. 1. The temperature profile of the PCR is highlighted in Tab. 13.

Tab. 12: Primer sequences for genotyping PCRs

Genotype	Forward primer	Reverse primer
BGT WT	5'-ctaagctattgcttctctctcac-3'	5'-ctgaggctcttgagttctctacga-3'
BGT KO	5'-ctaagctattgcttctctctcac-3'	5'-ataaacctcttgagttctctacga-3'
Bsn WT	5'-agttgtcaagcctgttccagaagc-3'	5'-acaccgtcggaggagtagcctgt-3'
Bsn (BsnΔEx4/5)	5'-ggtatcctgttctgaaagactttc-3'	5'-aagctgatatcgaattggcctg-3'

Tab. 13: PCR programs for genotyping PCRs

Process	BsnΔEx4/5		BGT KO	
	Time and Temperature	Number of Cycles	Time and Temperature	Number of Cycles
Initial denaturation	5 min at 95 °C	1	3 min at 95 °C	1
Denaturation	45 seconds at 95°C	34	30 sec at 95 °C	35
Annealing	45 seconds at 65°C		40 sec at 63 °C	
Extension	60 seconds at 72°C		30 sec at 72 °C	
Final extension	30 seconds at 72°C	1	2 min at 72 °C	1

2.2.1.2 PCR for amplification

If cDNA constructs were generated by PCR, specific primers were resuspended at a concentration of 100 pmol/µl and used in the amplification reaction at a final concentration of 10 pmol/µl. The concentration of the dNTPs was 0,2 mM plus 2 U of Phusion® DNA Polymerase in PCR buffer HF (Finnzymes). For reagents used see Tab. 1. The temperature profile used for PCR is highlighted in Tab. 14 (Annealing temperature is primer depending and was for this reason specific for the pair of primers; the amount of cycles varied between experiments).

Tab. 14: PCR program for cDNA fragment amplification

Process	Time and Temperature	Number of Cycles
Initial denaturation	1 min at 98 °C	1
Denaturation	30 seconds at 98°C	30-40
Annealing	30 seconds at 50-70 °C	
Extension	60 seconds at 72°C	
Final extension	60 seconds at 72°C	1

2.2.1.3 Introduction of point mutations by PCR

All mutations described were introduced by inverse PCR using primers with mutated sequence and corresponding Bassoon fragments subcloned in pBluescriptII SK⁻ (Agilent Technologies) as a template (Ausubel et al., 2003). The final PCR reaction mixture and the temperature profile used were the same as described in 2.2.1.2 part of this thesis.

2.2.1.4 DNA agarose gel electrophoresis

DNA fragments obtained after PCR (2.2.1.2) or after restriction digestion (2.2.1.8) were separated according to their size by one-dimensional agarose gel electrophoresis. Agarose gels (0.75-1.5 % w/v) were prepared by melting the agarose (UltraPure, Gibco). To visualize the DNA under UV light, 5-10 µl Ethidium bromide solution (10 mg/ml in H₂O) was added before gel polymerization. The DNA samples were prepared in 6x loading buffer and were loaded onto the gel. Gels were run at 80V in 1× TAE buffer. The DNA fragments were visualized under UV-light and photographed with an Eagle-Eye (Stratagene) using the gel documentation system Gel Doc (Biorad).

2.2.1.5 cDNA cloning into expression vectors

DNA fragments of interest were amplified by PCR (2.2.1.2). Following agarose gel electrophoresis in TAE buffer (2.2.1.4), the fragments were purified by the PCR cleanup gel extraction kit (Macherey-Nagel). The fragments were subjected to enzymatic digestion (2.2.1.8) and ligated with T4 DNA ligase to the pre-digested vector. The ligations were performed at 16–20°C for 2–8 hours. The used DNA fragment/vector ratio was 3:1. To select for positive clones, the ligated fragment-vectors were transformed into *E. coli* XL10 Gold competent cells for subsequent DNA mini-prep isolation.

2.2.1.6 Heat shock transformation of competent *E. coli* XL 10 Gold bacteria cells

The DNA ligation mixture (2.2.1.5) was incubated together with 100 µl of heat shock competent XL10 Gold bacteria for 10 minutes on ice. Heat shocking for 30 seconds at 42°C was followed

by incubation on ice for 1 minute. Then 1 ml of prewarmed SOC medium was added and the tube incubated at 37°C for 1 h shaking at low speed. Bacteria were spun down at 1000×g for 1 min and the supernatant was removed. The pellet was resuspended by vortexing in the remaining drops of liquid. The entire suspension was plated on LB agar plates containing the respective antibiotics. Plates were incubated over night at 37°C.

2.2.1.7 Plasmid isolation (Mini DNA preparation)

DNA plasmids were purified from a 2 ml LB overnight culture by alkaline lysis. The cells were pelleted, resuspended in 300 µl of P1 buffer and lysed with 300 µl of P2 buffer. In this step proteins and DNA were denatured and RNA hydrolyzed. With 300 µl of P3 buffer the mixture was neutralized, which leads to the precipitation of denatured proteins and chromosomal DNA. Debris was removed by centrifugation of the lysate at 6000×g for 10 minutes. The supernatant was transferred to a new tube and 630 µl of isopropanol were added and mixed. The plasmid DNA was precipitated by centrifugation at 13000×g for 10 minutes at 4 °C. The pelleted DNA was washed with ice-cold 500 µl of 70% (v/v) ethanol and centrifuged for 10 minutes at top speed. The pellet was dried, resuspended in 50 µl of dH₂O and stored at -20°C. For mammalian cell transfection, DNA with high concentration and purity was prepared using the Plasmid Midi Kit (Qiagen) and/or the EndoFree Plasmid Maxi Kit (Qiagen500-EF). The DNA concentration was determined by photospectrometrical quantification at 260 nm by $A_{260} * 50 = x \text{ µg/µl}$.

Tab. 15: Buffers for plasmid isolation

Buffer	Composition
P1 Buffer	50 mM Tris/HCl pH 8.0, 10 mM EDTA, 100 µg/ml RNase A (4°C).
P2 Buffer	200 mM NaOH, 1% (w/v) SDS
P3 Buffer	3 M potassium acetate, pH 5.5

2.2.1.8 DNA restriction enzyme digestion

For analytical digestions 1 µg of DNA, harboring 1 restriction site, was incubated with 1 U of enzyme for 1 h (alternatively, 0.5 U for 2 h; 0.25 U per 4 h). For preparative digestions 5 to 10 fold overdigestion was conducted. Reaction mixtures were incubated at 37°C, unless another temperature was recommended by the manufacturer.

2.2.2 Yeast experiments

Twenty five ml of yeast culture medium (YPDA) were inoculated with one AH109 colony (from a plate kept at 4°C) and were cultured overnight at 30°C shaking. 100 ml of fresh YPDA medium were inoculated with 10 ml of the overnight culture to a OD₆₀₀ of 0,1–0,2 and grown for 5 hours at 30°C with shaking till the OD₆₀₀ reached 0,9-1,0. Then, the yeast were

centrifuged at 500×g for 2 minutes at room temperature. The pellet was washed for 2 minutes with 50 ml of 1× TE buffer and again centrifuged for 2 minutes at 500×g at room temperature. A following pellet-washing step with 1× TE/LiAc was performed for 10 minutes at room temperature and centrifuged at the same conditions as before. The washed pellet was resuspended in 1,5 ml 1× TE/LiAc to finally get the competent yeast. 10 µl of Carrier DNA, minimum 500 ng of BD and AD-plasmid and 50 µl of competent yeast cells were added to one reaction tube. The components were mixed by shaking and 300 µl of PEG/TE/LiAc was added and vortexed at medium speed for 10 seconds. The plasmid incorporation was achieved with heat shock for 40 minutes at 42°C. Cells were subsequently chilled on ice for 2 minutes. The yeast were collected by centrifugation at 500 x g for 1 minute at room temperature and then resuspended in 200 µl of water. 100 µl of the resuspended pellet were plated on appropriate SD medium.

Co-transformed cells were selected by growth on –LW-medium. The interaction of co-expressed proteins activating expression of reporter genes was monitored as growth on –ALWH-medium after 4 and 7 days. Potential self-activation of constructs was always tested in parallel by co-transformation with empty prey or bait vectors.

2.2.3 Biochemical methods

2.2.3.1 Protein concentration determination: Amidoblack protein assay

Protein concentration was determined by the colorimetric amidoblack assay in a 96 well plate. To prepare the calibration curve, 0–20 µg BSA and 5–10 µl of sample were brought to a total volume of 100 µl with H₂O. 200 µl of amidoblack solution were added to both, the standard and sample solutions. All samples were incubated for 20 minutes at room temperature and centrifuged at maximum speed for 5 minutes. The supernatant was decanted and the pellet was washed three times with methanol-acetic acid. Finally the pellet was resuspended in 500 µl of NaOH (0.1 N). The absorption was measured at 620 nm against NaOH.

Tab. 16: Solutions for amidoblack assay

Solution	Composition
Amidoblack solution	14,4 g amidoblack in 1 l methanol-acetic acid
Methanol-acetic acid	Methanol:acetic acid = 9:1
BSA stock solution	0,5 mg/ml BSA

2.2.3.2 SDS-PAGE using Laemmli system

Proteins were separated using one-dimensional sodium dodecyl sulphate polyacrylamide gel electrophoresis (SDS-PAGE) under fully denaturing conditions (Laemmli 1970). SDS-PAGE

was performed in a gradient gel: a stacking gel was layered on top of a separating gel. The samples were first incubated with SDS-sample buffer at 95°C for 5 minutes and then loaded onto the gel. Gels were allowed to run at a constant current strength of 8 mA in an electrophoresis chamber (Hoefer Mighty Small System SE 250 from Amersham Biosciences) filled with 1x electrophoresis buffer. Subsequently the gels were either stained with Coomassie blue or were used for immunoblotting.

Tab. 17: List of Buffers for TRIS-Glycine SDS-PAGE

Buffer	Composition
4x SDS-sample buffer	250 mM Tris/HCl, pH 6.8, 1% (w/v) SDS, 40% (v/v), glycerol, 4% β -mercaptoethanol, 0.02% bromophenol blue
Electrophoresis buffer	192 mM glycine, 0.1% (w/v) SDS, 25 mM Tris-base, pH 8.3
4x separating buffer	0.4% (w/v) SDS, 1.5 M Tris/HCl, pH 6.8
Separation gel (20%)	8.25 ml separation buffer, 7.5 ml 87% Glycerol, 16.5 ml 40% Acrylamide, 330 μ l EDTA (0.2 M), 22 μ l TEMED, 120 μ l 0.5% Bromophenol blue and 75 μ l 10% APS
Separation gel (5%)	8.25 ml separation buffer, 17.94 ml dH ₂ O, 1.89 ml 87% Glycerol, 4.12 ml 40% Acrylamide, 330 μ l EDTA (0.2 M), 22 μ l TEMED and 118 μ l APS
Stacking gel (5%)	6 ml stacking buffer, 7.95 ml dH ₂ O, 5.52 ml 87% Glycerol, 3.90 ml 30 % Acrylamide, 240 μ l EDTA (0.2 M), 240 μ l 10% SDS, 17.2 μ l TEMED, 30 μ l Phenol red and 137 μ l 10% APS

2.2.3.3 Coomassie staining of SDS-PAGE

Polyacrylamide gels were stained with Coomassie solution for 30 minutes. Proteins were visualized by incubating the gel in destaining solution for 2 hours or overnight by shaking. Gels were visualized by Odyssey Infrared Imaging System (LI-COR Bioscience).

Tab. 18: List of solutions for Coomassie staining of SDS-PAGE gels

Solution	Composition
Coomassie blue staining solution	1 mg/1000 ml Coomassie brilliant blue R-250, 60% (v/v) methanol, 10% (v/v) acetic acid
Destaining solution	7% (v/v) acetic acid, 5% (v/v) methanol
Drying solution	5% (v/v) glycerin, 50% (v/v) methanol

2.2.3.4 Western blotting and blot overlay

Proteins were electrotransferred from polyacrylamide gels to Millipore Immobilon-FL transfer membranes (polyvinylidene fluoride membrane (PVDF)). The transfer was performed in blotting buffer (192 mM Glycine, 0,2 % (w/v) SDS, 18 % (v/v) methanol, 25 mM Tris-Base, pH 8,3) at 4°C for 2 h with 200 mA.

2.2.3.5 Immunoblot detection

For immunodetection, blots were blocked with 1% BSA in PBS with 0,1% Tween-20, incubated with primary antibodies for 1h at room temperature and after several washing steps probed with peroxidase coupled secondary antibodies for 1h at room temperature. The visualisation was performed by chemiluminescent detection (Pierce or Millipore) and detected

with Amersham hyperfilms (GE Healthcare) or a ChemoCam Imager HR16-3200 (Intas Science Imaging). For blotoverlay experiments each blot was incubated with 25 µg of purified GST or 50 µg GST-14-3-3h fusion proteins for 1 h at RT and subsequently processed for immunodetection of the bound proteins.

2.2.3.6 Purification of fusion proteins

2.2.3.6.1 Induction of fusion protein synthesis (GST and His-Trx)

E.coli BL21 cells were transformed either with pGEX- or pET-vector. 100 ml of LB medium containing appropriate antibiotics were inoculated with one colony and cultured overnight at 37°C shaking. 1000 ml of 2×YT culture medium including the appropriate antibiotics and 0,2% glucose was inoculated with 50 ml overnight culture. The dilution was incubated shaking at 37°C until OD600 reached 0,5-0,7. Then the culture was induced with 0,3 mM IPTG and incubated at 20 °C for 10 h (overnight). Cells were harvested at 3000×g for 5 min at 4°C. Then bacteria were resuspended in 25 ml of ice-cold PBS; transferred in 50 ml Falcon tube and stored at -80°C.

2.2.3.6.2 Bacterial extract preparation

Frozen bacterial pellet was mixed with volume (25 ml) of 2× PBS buffer containing 1 tablet of EDTA-free Complete TM protease inhibitor (Roche), DNase I (5 µg/ml) and RNase A (10 µg/ml) and thawed on ice. Bacteria were lysed at 20000 psi using the french press. The lysate was diluted 1:1 with 2× PBS and 20% Triton X-100 was added to the final concentration 0,1%. The final dilution was stirred gently for 30 min at 4° and then centrifuged for 10 min at 4°C. The supernatant was then transferred into a 50 ml centrifugation tube containing the affinity resin.

2.2.3.6.3 Affinity purification

Equilibration of 2 ml Talon Metal Affinity Resin (BD/Clontech) or glutathione Sepharose 4 Fast Flow (GE Healthcare) for purification of His-Trx- or GST-fusion proteins, respectively, was made in 50 ml centrifugation tube by washing two times with 2× PBS (pH 7.0). Then bacterial extract was transferred to the beads; mixed end-over-end for 1 h at 4 °C and centrifuged for 3 min at 500×g. Supernatant was discarded. Talon beads were washed 3 times with 50 ml 2× PBS (pH 7,0) at 4°C for 3 min each and transferred to a disposable column. 10 ml of 2× PBS was used for the last washing step. Fusion proteins were eluted by adding 2 ml

elution buffer 3 times with 5 min incubation at room temperature. Three elution fractions were combined and elution buffer was exchanged by overnight dialysis against 1× PBS. Dialysed protein fractions were stored at -80°C or, alternatively, were mixed with glycerol 1:1 and stored at -20°C.

Tab. 19: Buffers for affinity purification

Buffer	Composition
Elution buffer for GST-tagged proteins	10 mM Glutathione in 50 mM Tris/HCl, pH 8,0
Elution buffer for His-Trx-tagged proteins	150 mM imidazol in 2× PBS, pH 7,0

2.2.3.7 Pull-downs and Co-immunoprecipitation proteins from transfected HEK293-T cells

HEK293T (ATTC) were grown in 6-well plates and transfected using the calcium phosphate method (2.2.4.7.1). Cells were lysed in 10 mM HEPES, pH 7.5, 150 mM NaCl, 0.5 % Triton-X-100, for pull downs, or 10 mM Tris-HCl, pH 8.0, 150 mM NaCl, 1% NP-40, 10% glycerol, for co-immunoprecipitations, containing Complete protease inhibitors (Roche) and PhosStop (Roche) for 10 min at 4°C. Insoluble material was removed by centrifugation. For dephosphorylation of proteins 10 units of calf intestine alkaline phosphatase (Fermentas) were added to the cell lysates and incubated for 1 h at 37°C. For pull downs 25 µg purified GST or 50 µg purified GST-14-3-3η were coupled to Glutathion sepharose Fast Flow (Amersham) and incubated with cell lysates overnight at 4°C. Unspecific material was removed by washing with lysis buffer and bound material was eluted by incubation with 10 mM glutathione, 50 mM Tris-HCl, pH 7,5, for 30 min at RT. Co-immunoprecipitations were done using MicroMACS anti-GFP MicroBeads and MicroColumns (Miltenyi Biotec) according to the manufacturer's protocol but using the lysis buffer in all washing steps.

2.2.3.8 Brain extract preparation

Bassoon mutant mice (BsnDEx4/5; (Altrock et al., 2003)) were used for blotoverlay experiments and for characterisation of α-pS2845 Bsn. Mice were killed by neck dislocation and brains were homogenised in 320 mM sucrose, 25 mM Tris-HCl, pH 7.4, containing Complete protease inhibitor and PhosStop, and centrifuged at 1,000 x g for 10 min. The supernatant was centrifuged at 12,000 x g for 20 min and the pellet was resuspended in 25 mM Tris HCl, pH 7.4, 150 mM NaCl, 1% Triton-X-100 to obtain the crude membrane fraction (pellet P2). All steps were performed at 4°C. For hyperphosphorylation of proteins 5 mM MgCl₂ and 1 mM ATP (Sigma-Aldrich) was added and incubated at 30°C for 30 min. The reaction

was stopped by addition of 10 mM EDTA. Protein concentrations were determined by amidoblack assay and the samples were used for Western blots.

2.2.3.9 In vitro phosphorylation

His-Bsn11 and the His tag alone were expressed in bacteria (BL21 Codon Plus (DE3) RIPL, Stratagene) and purified following the manufacturer's protocol. 5 μ mol of His fusion proteins were incubated with 0 to 40 mU RSK protein (RSK1 #14-509, RSK2 #14-408, RSK3 #14-462, RSK4 #14-702; Millipore) in 50 mM Tris-HCl, pH 7.5, 10 mM MgCl₂, 1 mM EGTA, 1 mM DTT, 1 mM ATP for 45 min at 37°C. Phosphorylation of proteins was analysed by Western blots using phosphorylation specific antibodies.

2.2.4 Cell culture techniques

Primary neurons, HEK293-T and COS-7 cells were cultured in 5% CO₂ at 37°C and a humidity of 95%. All supplemented cell culture media were filtrated using sterile filtration bottles with a pore size of 0.22 μ m and kept at 4°C until usage. Media and reagents used for eukaryotic culture are listed in Tab. 20. All media were preincubated at 37°C before addition to cells.

Tab. 20: Media and reagents for eukaryotic cell culture

Media and reagents for eukaryotes	Ingredients/Company
DMEM (mouse culture)	2% B27 (Gibco); 1 mM sodium pyruvate 100x (Gibco); 5 g/l AlbuMax II (Gibco); 2 mM L-glutamine 100X (Gibco) in DMEM (without: phenol red, Lglutamine, sodium pyruvate) (Gibco)
DMEM (10% FCS)	10% FCS (Gibco); 1% Penicillin/Streptomycin 100x (Gibco); 2 mM L-Glutamine 100x (Gibco) in DMEM (Gibco)
NB (Neurobasal)	2% B27 (Gibco); 2 mM L-glutamine (Gibco); 1% Penicillin/Streptomycin 100x (Gibco) in Neurobasal
Distilled Water	Gibco /Millipore
HBSS+ (with Mg ²⁺ and Ca ²⁺)	Gibco
HBSS-	Gibco
Optimem	Gibco
AraC 1.5 mM	Calbiochem
10x Trypsin	Gibco
1x Trypsin	10% 10x Trypsin (Gibco); DMEM (10%FCS)
Paraffin	Paraplast embedding medium (Fischer)

2.2.4.1 Splitting of cells into culture plates

HEK293-T and COS-7 cells were split by Heidi Wickborn, Sabine Opitz and Janina Juhle. Cells were washed twice with pre-warmed HBSS- and subsequently incubated with 1 ml of 1x Trypsin per 75 cm² flask for 5 minutes at 37°C. After checking the dissociation of the cells from the plate, degradation of extracellular proteins by the protease trypsin was blocked by

adding 9 ml of fresh, pre-warmed DMEM (10% FCS). The cells then were transferred into plates with additional medium as indicated in each section.

2.2.4.2 Preparation of glass coverslips

Washing: Glass coverslips for cell culture were placed into 50 ml tubes with 50% HNO₃ and incubated in an end-over-end shaker overnight. On the next day, pH was neutralized by washing with cell culture or milipore water. Coverslips then were boiled in cell culture water using a microwave oven three times with exchanging the water in between. After washing one additional time they were separately dried on precision wipes and baked for 4 h at 200°C for sterilisation.

Coating: Coverslips were transferred into a Ø 10 cm microbiological plastic dish and three paraffin dots were attached to each of them (paraffin heated to 150°C) (only for neuronal cell culture). They were coated with 100 µl of poly-D-lysine working solution (see Tab. 8) per coverslip and incubated overnight in the cell culture incubator. On the next day cell culture water was added to each plate. Before usage of the coverslips they were washed three times with cell culture water and dried completely prior to plating of the cells.

2.2.4.3 Glial cells

Plating: P1 to P3 pups (C57Bl6|J cre strain for mice culture and Wistar rat strain for rat culture) were decapitated and both brain hemispheres were removed, washed twice with HBSS- and incubated in 4,5 ml HBSS- with 0,5 ml 10× Trypsin for 20 minutes at 37°C. After washing once with HBSS+ medium was exchanged for 1 ml DMEM (10% FCS). Trituration of the hemispheres followed using a 1 ml pipette to obtain a nearly homogeneous cell solution. The material from two hemispheres filled up to a volume of 10 ml with DMEM (10% FCS) and was plated in one 75 cm² or it was filled up to a volume of 50 ml and plated into ten Ø 6 cm plates for direct usage.

Freezing: Before freezing, glial cells were brought in solution using trypsin. The cell suspension of one bottle was transferred to 50 ml tubes and spinned down for 5 minutes at 1000×g. Resuspension in 1 ml ice cold DMEM (10 % FCS) containing 10 % DMSO followed. Slow freezing of the sample was performed by quick transfer into a bio safe freezing tube, initially on ice and then at -80°C. On the next day aliquots were transferred to -150°C and stored until usage.

Plating: from stocks 2-4 frozen glial cell aliquots were incubated at 37°C until melting started. Then 1 ml of prewarmed DMEM (10% FCS) was added. Cells were triturated and transferred to fresh DMEM (10% FCS) and plated on twenty Ø 6 cm plates with a final volume of 5 ml each.

2.2.4.4 Mouse hippocampal neurons

Mouse hippocampal cultures were prepared by Carolina Montenegro and Claudia Marini. P0 mouse pups were genotyped (see 2.2.1.1) and decapitated and the heads were kept in HBSS+ on ice until dissection. Hippocampi were collected in fresh tubes on ice with HBSS+ and washed three times with cold HBSS-. After the last washing step, 4.5 ml HBSS- and 500 µl of 10× trypsin were added and incubated for 20 min at 37°C. Hippocampi were washed once with HBSS+ and the medium was replaced by 1 ml DMEM (10% FCS). Trituration using a 1 ml pipette was performed by pipetting up and down 10 times. After counting the cells, the suspension was diluted to 250000 cells/ml. 100 µl of cell suspension were plated on the coated, washed and dried Ø 18 mm coverslips (see 2.2.4.2) and incubated for 1 h in the cell culture incubator. The media of the Ø 6 cm glial cell plates was exchanged by 5 ml DMEM (mouse culture) and five coverslips were turned into each plate with neurons and paraffin dots facing down. After two days 5 µl AraC (100×) were added to inhibit glial cell proliferation. The cells were fed every week by replacing 1 ml of old media with fresh one.

2.2.4.5 Rat hippocampal neurons

Rat hippocampal neuron cultures were prepared by Sabine Opitz, Heidi Wickborn and Janina Juhle from E16 to E17 rats. The general procedure for preparing rat hippocampal neurons is equivalent to the protocol for mouse hippocampal neurons 2.2.4.4. Neurons were cultivated in NB medium. 7,5 µl AraC were added to the cells at DIV3.

2.2.4.6 Manipulation of the Bassoon phosphorylation status

To manipulate the phosphorylation of Bassoon, rat cortical neurons grown in 6 well plates were washed with HBSS and incubated for 30 min at 37°C with the kinase inhibitors 100 nM BI-D1870 (Symansis), 10 µM UO126 (Cell Signaling Technology) or 10 µM PD98056 (Promega) dissolved in Hanks buffered salt solution (HBSS). Global phosphorylation of cellular proteins was induced by addition of 50 nM okadaic acid (Tocris) for 30 min at 37°C.

2.2.4.7 Transfections

2.2.4.7.1 Transfection of HEK293-T cells with calcium-phosphate

HEK293-T cells were grown in 75 cm² flasks in DMEM (10% FCS). 150 µl of 0.5 M CaCl₂ were mixed with 4 µg DNA. Then, 50 µl of 140 mM NaCl, 50 mM HEPES, and 1,5 mM Na₂PO₄, pH 7,05, were added and after 1 min applied to cells in culture. The cells were incubated for 4 to 6 h at 37°C in 5% CO₂ atmosphere before exchanging growth media. Cells were grown for 24 hours before using them for further analyses.

2.2.4.7.2 Transfection of COS-7 cells on 24 well plates

The cells were grown on poly-D-lysine coated glass coverslips to 50–70 % confluency. For a single construct transfection 1.5 µg DNA were used for 4 wells. For a double transfection 1 µg of each construct was used for the same number of wells. The DNA was resuspended in 200 µl DMEM without supplements, 8 µl of Polyfect (Qiagen) was added and the transfection reaction was mixed. After 5 minutes at room temperature 400 µl of COS-7 cells culture medium was added and 150 µl of this mixture was carefully dropped to each 4 wells and incubated for 24 hours. After 24 h, cells were fixed in 4% paraformaldehyde and 4% sucrose in PBS, pH 7.4, for 5 min at room temperature and embedded in Mowiol 4-88.

2.2.4.7.3 Transfection of rat hippocampal neurons with calcium phosphate

Hippocampal neurons were transfected using the calcium phosphate method at 3 DIV. Prior transfection Ø 18 mm coverslips cultured with neurons were transferred into a new 12-well plate containing 1 ml/well of prewarmed and equilibrated Optimem media (see Tab. 20) and kept in the incubator for 30 min. To prepare the precipitates 180 µl of transfection buffer (274 mM NaCl, 10 mM KCl, 1.4 mM Na₂HPO₄, 15 mM Glucose, 42 mM HEPES) was added dropwise to a solution containing 12 µg of DNA and 250 mM CaCl₂, under gentle stirring. The mixture was placed for 20 min at room temperature in the dark; 60 µl of the mix was then added per well, and neurons were placed in the incubator for 40 to 60 min. Medium was exchanged for 1 ml 37°C pre-warmed Neurobasal (see Tab. 20), followed by two 750 µl washes. Finally, the coverslips were transferred back into the original medium.

2.2.5 Immunocytochemistry, microscopy and image analysis

All primary antibodies for immunocytochemistry (ICC) were prediluted in 50% glycerol and stored at -20 °C (Tab. 10). Secondary antibodies were stored at 4 °C.

2.2.5.1 Immunostaining of cell cultures

Cells were grown on Ø 18 mm (mouse and rat hippocampal neurons) and Ø 12 mm (COS-7 cells) coverslips and fixed for 3 to 5 minutes with 37 °C pre-warmed 4 % PFA, 4 % sucrose in PBS. Blocking of PFA-reactivity and permeabilization of the cells was achieved by 15 minutes incubation in 10 % FCS, 0,1% glycine, 0,3 % Triton X-100 in PBS. The antibodies were diluted in 50 µl 3 % FCS in PBS per Ø 18 mm coverslip and pipetted on a paraffin film in a wet chamber (for list of antibodies and corresponding dilutions see Tab. 10). The coverslips were turned with cells facing down on top of the antibody drop. Incubation with the primary antibody at 4°C overnight was followed by three times washing with PBS. The secondary antibody was applied at RT for one hour. After washing three times for 15 min in PBS, coverslips were mounted in Mowiol (10 µl per Ø 18 mm coverslip). Mounted coverslips were stored at 4°C until usage.

2.2.5.2 Synaptotagmin uptake assay

For the synaptotagmin assay transfected hippocampal neurons from wt and Bassoon KO mice were transferred to a 12 well plate and washed two times with 1 ml Tyrodes buffer (2,5 mM KCl, 119 mM NaCl, 25 mM Hepes, 30 mM sucrose, 2 mM MgCl₂, 2 mM CaCl₂, pH 7,4). Then Oyster 550 labeled α -Synaptotagmin1 antibody was added in a 1:200 dilution and the mixture was incubated for 5 min to allow uptake of the antibody into the cells. Not internalised antibody was washed away by two washing steps with Tyrodes buffer. Cells were then fixed with 4 % PFA and 4 % sucrose in PBS for 3 min and further processed for immunostaining as above (2.2.5.1).

2.2.5.3 Microscopy and image analysis

Hard- and software Images were taken using a Zeiss Axioplan 2 epifluorescence microscope equipped with a camera (Cool Snap EZ camera; Visitron Systems, or Spot RT-KE; Diagnostic Instruments, Inc.) and MetaVue software (MDS Analytical Technologies). Image processing and analysis were performed using ImageJ (MacBiophotonics ImageJ Version 1.41a), Adobe Photoshop (Version 8.0) and Openview (Version 1.5 from Noam Ziv) software.

2.2.5.4 Analysis of synaptic immunofluorescence

To analyze immunofluorescence at synapses as a relative measure for the synaptic amount of a protein, mouse or rat hippocampal cultures were fixed and stained for a synaptic marker in the infrared channel (Cy5) and the protein of interest in the red channel (Cy3). The analysis of co-

localisation of proteins expressed in neurons was performed using the ‘Colocalisation Analysis’ plug-in of ImageJ (Li et al., 2004; Schneider et al., 2012). To analyse of synaptic targeting of GFP-Bsn and GFP-Bsn S2845A, transfected neurons were fixed and stained for synaptic markers Homer and Synaptophysin. Bsn-positive puncta were detected using Openview (Tsuruel et al., 2006). Homer and Synaptophysin intensities were then measured at the location of Bsn-positive puncta in the according channels. After subtraction of an intensity threshold to exclude background levels the percentage of Bsn-positive puncta also positive for Homer or Synaptophysin was calculated.

2.2.5.5 Live imaging microscopy, fluorescence recovery after photobleaching (FRAP) experiments

Live imaging was performed at 37°C using an inverted microscope (Observer. D1; Carl Zeiss, Inc.) in a heated imaging chamber TC-344B (Warner Instruments) and an EMCCD camera (Evolve 512; Photometrics) controlled by MetaMorph Imaging (MDS Analytical Technologies) and VisiView (Visitron Systems GmbH) software. The FRAP laser DL-473 (Rapp Optoelectronics) was driven by the FRAP targeting device Visifrap 2D (Visitron Systems GmbH). Videos were taken prior to bleaching 10 s (10 pictures, 250 ms exposure time), then for fluorescence bleaching a laser pulse of 10 ms was applied and the recovery was monitored for 25 s (100 pictures, 250 ms exposure) and additional 300 s (300 pictures, 250 ms exposure). For image analyses ImageJ (Schneider et al., 2012) and MetaMorph Imaging (MDS Analytical Technologies) was used. Recovery rate was determined after background subtraction (from three independent spots) and bleaching correction, which was performed by selection of five fluorescence spots which were not used for FRAP, by calculating the ratio of the spot intensity for every time point versus the intensity before (set to 100%) and after (set to 0%) bleaching.

For vesicle mobility experiments video streams of 25 s recorded at 4 Hz with an exposure time of 250 ms were analysed using Metamorph software. To determine velocities and running distances of vesicles carrying GFP-Bsn or GFPBsn14- 3-3BM, traces of mobile particles were visualised on kymographs of axonal segments. Traces showing processive movement (without stops and changes in velocities or movement directions) were analysed. Statistical analysis of all data was done with the software GraphPad Prism 5 (GraphPad Software).

2.2.6 Transferrin uptake and fluorescence activated cell sorting (FACS)

HEK293T cells were cultured in 75cm² flasks and transfected with GFP-tagged constructs. After 24h of expression cells were washed with pre-warmed PBS (37 °C). Cells were trypsinised and trypsin activity was stopped by addition of 8,5 ml of serum containing DMEM after detachment. Cells were detached further by pipetting up and down several times. The cells were pelleted by centrifugation for 5 min at 220 x g and the pellet was washed with 10 ml PBS. Subsequently pellets were resuspended and the cells were starved in 10 ml serum free DMEM for 30 min at 37 °C in a slowly turning end-over-end shaker. Negative control samples were supplied with 100µM Dynasore in this and the next steps to inhibit dynamin and thereby CME. The suspensions were cooled to 4 °C on ice for 5 min. Alexa 647 labelled transferrin was added to the cells in 1:200 dilution and incubated for 5 min on ice. Then the uptake was performed by incubation of the suspensions at 37°C in the water-bath for 10 min. To stop the uptake cells were cooled down again to 4°C on ice for 5 min and subsequently washed with 10 ml cooled PBS (4 °C). Then they were washed two times with a buffer containing 0,1 M Glycin, 150 mM NaCl, pH 3 to strip extracellularly attached transferrin from the cell surface. Cells were resuspended in ice cooled PBS with 1 % BSA. Now the samples were measured with a FACSCalibur flowcytometry device (BD Bioscience). Resulting datasets were analysed by WinMDI flowcytometry software.

2.2.7 Statistical data analysis

Statistical data analysis (t-test, ANOVA) was performed using GraphPad Prism 4.

3 Results

This work comprises the analysis of the interaction of two different adaptor proteins with the presynaptic scaffolding protein Bassoon. The project is based on a Y2H screening for binding partners of Bassoon done by Wilko Altmann. Two of the proteins that have been found by this assay are the μ subunit of the Adaptor Protein Complex 2 (AP2 μ 1) and the η isoform of the 14-3-3 family (14-3-3 η). Both proteins are besides other tasks well known for their contribution in presynaptic function and performance (1.4 and 1.4.2). Therefore the aim of this study was to confirm the interaction observed in yeast cells and to elucidate the functional relevance of their interaction with Bassoon, especially focused on presynaptic mechanisms like vesicle control and dynamic network regulation. In the following sections the results of the analysis of the two interactions are presented subsequently, first referring to AP2 in chapter 3.1 and second to 14-3-3 in chapter 3.2.

At this point it must be mentioned that to assure comprehensibility of the study it was necessary to include experimental data, which were obtained together with or provided by other members of our laboratory. These experiments will be clearly marked as work of others below the corresponding figures.

3.1 Interaction of Bassoon with Adaptor Protein Complexes

The first adaptor protein investigated for a functional interaction with Bassoon was the μ subunit of the AP2 complex. This subunit is responsible for the binding of the complex to cargo proteins. AP complexes are well known for their important role in the maintenance of the SVC. Therefore the interaction represented an interesting target in the process of revealing more of the physiological significance of Bassoon at the presynaptic bouton. The main question of this project was if and, if yes how Bassoon could be involved in endocytosis and vesicle recycling mechanisms providing the basis for sustained signalling capacities at the presynaptic terminal.

3.1.1 The AP2 μ subunit and Bassoon interact in yeast

The initial step was to confirm the interaction of AP2 μ 1 with Bassoon fragments used for the original screening of Bassoon interaction partners in the Y2H system. For this purpose AP2 μ 1 was cloned from a rat brain cDNA library and subcloned into a Y2H prey vector to facilitate the conduction of direct Y2H experiments. The smallest bait fragment of Bassoon that was interacting with AP2 μ 1 contained the aa 608-1204 of rat Bassoon (Fig. 6A, Tab. 21). The goal

of the subsequent Y2H experimental series was to identify the exact binding site of AP2 μ 1 on Bassoon and to provide evidence for its functionality by single aa exchange mutations of the motif. Since the consensus prerequisites for AP binding sites are well described (see section 1.4) the next step was to perform an *in silico* prediction of functional sites of Bassoon to close up on potential target regions for the AP2 μ 1 interaction. The online database “The Eukaryotic Linear Motif resource for Functional Sites in Proteins” (ELM) is a comprehensive tool to screen proteins for a huge number of aa motifs like recognition sites or target sequences for posttranslational modifications described in the literature (Puntervoll et al., 2003).

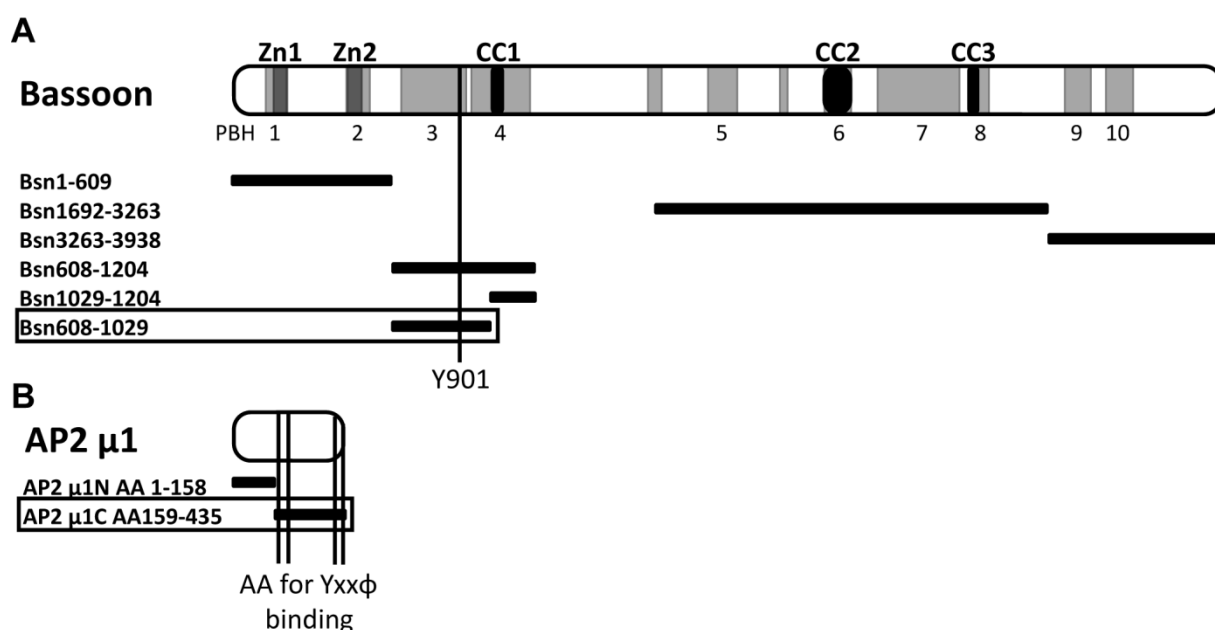


Fig. 6: Scheme of constructs used in the Y2H Assay for AP2 interaction.

(A) Scheme of Bassoon with functional domains and aa sequence sections covered by the Y2H bait constructs. Tyrosine 901, essential for interaction of Bassoon with AP2 μ 1 constructs is marked by a line. The smallest interacting Bassoon fragment Bsn608-1029 is boxed. **(B)** Scheme of AP2 μ 1 Y2H prey constructs. Aa essential for Yxx ϕ motif interaction are marked by lines. Only boxed Ap2 μ 1C containing the Yxx ϕ binding pocket interacted with Bassoon.

The list of sites predicted for Bassoon by this software included two potential Yxx ϕ motifs as possible binding locations for AP2 μ 1 in the region of the interacting prey construct Bsn608-1204. The first motif comprised Bassoon aa 901-904, the second one Bassoon aa 1182-1185. The routine of the ELM software also permitted a prediction of the accessibility of the presented motifs by a combination of hydrophobicity analysis and assumptions of structural conformation of the screened protein. While aa 901-904 are regarded accessible by ELM, aa 1182-1185 are positioned inside a so called SMART/Pfam domain and are therefore considered unlikely to be accessible. Nevertheless it was decided to check both motifs in further experiments. To test the

functionality of the predicted binding sites two smaller fragments of rat Bassoon (Bsn608-1029 and Bsn1029-1204) each containing one of the two potential binding motifs were cloned and used as bait constructs in the same Y2H setup as before (Fig. 6A, Tab. 21). Only Bsn608-1029 containing the first potential binding site but not Bsn1029-1204 containing the second site showed an interaction with the AP2 μ 1 bait construct.

To confirm that the identified interaction was established in the conventional way via the Yxx ϕ binding pocket of the AP2 μ subunit, two additional AP2 μ 1 deletion constructs (Fig. 6B) were designed and cloned. One contained the binding pocket (AP2 μ 1C) in the other one it was absent (AP2 μ 1N). Only AP2 μ 1C including the binding pocket for the Yxx ϕ motif was interacting with Bsn608-1204 or Bsn608-1029, while AP2 μ 1N did not interact with any of the Bassoon prey constructs (Tab. 21).

Tab. 21: Intensities of Y2H interaction of Bassoon bait with AP2 μ 1 prey constructs.

Intensities were judged by comparison of colony numbers on the control plates. -: no interaction, +: weak interaction, ++: medium interaction, +++: strong interaction.

Bait constructs	Prey constructs	Interaction
Bsn1692-3263	AP2 μ 1	–
Bsn3263-3938	AP2 μ 1	–
Bsn1-609	AP2 μ 1	-
Bsn608-1204	AP2 μ 1	++
Bsn608-1029	AP2 μ 1	++
Bsn1029-1204	AP2 μ 1	–
Bsn608-1204	AP2 μ 1N	–
Bsn608-1029	AP2 μ 1N	–
Bsn1029-1204	AP2 μ 1N	–
Bsn608-1204	AP2 μ 1C	++
Bsn608-1029	AP2 μ 1C	++
Bsn1029-1204	AP2 μ 1C	–

The only Yxx ϕ motif in Bsn608-1029 has the aa sequence YEEL and spans the aa 901-904 of Bassoon. Furthermore this fragment does not contain any of the other functional motifs known to interact with AP μ subunits. To provide direct evidence that the identified motif is really responsible for the interaction with AP2 μ 1, a mutant of Bsn608-1029 (Bsn608-1029^{Y901A, L904A}) was generated by site directed mutagenesis. The sequence of the potential binding motif was

changed from YEEL to AEEA to disrupt both of the aa essential (1.4) for a successful interaction with $\mu 2$.

The mutated construct was tested and compared to the wt counterpart in the same Y2H setup as before. Bsn608-1029^{Y901A, L904A} did not show any interaction with any of the $\mu 2$ bait constructs (Tab. 22). The disruption of the interaction between Bassoon and AP2 μ 1 by mutation of the essential aa of the predicted binding motif provides an evidence for the aa 901-904 of rat Bassoon to act as functional interaction site for the binding of AP2 μ 1. Further it can be concluded from the Y2H experimental series, that the identified motif is the only functional AP2 μ 1 binding site on Bassoon. This motif is not conserved in Piccolo indicating that possible endocytosis or sorting processes of Bassoon mediated by AP complexes can work independently and differently than for Piccolo.

Tab. 22: Intensities of Y2H interaction of Ap2 μ 1 prey constructs with Bassoon bait constructs containing mutated Yxx ϕ motifs.

Intensities were judged by comparison of colony numbers on the control plates. -: no interaction, +: weak interaction, ++: medium interaction, +++: strong interaction.

Bait constructs	Prey constructs	Interaction
Bsn608-1029	AP2 μ 1	++
Bsn608-1029 ^{Y901A, L904A}	AP2 μ 1	-
Bsn608-1029	AP2 μ 1N	-
Bsn608-1029 ^{Y901A, L904A}	AP2 μ 1N	-
Bsn608-1029	AP2 μ 1C	++
Bsn608-1029 ^{Y901A, L904A}	AP2 μ 1C	-

3.1.2 The AP2 μ subunit and Bassoon interact in mammalian cells

The interaction was observed in the model organism yeast in which Bassoon is naturally not expressed. Therefore the next aim was to further support the assumption of a physiological relevance for the binding of AP2 μ 1 to Bassoon in mammalian cells. For this cause the results from the Y2H system, the interaction and also the disruption of the interaction by mutation of the binding site, were tested in additional independent mammalian experimental systems.

3.1.2.1 Co-clustering of the AP2 μ subunit and Bassoon in COS-7 cells

The first step to confirm the interaction in a mammalian system was a rather crude approach, the blob assay (Kirsch et al., 1995). Therefore a mRFP tagged construct of AP2 μ 1 (AP2 μ 1-mRFP) was cloned and co-expressed with two previously established GFP-tagged Bassoon constructs in COS-7 cells. Both of the used Bassoon fragments form distinct clusters upon heterologous expression and the aim of the experimental setup was to look for a recruitment of the co-expressed AP2 μ 1 to these Bassoon clusters.

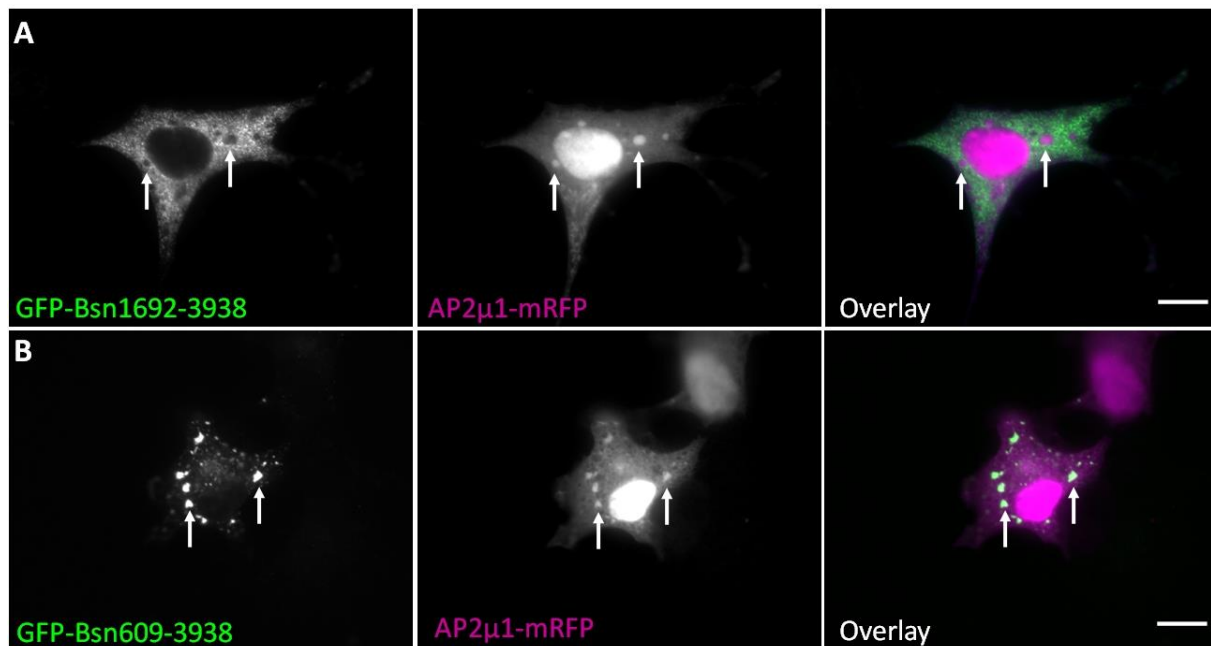


Fig. 7: AP2 μ 1 is co-recruited to Bassoon clusters in COS-7 cells.

AP2 μ 1-mRFP was co-expressed with **(A)** GFP-Bsn1692-3938 missing, or **(B)** GFP-Bsn609-3938 containing the AP2 binding site in COS-7 cells. AP2 μ 1-mRFP is co-localised with clusters formed by GFP-Bsn609-3938 but not with clusters formed by GFP-Bsn1692-3938 (arrows). Scale bar is 20 μ m.

Co-expression of AP2 μ 1-mRFP with the Bassoon constructs confirmed the Y2H results and showed that only the Bassoon fragment including the identified binding motif (GFP-Bsn609-3938) but not a construct lacking the motif (GFP-Bsn1296-3263) was able to co-recruit mRFP-AP2 μ 1 into the formed clusters (Fig. 7).

3.1.2.2 Co-IP of the AP2 μ subunit and Bassoon from HEK cells

To provide additional evidence for the protein-protein interaction, it was aimed to support the previous results biochemically by using a co-immunoprecipitation experiment employing the Bassoon point mutant. Therefore HEK293T cells were co-transfected with myc-tagged AP2 μ 1C (myc-AP2 μ 1C) and the same wt/mutant Bassoon constructs which were already used

for the Y2H experiments but fused to GFP (GFP-Bsn608-1029 and GFP-Bsn608-1029^{Y901A, L904A}). After immunoprecipitation of the fusion proteins by antibodies against GFP, co-precipitation of myc-AP2 μ 1C was checked by an antibody directed against the myc-tag. The results showed that only GFP-Bsn608-1029 but not the dominant negative mutant could co-precipitate myc-AP2 μ 1C from the HEK cell lysates (Fig. 8). At this point it should be noticed that the relative efficiency of the co-precipitation was rather weak despite the applied subtle buffer and washing conditions. This could be explained by the transient nature of AP-cargo interactions with dissociation constants in the μ M range (Aridor and Traub, 2002; Nakatsu and Ohno, 2003).

Until this step the question if the interaction was specific for AP2 or if μ subunits of other AP complexes could also bind to the same motif on Bassoon remained unanswered. To address this question the μ subunits of the other clathrin-dependent AP complexes AP1, AP3A and AP3B were cloned and myc tagged C-terminal constructs of them, comparable to AP2 μ 1C, were designed (myc-AP1 μ 1C, myc-AP3 μ 1C, myc-AP3 μ 2C). The co-immunoprecipitation was subsequently repeated with these constructs in the same way as for AP2 μ 1 (Fig. 8). Since the cargo recognition specificity of the different APs for their target sequences is overlapping (see section 1.4), it was expected to find similar results as for AP2 μ 1C also for the other AP complexes. Indeed the co-immunoprecipitation worked for AP1 and AP3A in a degree, which was comparable to AP2. Surprisingly the only μ subunit that failed to co-precipitate with the wt Bassoon construct was AP3 μ 2C belonging to the neuron-specific subtype AP3B. By this experiment the interaction itself and further also the functionality of the identified binding motif was confirmed for AP2 as well as for AP1 and AP3A but not for AP3B in another independent mammalian experimental setup.

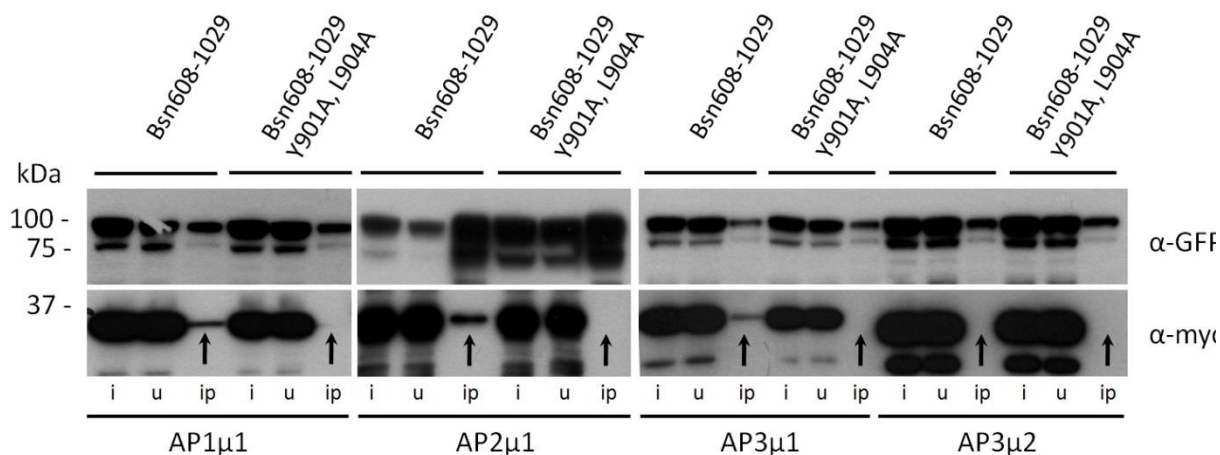


Fig. 8: Co-IP of myc-tagged c-terminal constructs of AP μ subunits with GFP tagged Bassoon wt and mutant constructs.

The upper blots show the IP by detection with α -GFP antibody, the lower blots show the co-IP detected by anti-myc antibody. The arrows show successful (visible band) and unsuccessful (no band) co-IPs of the μ constructs in the ip fractions. AP3 μ 2 of the AP3B complex was the only tested μ subunit, which did not interact with the wt Bsn constructs. i: input, u: unbound fraction, ip: immunoprecipitation.

3.1.2.3 AP complexes and Bassoon co-localise in neurons

After having demonstrated that interactions between over-expressed Bassoon and μ subunit fragments of various AP complexes can be established in mammalian model cells the next question was if and, if yes, where and when this event could endogenously occur in neurons. In mature neurons Bassoon is almost exclusively localised at synapses and it is known to be among the earliest proteins transported to and localised at forming presynaptic compartments (tom Dieck et al., 1998; Zhai et al., 2000). AP complexes do not only mediate SV recycling at the presynapse but are also responsible for diverse sorting and budding processes for cargo transport between other membranous structures in the cell. Two possible scenarios for the Bassoon AP interaction therefore were (i) the regulation of the SVC at the presynaptic active zone and (ii) the sorting of Bassoon at the TGN. To cover both possibilities co-localisation of the endogenous proteins was studied in young (DIV5) and mature (DIV21) cultured hippocampal neurons. From previous studies it is known that in young neurons Bassoon accumulates at the TGN (Dresbach et al., 2006; Maas et al., 2012) but at the same time is also already present in axonal growth cones (Zhai et al., 2000). Since AP1 is predominantly localised at the TGN while AP2 is mostly employed at the plasma membrane both somata and growth cones were analysed for co-localisation of Bassoon with AP1 or AP2 in young neurons

respectively. In mature neurons the focus was laid especially on the synaptic compartment and co-localisation with the AP2 complex.

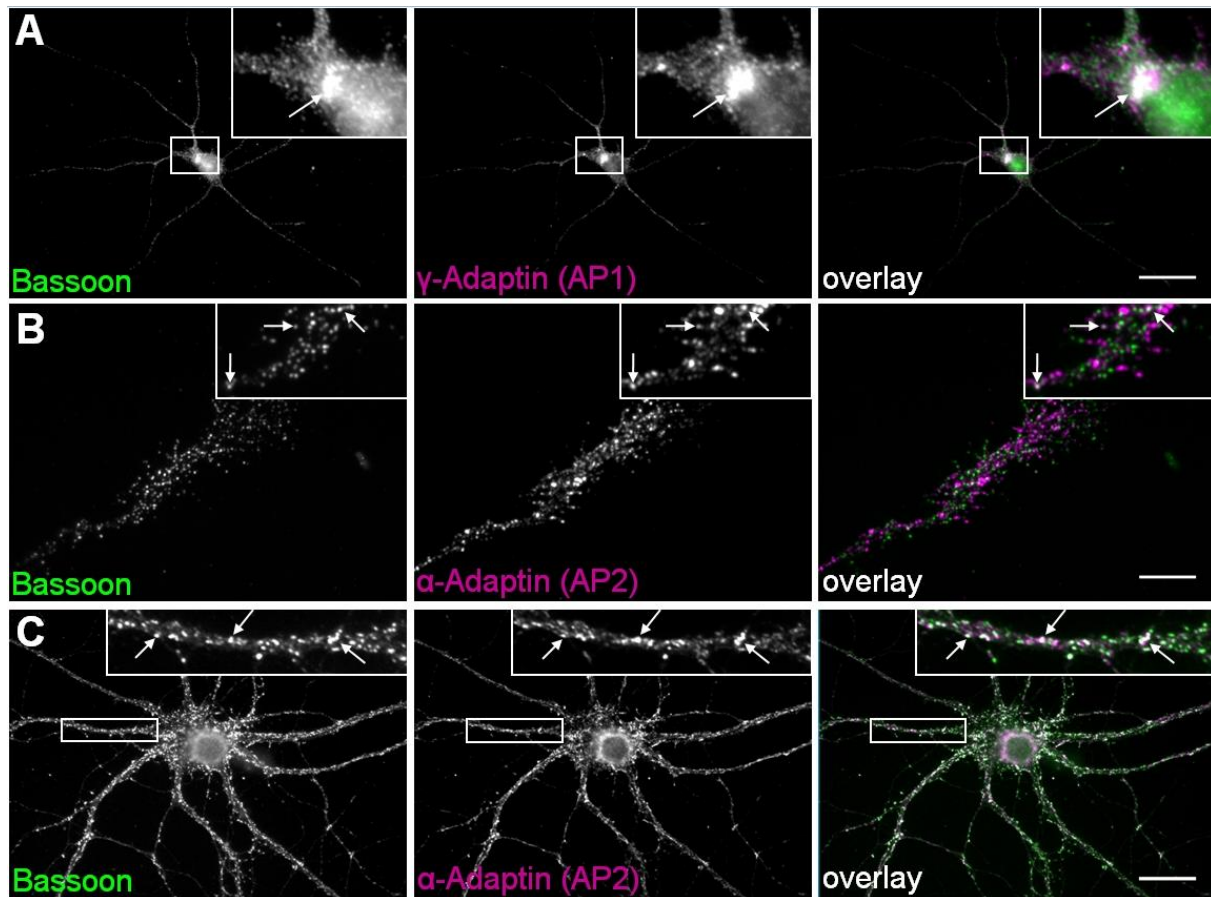


Fig. 9: Bassoon and AP complexes co-localise in neurons.

(A) Bassoon and AP1 co-localise in a somatic region of DIV5 hippocampal neurons representing the TGN. (B) At the same developmental level (DIV5) Bassoon also co-localises with AP2 at axonal growth cones. (C) Later in development (DIV21) AP2 and Bassoon co-localise at synapses. Scale bar is 20 μm .

In all three cases it was found that endogenously expressed Bassoon and AP complexes co-localise in living neurons. The strongest overlap of expression patterns was found in a somatic region in young neurons where both Bassoon and the AP1 complex were substantially enriched compared to other parts of the cells (Fig. 9A). At the same time but to a lower content the AP2 complex co-localised with Bassoon in axonal growth cones of neurons of the same age (Fig. 9B). Finally in the somatodendritic area of adult neurons the distribution pattern of AP2 was found to resemble the synaptic localisation of Bassoon much stronger than observed for the growth cone at early developmental stages (Fig. 9C). The overlap of both proteins showed that Bassoon was enriched at every spot where AP2 was present but not vice versa.

3.1.3 Bassoon does not influence clathrin-mediated endocytosis of the transferrin Receptor

Based on the previous results a functional assay was designed to elucidate whether the interaction of Bassoon with AP complexes has an impact on the mechanism of CME. Since CME is critically relevant for SV recycling this experiment should provide a proof of principle to confirm the hypothesis of a role of the interaction in regulation of neurotransmitter signalling. A classical way to measure the functionality of CME is to quantify the cellular uptake of fluorescence labeled and iron associated transferrin into cultured model cells (Fig. 10).

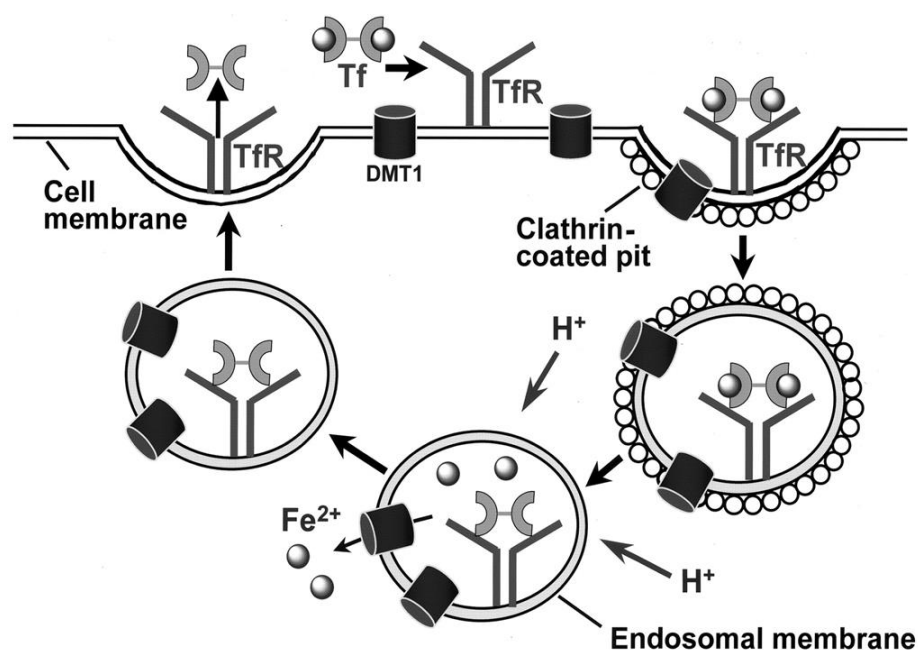


Fig. 10: Transferrin uptake mechanism.

Iron-loaded transferrin binds to the transferrin receptor at the cell surface. The complex gets internalised by CME. Acidification of the endocytic vesicle leads to dissociation of Fe²⁺ from transferrin and the ions translocate into the cytosol. The vesicle fuses with the plasma membrane and the receptor and transferrin get reexposed to the extracellular space. Unloaded transferrin dissociates from the receptor and is free for the next cycle (Qian et al., 2002).

Upon binding of transferrin to the transferrin receptor (TfR) the entire complex gets internalised by CME engaging also the AP2 complex (Qian et al., 2002; Motley et al., 2003). The goal of the experiment was initially to check if the Bassoon-AP2 interaction had any influence on the general performance of CME. Therefore HEK293T cells were transfected with constructs of GFP-tagged wt and AP2 μ 1 binding-deficient Bassoon fragments (GFP-Bsn608-1029, GFP-Bsn608-1029^{Y901A, L904A}). The transfected cells were supplied with Alexa647-labeled transferrin and allowed for a period of uptake of subsequently formed TfR-transferrin complexes into the

cells. After uptake the cells were cooled down to inhibit subsequent exocytosis of the previously internalised transferrin. Unbound extracellular transferrin was washed away and the endocytosed transferrin was quantified by measuring fluorescence intensities of the Alexa dye in the cells by flow cytometry. Cells transfected with GFP alone were used as a negative control. As positive control to compare the results to a successful inhibition of CME GFP-transfected cells were treated with the inhibitor Dynasore (100 μ M). This Dynamin inhibitor is known to disturb the fission process of budded vesicles during the process of endocytosis (Macia et al., 2006; Newton et al., 2006). The positive control showed a clear reduction of intracellular Alexa647 fluorescence intensity by application of Dynasore. Neither the wt Bsn construct nor the AP2 μ 1 binding-deficient Bassoon fragment or GFP alone had any influence on transferrin uptake in this assay. The FACS results confirmed the notion of previous experiments with the same system but different read out techniques (microscope, plate reader; data not shown). One hypothesis to explain the missing effect was that usually AP complexes interact with transmembrane or membrane attached proteins. In neurons, wt Bassoon is normally anchored to membranes by N-myristoylation. Since the Bassoon fragments used in this assay lacked the n-terminal 607 aa and therefore missed the essential sequence for N-myristoylation they showed mainly diffuse localisation patterns with some enrichment in a perinuclear region and in membrane ruffles. Despite the missing nuclear localisation due to the size difference the distribution of the constructs was comparable to that of the expressed soluble GFP control (Fig. 11A). To test the hypothesis that missing membrane association of the fragments was the reason for the lacking influence on CME, constructs with the N-myristoylation sequence of c-src (Maroun et al., 2003) inserted N-terminally of the GFP tag were cloned. This modification was sufficient to successfully target the constructs to membranous compartments and to the plasma membrane of the cells (Fig. 11B). Since N-myristoylation of GFP alone abolished its nuclear enrichment, the overlap between the distribution patterns of myristoylated GFP (Myr-GFP) and the myristoylated Bassoon constructs was even better than for the non-myristoylated fragments. In all cases, there was now a strong enrichment in a perinuclear membranous compartment potentially representing the TGN. The accumulation in membrane ruffles and in the tips of filopodia seemed slightly more prominent for the myristoylated Bassoon constructs than for Myr-GFP alone.

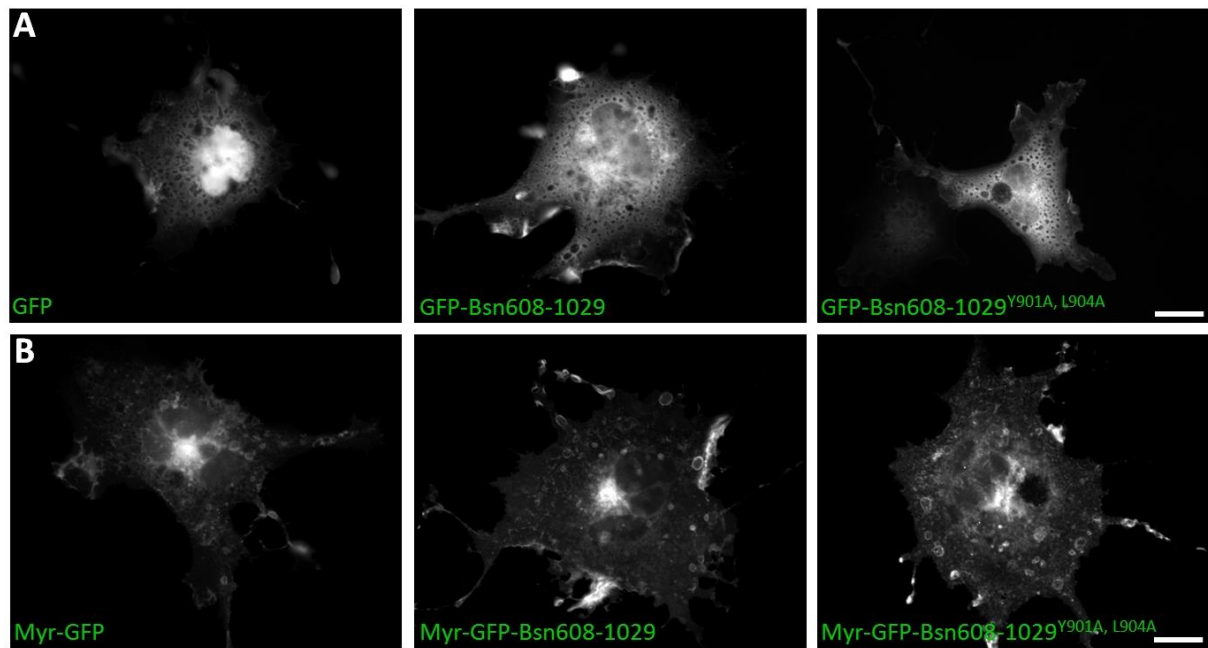


Fig. 11: Intracellular distribution patterns of the Bassoon constructs used for FACS analysis.

(A) Spatial expression patterns of GFP and the GFP-fused Bassoon fragments RB86 and RB174 in HEK293T cells. **(B)** Spatial expression patterns of the same constructs anchored to membranes by myristoylation. Scale bar is 10 μm .

Subsequently, the transferrin uptake experiment was repeated with the myristoylated constructs. It turned out, that also membrane association of the fragments did not have any effect on CME measured by the uptake of transferrin into the cells. The graph in Fig. 12 showing the flow cytometry results of the myristoylated proteins is therefore also representative for the results with non-myristoylated constructs used in the first instance. The four curves show relative fluorescence intensities of internalised transferrin from cells expressing constructs tagged with myristoylated GFP. The peaks of the red and blue curves representing wt and mutant Bassoon constructs, respectively, completely matched the peak of the Myr-GFP control in green in respect to transferrin intensities. This indicates that over-expression of Bassoon neither promotes nor inhibits CME of transferrin as compared to the GFP control, no matter whether it is able to bind to AP complexes or not. The functionality of the assay was confirmed by a clear shift of the purple curve towards lower fluorescence intensities. It demonstrated that inhibition of CME by the Dynamin inhibitor Dynasore was clearly detectable by the assay. Taken together, the data do not provide any evidence for an influence of the interaction of Bassoon with AP complexes on general CME.

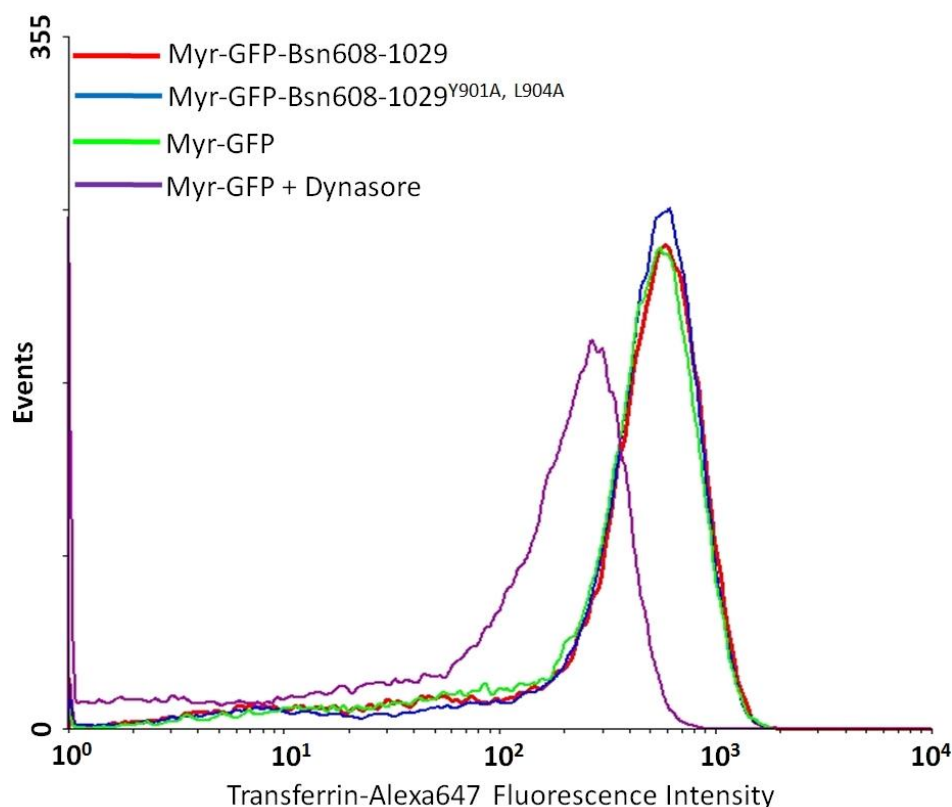


Fig. 12: Expression of Bassoon constructs does not influence CME of fluorescently labeled transferrin in HEK293T cells.

HEK293T cells were transfected with Myr-GFP, Myr-GFP-Bsn608-1029 or Myr-GFP-Bsn608-1029^{Y901A, L904A}. Cells were incubated with Alexa647-labeled transferrin. After the uptake, cells were cooled down to 4°. Residual extracellular transferrin was washed away and the endocytosed transferrin was quantified by measuring relative fluorescence intensities of the Alexa dye in the cells by flow cytometry. As positive control for successful inhibition of CME a batch of Myr-GFP transfected cells were treated with the Dynamin inhibitor Dynasore (100 μ M).

3.1.4 AP binding-deficient Bassoon can rescue KO-induced SV recycling phenotype

Recent unpublished data of our group showed significantly reduced synaptotagmin cycling in synapses of Bassoon KO mice (Claudia Marini and Carolina Montenegro). The assay by which this phenotype was detected is termed synaptotagmin uptake and is functionally very similar to the described transferrin uptake. To measure the uptake of synaptotagmin into neurons, the cells are supplied with fluorescently labeled antibodies directed against the luminal domain of synaptotagmin. The protein is localised specifically in the membrane of SVs and shuttles between the presynaptic plasma membrane and vesicular membranes with every exo-

endocytosis cycle. Quantification of fluorescence intensities after an internalisation period thus provides a measure of SV recycling and thereby indirectly indicates synaptic activity. The observed reduction of synaptotagmin uptake in Bassoon deficient neurons led to the conclusion of a reduced SV turnover and subsequently a presumed lower synaptic activity. This effect was rescued by expression of GFP-Bsn95-3938 (called GFP-Bsn in the following) partially restoring synaptotagmin uptake in transfected Neurons (Fig. 13). This construct is substantially larger than the fragments used in the previous experiments and comprises almost the complete Bassoon sequence. It is known to behave in many respects like wt Bassoon when expressed in primary neurons (Dresbach et al., 2003; Bresler et al., 2004; Dresbach et al., 2006; Tsuriel et al., 2009). While a disruption of presynaptic activity can have many causes, a disturbance of the SVC in exo- or endocytosis would probably produce such a synaptotagmin uptake phenotype.

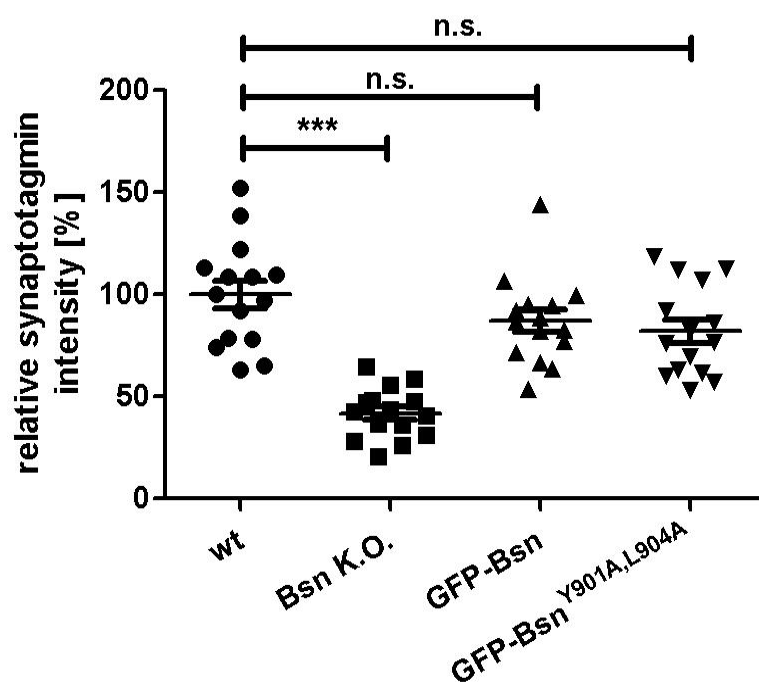


Fig. 13: AP binding-deficient Bassoon rescues Bassoon KO phenotype of reduced synaptotagmin uptake.

Synaptotagmin uptake of wt and Bassoon-deficient neurons and Bassoon-deficient neurons transfected with GFP-Bsn or GFP-Bsn^{Y901A,L904A} was measured and compared. Values are presented as % of average wt synaptotagmin intensity \pm SEM. Significance was determined via 1 way ANOVA test. *** means $P < 0,0001$. This experiment was conducted by Carolina Montenegro.

Since AP complexes are essential for the recycling of SVs and even interact with synaptotagmin (Haucke et al., 2000) the question arose if the interaction with Bassoon may play a role for the observed effect. Therefore it was investigated if diminished synaptotagmin uptake could also be rescued with the AP binding-deficient mutant of GFP-Bsn (GFP-Bsn^{Y901A, L904A}). In contrast to the hypothesis, expression of the AP binding-deficient Bassoon construct rescued the phenotype as efficiently as the wt (wt: $100 \pm 14,9$ %; Bsn KO: $41,8 \pm 7,1$ %; GFP-Bsn: $86,9 \pm 12,4$ %; GFP-Bsn^{Y901A, L904A}: $81,9 \pm 12,8$ %; in % of wt average \pm t; n = 3 experiments with 5 pictures each; P < 0,0001 determined by 1 way ANOVA). This demonstrated that the interaction of Bassoon with AP complexes seems not to be involved in diminished synaptotagmin uptake of Bassoon-deficient neurons (Fig. 13). The function of the interaction of Bassoon with AP2 therefore remains unclear.

3.2 Interaction of Bassoon with 14-3-3

The second adaptor protein investigated for a functional interaction with Bassoon was the η -isoform of the 14-3-3 protein family. While the function of AP complexes is restricted to sorting and trafficking processes of membrane proteins, the 14-3-3 family is known as highly multifunctional. This characteristic trait marked 14-3-3 as an interesting research subject, but also made it more complicated to develop a straight-forward working hypothesis. One of the major effects 14-3-3 interactions can have on other proteins is the regulation of their subcellular localisation. Since Bassoon is a protein strictly positioned at presynaptic boutons the major aim was to investigate whether 14-3-3 plays any role in the regulation of this defined allocation and the connected scaffolding characteristics.

3.2.1 Bassoon interacts directly with 14-3-3 proteins in a phosphorylation-dependent manner

Initial clues for an interaction of Bassoon with 14-3-3 proteins came from the previously mentioned Y2H screen of a rat brain cDNA library for Bassoon interaction partners. One clone interacting with the bait fragment Bsn28 covering aa residues 2715-3013 of rat Bassoon (Fig. 14A) contained the full coding sequence of 14-3-3 η . The consensus 14-3-3-interaction motifs were defined previously (Muslin et al., 1996; Yaffe et al., 1997; Wu et al., 2006) and could be identified using online accessible tools such as The Eukaryotic Linear Motif resource (ELM, (Puntervoll et al., 2003)). Aa residues 2842-2847 of rat Bassoon with the sequence RSLSDP form a putative interaction site for 14-3-3, which fits to the described classical mode 1 binding

motif (RSXpSXP) (Muslin et al., 1996). This sequence is highly conserved between all analysed Bassoon orthologues (Fig. 14B) suggesting a high evolutionary pressure for integrity of the 14-3-3 binding interface on Bassoon.

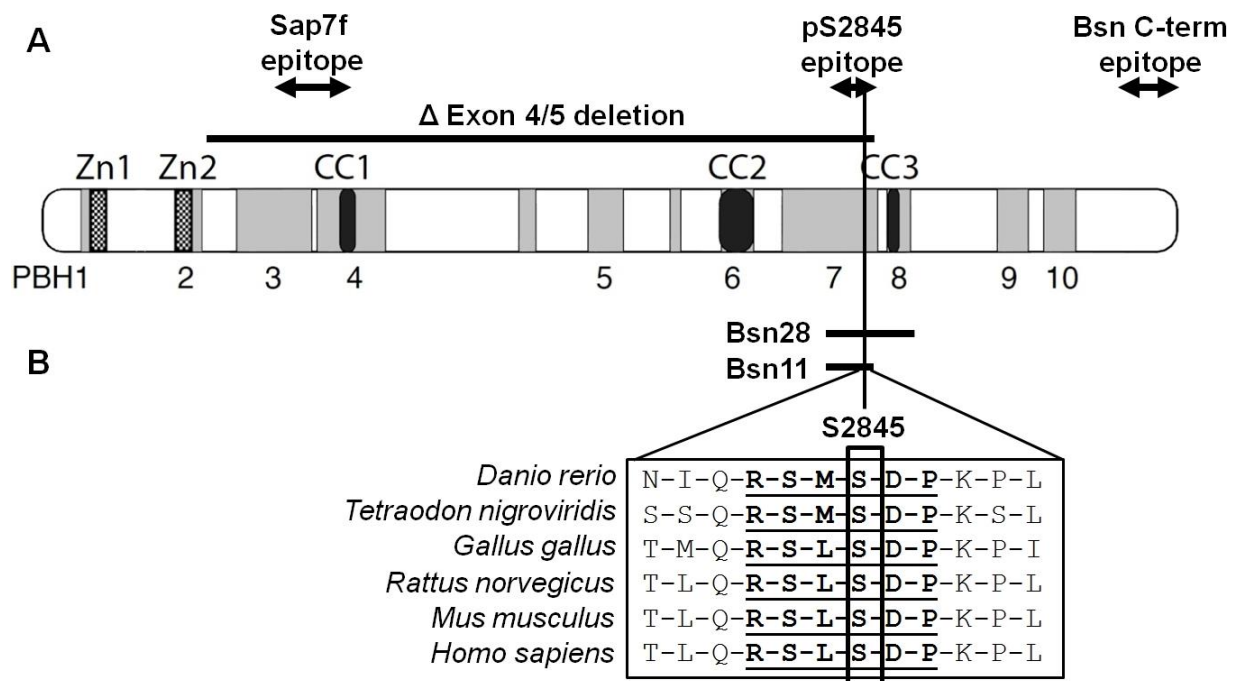


Fig. 14: Bassoon contains a 14-3-3 interaction interface.

(A) The domain structure of Bassoon with the position of the fragments Bsn28 and Bsn11 (horizontal bars) containing serine-2845 (vertical line) critical for 14-3-3 η interaction is presented (PBH 1-10: Bassoon/ Piccolo homology domains 1-10; Zn: Zinc finger domain; cc: coiled coil domain). The deletion of exons 4 and 5 in Bsn Δ Ex4/5 mutant mice and positions of epitopes of antibodies used in the study are depicted. **(B)** Alignment of the aa sequences of the region containing the 14-3-3 binding motif from Bassoon orthologues of different species. The RSM/LpSDP 14-3-3 binding motif is bold and the critical serine residue S2845 is boxed.

To confirm that this particular motif mediates an interaction of Bassoon with 14-3-3 η a series of pull-down experiments was performed. To this end, GST-tagged 14-3-3 η was expressed and affinity-purified from bacteria. The GFP-tagged Bassoon fragment Bsn28 (GFP-Bsn28) and its mutant (GFP-Bsn28^{S2845A}), in which the critical serine residue S2845 was changed to alanine, were expressed in HEK293T cells. The expression of the Bassoon fragments in mammalian model cells was chosen to allow the phosphorylation of the binding motif, which was previously reported to be a necessary prerequisite for 14-3-3 binding to almost all reported targets (Dougherty and Morrison, 2004). Purified GST-14-3-3 η , but not GST alone, successfully pulled down GFP-Bsn28 from the cell lysates. The mutated Bassoon fusion protein GFP-Bsn28^{S2845A} showed no binding to GST-14-3-3 η confirming that the intact S2845-containing motif is required for interaction of Bassoon with 14-3-3 η (Fig. 15A). To test whether phosphorylation of S2845 is necessary for the interaction with 14-3-3 η , lysates of HEK293T

cells expressing GFP-Bsn28 were prepared under two different conditions. First: without the addition of phosphatase inhibitors to destabilise the phosphorylated state of the expressed proteins. Second: with addition of alkaline phosphatase to dephosphorylate the proteins prior to the pull-down experiment. In both conditions the pull-down efficiency was almost completely diminished compared to the controls containing phosphatase inhibitors (Fig. 15B). Accordingly it was concluded that the interaction of 14-3-3 critically relies on the phosphorylation of S2845 of Bassoon, which is in line with the general phosphorylation dependency of 14-3-3 protein interactions. To mimic the phosphorylation of S2845 the residue was substituted by glutamate or aspartate. However, none of the phosphomimetic mutants was able to bind 14-3-3 η (Fig. 15A), which is in agreement with the previously described high selectivity of 14-3-3 to phosphoserine- or phosphothreonine-containing binding motifs (Johnson et al., 2010). In order to address the question, whether the physical interaction of Bassoon and 14-3-3 proteins is direct a blot-overlay assay was performed. For this goal, control and hyperphosphorylated brain extracts of adult wt and Bassoon-mutant mice (Bsn Δ Ex4/5; (Altrock et al., 2003) were separated by SDS-PAGE and transferred to PVDF membrane. In the Bsn Δ Ex4/5 mice the exons 4 and 5 of Bassoon coding for aa 505 to 2889 have been deleted. This deletion includes the identified 14-3-3 binding site in the residual Bassoon fragment. The immunodetection with specific Bassoon antibodies (α -Bsn C-term) revealed the expected bands of 420 kDa in the wt and of 180 kDa in the Bsn Δ Ex4/5 brain extracts (Fig. 15C). Application of the hyperphosphorylation protocol led to a shift of the Bassoon bands to higher molecular weights suggesting a change in the charge and conformation of Bassoon due to increased phosphorylation. Further blot membranes prepared in parallel were incubated with purified recombinant GST or a GST-14-3-3 η fusion protein. Immunodetection by α -GST antibodies showed the binding of GST-14-3-3 η at the exact location of the Bassoon band in lysates from wt animals, but not in lysates from Bsn Δ Ex4/5 mice indicating the interaction of 14-3-3 with full length Bassoon (Fig. 15C). The interaction was specific for 14-3-3 η since GST alone did not bind to proteins immobilised on the blot membrane. Due to the denaturing conditions and the separation of the brain extracts by SDS-PAGE the binding could not involve any other proteins and was therefore direct. At this point it should be mentioned, that the overlay experiment was only successful when hyperphosphorylated brain extracts were used, which suggested a low abundance or a short lifetime of phosphorylated S2845 of Bassoon in the adult mouse brain.

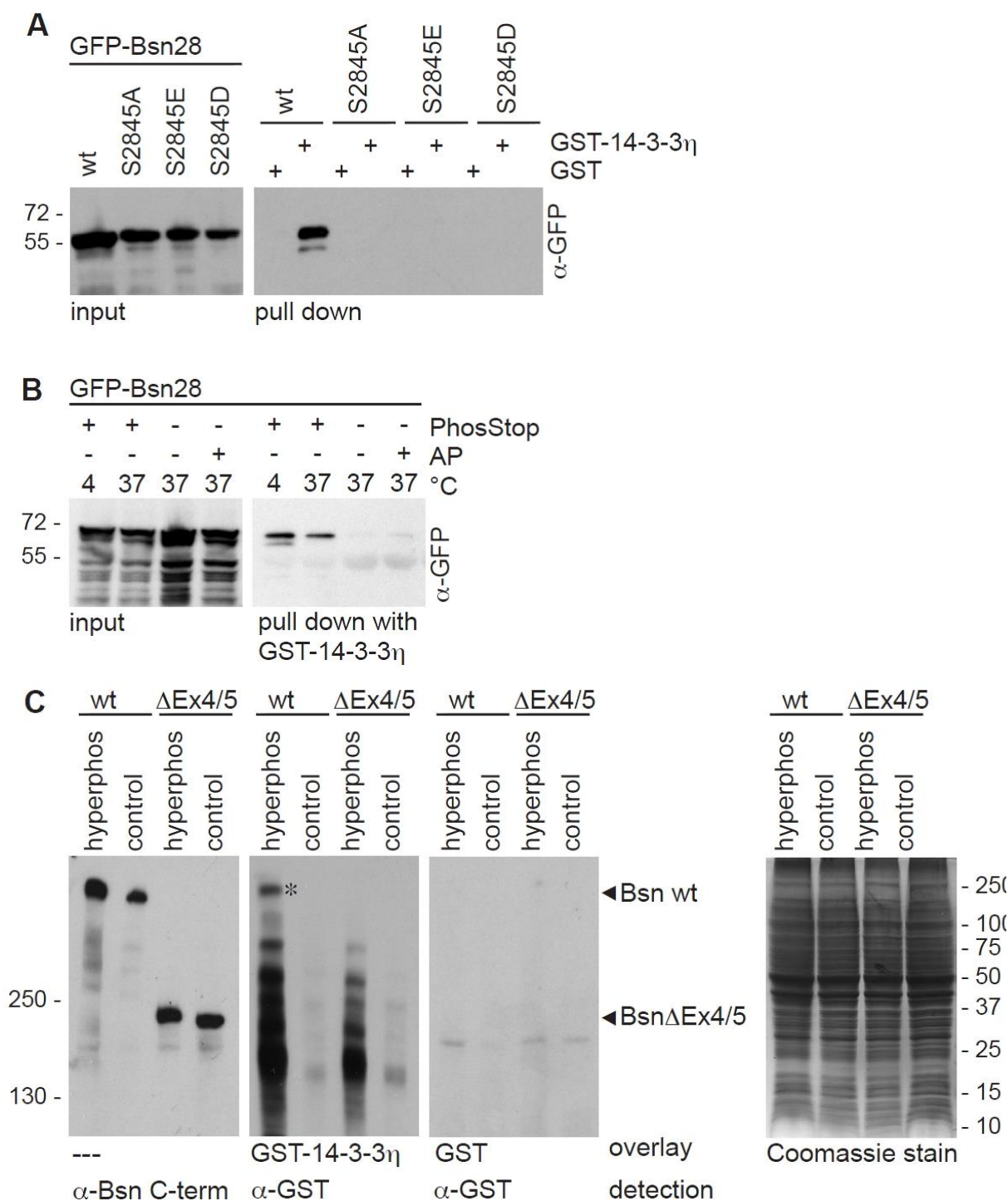


Fig. 15: Direct binding of Bassoon to 14-3-3 depends on phosphorylation of Serine-2845.

(A) GFP-Bsn28 wt and its variants containing mutation in the critical S2845 residue (S2845A, S2845E, S2845D) were expressed in HEK293T cells and employed for pull-down experiments with bacterially expressed and purified GST-14-3-3 η or GST as a control. Detection of GFP-tagged proteins in the cell lysates (input) and the bound fractions (pull down) was performed using α -GFP antibody. GFP-Bsn28 was successfully co-precipitated by GST-14-3-3 η , but not with GST. All tested mutations interfered with the binding. **(B)** Cell lysates from HEK293T cells expressing GFP-Bsn28 without any additives or supplemented with phosphatase inhibitors (PhosStop) or alkaline phosphatase (AP) and incubated at 4° or 37° C were used for pull-down experiments with immobilised GST-14-3-3 η . GFP-Bsn28 was detected in cell lysates (input) and the bound fractions (pull down)

using α -GFP antibodies. **(C)** Hyperphosphorylated and control P2 fractions from brains of wt and Bassoon-mutant mice (Bsn Δ Ex4/5) were separated by SDS-PAGE. Equal amounts of protein in each sample was controlled by Coomassie Blue staining for all proteins (right panel). Immunodetection with α -Bsn C-term antibodies revealed the immunoreactivity of wt Bassoon (420 kD) and the mutant Bassoon Δ Ex4/5 residual protein (180 kD). Purified GST-14-3-3 η or GST fusion proteins were used for the overlay and detected by α -GST antibody. Note the presence of the band (marked by asterisk) corresponding to Bassoon in lysates from wt but not from Bsn Δ Ex4/5 mice showing binding of GST-14-3-3 η , but not GST alone. Bars and number on the left side of the blots and on the right side of the Coomassie-stained gel show sizes and positions of molecular weight markers. These experiments were conducted by Anne Stellmacher.

3.2.2 14-3-3 interacts with Bassoon in mammalian cells

Similar as for the AP interaction, the next step was to support the assumption of a physiological relevance of the 14-3-3 binding to Bassoon. Therefore it was checked if the interaction observed in the model organism yeast can also occur in mammalian cells. For this reason the results from the Y2H system, the interaction and also the disruption of the interaction by mutation of the binding site, were tested in several independent mammalian experimental systems.

3.2.2.1 Co-IP and co-recruitment of 14-3-3 by Bassoon in HEK293T cells

Biochemically the results from the Y2H assay were supported by co-immunoprecipitation experiments of endogenous 14-3-3 from lysates of HEK293T cells transfected with GFP-Bsn28 (Fig. 16A). For this purpose the expressed Bassoon fragments were immunoprecipitated from the cell lysates by antibodies against the GFP tag. Detection of the subsequently produced Western blots with α -14-3-3 η antibodies showed a successful co-immunoprecipitation of the η isoform by GFP-Bsn28. The α -pan 14-3-3 antibodies even detected two distinct bands. The less prominent upper band represents the slightly larger 14-3-3 ϵ isoform, while the other isoforms run together at the height of the more prominent lower band (Isobe et al., 1991). At the same time the mutated GFP-Bsn28^{S2845A} was not able to co-precipitate any 14-3-3.

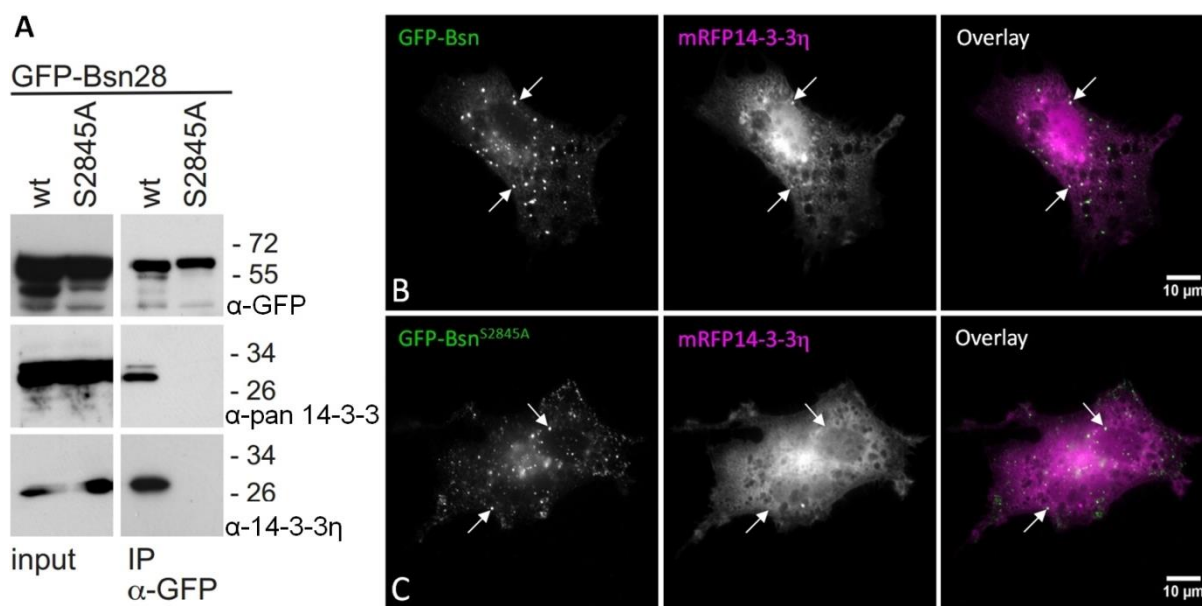


Fig. 16: Bassoon interacts with 14-3-3 in HEK293T cells.

(A) GFP-Bsn28 wt or its mutant GFP-Bsn28^{S2845A} were expressed in HEK293T cells and cell lysates were used for immunoprecipitations with α -GFP antibody. Successful expression of GFP-tagged proteins was shown in cell lysates (input) and bound fraction (IP) using α -GFP antibody. The endogenously expressed 14-3-3 proteins were co-precipitated with GFP-Bsn28 but not with its mutant Bsn28^{S2845A} as demonstrated by detection with α -pan 14-3-3 and α -14-3-3 η antibody. Note two bands detected in the bound fractions using α -pan 14-3-3 antibody suggesting immunoprecipitation of multiple 14-3-3 isoforms. The bars and number on the left side of blots show the sizes and positions of molecular weight markers. This experiment was conducted by Anne Stellmacher. **(B, C)** HEK293T cells were transfected with GFP-Bsn or GFP-Bsn^{S2845A} and mRFP-14-3-3 η . Clusters formed by GFP-Bsn (arrows in B) but not clusters formed by the corresponding 14-3-3 binding mutant GFP-Bsn^{S2845A} (arrows in C) recruited mRFP-14-3-3 η .

The additional information gathered by this experiment was, that the expressed Bassoon fragment GFP-Bsn28 could interact not only with over-expressed and mRFP-tagged 14-3-3, but also with a set of endogenous 14-3-3 isoforms. Additionally to the Co-IP an intracellular co-recruitment experiment was performed in HEK293T cells. To this end cells were co-transfected with mRFP-14-3-3 η and the substantially larger GFP-Bsn construct, which only misses the first 95 aa residues of the Bassoon sequence. A corresponding 14-3-3 binding-deficient Bassoon construct (GFP-Bsn^{S2845A}) was created by introduction of the same point mutation, which disrupted the 14-3-3 interaction in all previous experiments. Expression of both constructs led to the formation of cytoplasmatic Bassoon clusters in the cells. In line with the results from a mito-targeting assay performed in parallel (Schroder et al., 2013), co-expressed mRFP-14-3-3 η was only recruited to clusters formed by GFP-Bsn, but not to those formed by GFP-Bsn^{S2845A} (Fig. 16B, C). Since the GFP-Bsn^{S2845A} construct did not recruit 14-3-3 η and no 14-3-3 binding motif was predicted in the first 95 aa of Bassoon this result

demonstrated that the described binding motif containing S2845 represents the only interaction interface for 14-3-3 in Bassoon.

3.2.2.2 Bassoon recruits 14-3-3 in hippocampal neurons

After the basic characteristics of the interaction were assessed, the next important aim was to certify that the gathered information also applies to the behaviour of the proteins in neurons. For this reason the co-recruitment experiment with the large Bassoon constructs was repeated in primary hippocampal neurons. The neurons were co-transfected with mRFP-14-3-3 η and GFP-Bsn or GFP-Bsn^{S2845A}. In accordance with previous observations, both GFP-fusion proteins were located at synapses in a similar way as the endogenous Bassoon protein (Fig. 17A, B; see also Fig. 21). In addition, GFP-Bsn and GFP-Bsn^{S2845A} were located in ectopic cytoplasmic clusters formed by mis-targeted over-expressed protein in the transfected neurons as it was shown before (Dresbach et al., 2003; Fejtova et al., 2009). Co-transfected mRFP-14-3-3 η could be found at synapses when co-expressed with both GFP-Bsn and its S2845A mutant. This was most likely due to interactions with its multiple synaptic binding partners (1.4.2.) Interestingly, and confirming the data from HEK293T cells, mRFP-14-3-3 η was recruited to ectopic cytoplasmic clusters only in cells expressing GFP-Bsn but showed a diffuse cytoplasmic localisation when co-expressed with GFP-Bsn^{S2845A}.

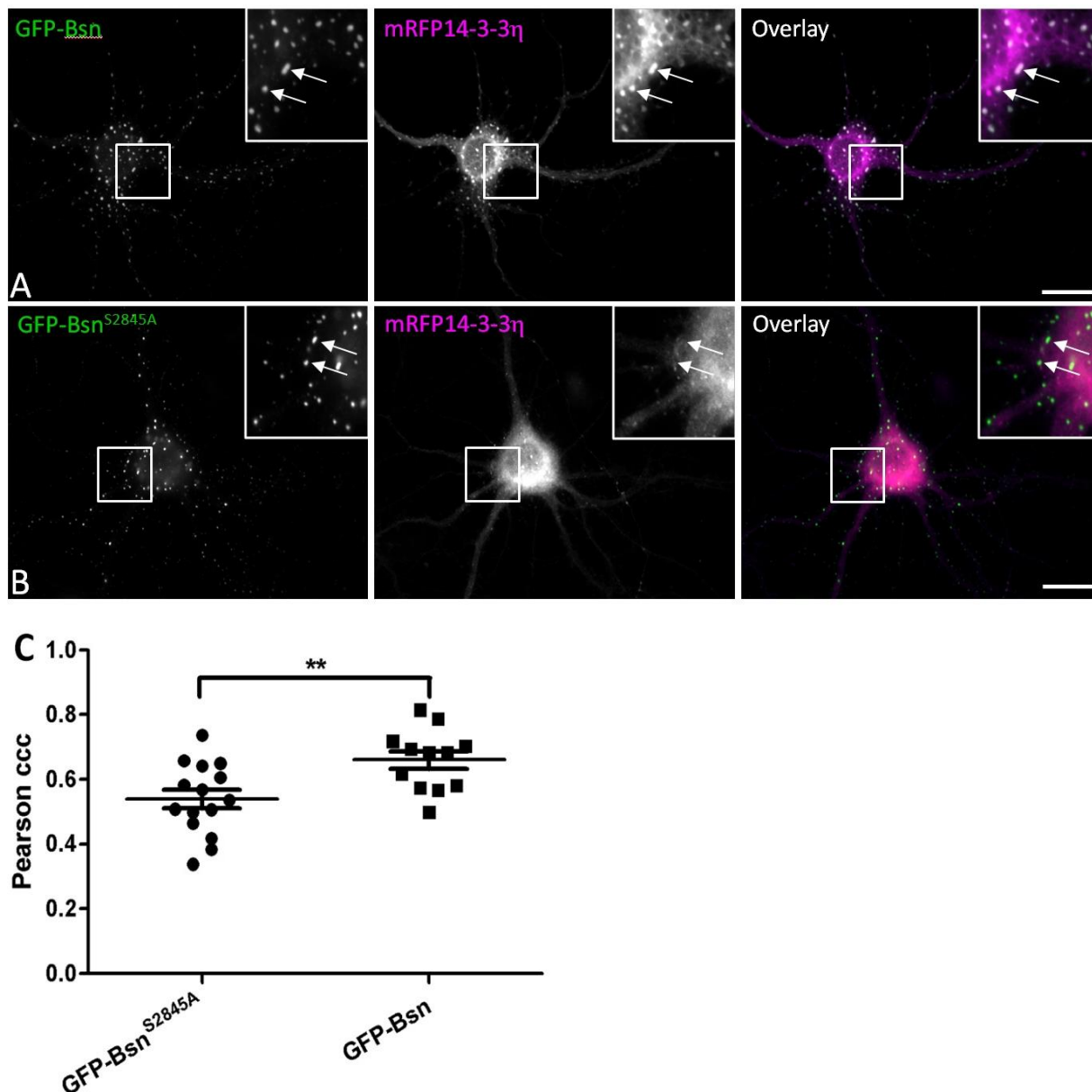


Fig. 17: Bassoon recruits 14-3-3 in neurons.

Primary hippocampal neurons were transfected with GFP-Bsn or GFP-Bsn^{S2845A} and mRFP-14-3-3 η . Clusters formed by GFP-Bsn (arrows in **A**) but not clusters formed by the corresponding 14-3-3 binding mutant GFP-Bsn^{S2845A} (arrows in **B**) recruited mRFP-14-3-3 η . (**C**) Pearson's cross correlation coefficient was calculated to quantify the co-localisation with mRFP-14-3-3 η and was significantly higher for GFP-Bsn than for GFP-Bsn^{S2845A}. Scale bar is 20 μ m. ** means $P < 0,01$.

The degree of co-recruitment was quantified by calculation of the Pearson's correlation coefficient (Li et al., 2004) for mRFP and GFP fluorescence in double transfected cells (Fig. 17C). The correlation coefficient was significantly higher for mRFP-14-3-3 η expressed with GFP-Bsn than for GFP-Bsn^{S2845A} ($0,66 \pm 0,03$ vs. $0,54 \pm 0,03$; mean \pm SEM; $n = 15$ vs. 12 cells; $P < 0,01$; unpaired t-test). This demonstrated that Bassoon could sequester 14-3-3 η also in neurons and that the recruitment was crucially dependent on presence of S2845 in Bassoon.

3.2.3 Generation of a phosphorylation-specific antibody for pS2845 of Bassoon

In order to analyse the phosphorylation state of S2845 of Bassoon, which is critical for its interaction with 14-3-3, a phosphorylation-specific antibody (further named α -pS2845 Bsn) was generated. To testify the specificity of the antibody for the epitope and its phosphorylation, the same Bassoon fragments already used for the pull-down assays were employed. The wt and the S2845A-mutated version of GFP-Bsn28 were expressed in HEK293T cells and precipitated from the cell lysates by α -GFP antibodies. To control phospho-specificity of α -pS2845 Bsn the wt sample was divided in two. One half was treated with alkaline phosphatase for the purpose of general dephosphorylation, while the other half and the mutant sample were treated with phosphatase inhibitors to preserve the phosphorylation status. Western blots of the precipitates were then analysed with α -pS2845 Bassoon (Fig. 18A). The results showed that mutation of the critical serine residue of the motif disrupted the detection of the constructs by α -pS2845 Bsn. Furthermore the dephosphorylation of fragments by alkaline phosphatase, as controlled by an antibody generally recognising phospho-serine or -threonine residues had the same effect. Therefore the antibody was considered capable of distinguishing between intact or mutated as well as phosphorylated or dephosphorylated epitope. To check the specificity of the antibody for Bassoon in brain samples, it was then tested on brain extracts (membrane enriched P2 fractions) from wt and Bsn Δ Ex4/5 mutant mice. The α -pS2845 Bsn antibody reliably recognised a band with a molecular weight of ~450 kDa corresponding to Bassoon in hyperphosphorylated extracts from wt mice. In contrast, no corresponding immunoreactivity was observed in the extracts from mutant mice, confirming the specificity of this antibody for Bassoon (Fig. 18B). Still, as can be seen on the blot, Bassoon represented the major but not the only substrate that was detected by α -pS2845 Bsn in this assay. Additionally, at this point the phosphorylation of S2845 was not detectable under control conditions in the wt samples although P2 fractions were treated with phosphatase inhibitors to preserve phosphorylation. Both points may indicate reasons why the antibody was not suited for the use in immunocytochemistry staining experiments.

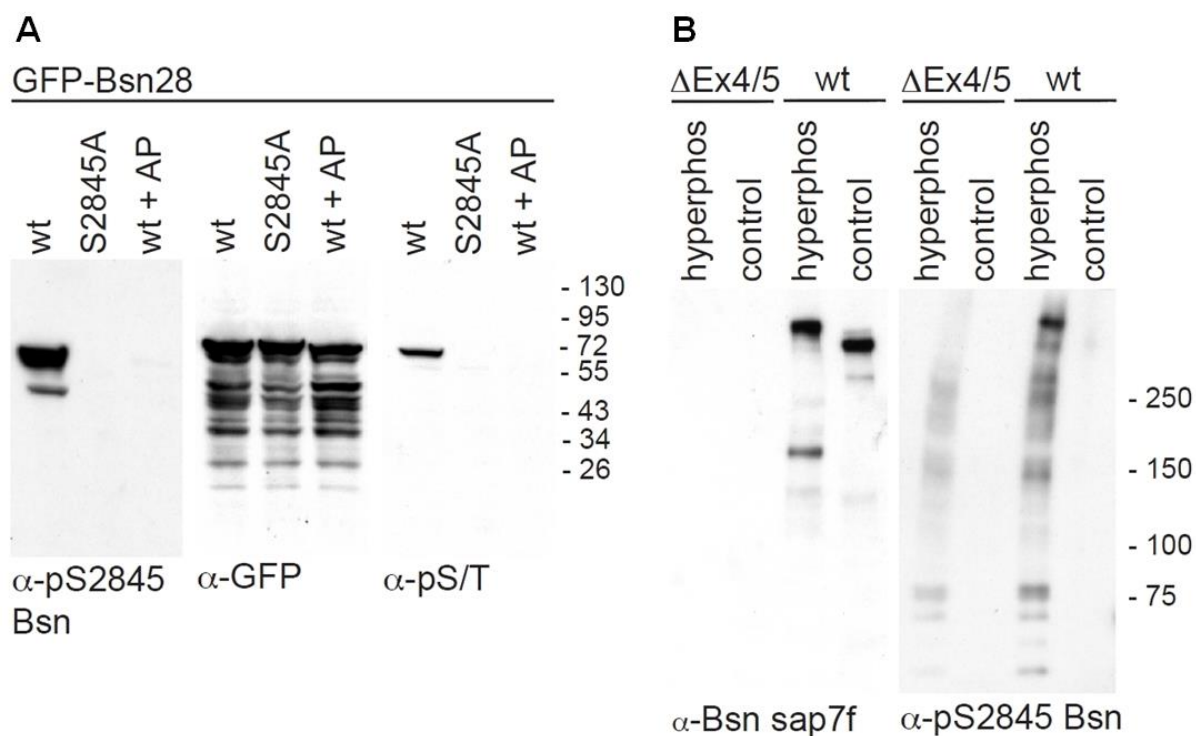


Fig. 18: Characterisation of the antibody against phosphorylated S2845 of Bassoon.

(A) GFP-Bsn28 (wt) or its mutant (S2845A) were expressed in HEK293T cells. The cell lysates were either treated with phosphatase inhibitors to prevent dephosphorylation or the alkaline phosphatase (AP) was added to reduce phosphorylation of the proteins. Comparable expression of all constructs was demonstrated by the α -GFP staining. Immunodetection using α -pS/T antibodies revealed that GFP-Bsn28 but not S2845A mutant is phosphorylated under the tested conditions. α -pS2845 Bsn recognised only phosphorylated GFP-Bsn28 but not the S2845A mutant or the dephosphorylated GFP-Bsn28 in samples treated with AP. Images shown are representative for one of at least three independent experiments. The bars and number on the left side of blots show the sizes and positions of molecular weight markers. **(B)** α -pS2845 Bsn antibody was tested on P2 fractions from brains of wt and Bassoon mutant (Bsn Δ Ex4/5) mice. Bassoon was detected by α -Bsn sap7f antibody in the samples from wt mice but not from mutant. The Western blot, which was prepared in parallel and incubated with the phosphorylation-specific antibody α -pS2845 Bsn preferentially detects Bassoon in the hyperphosphorylated sample and showed only weak unspecific immunoreactivity in the samples of the Bassoon-mutant mice. These experiments and the corresponding figure are the work of Anne Stellmacher.

3.2.4 The 14-3-3 binding site on Bassoon can be phosphorylated by RSK kinases

The phosphospecific antibody represented an ideal tool for the identification of the protein kinases driving the modification. To gather information about the responsible kinase was the next aim on the way to understand the physiological context in which the phosphorylation of Bassoon on S2845 occurs. Addressing this point, in silico predictions by the online services NetPhosK (Blom et al., 2004) and MnM 3.0 (Balla et al., 2006) were applied, which both

pointed towards a possible phosphorylation by kinases of the RSK family. Since detection of pS2845 under untreated control conditions failed in the previous experiment, it was further tested if the miss of detection was due to a lack of sensitivity of the detection method. Therefore Western blot immunodetection was optimised by switching from X-ray films to a CCD camera-based imaging system and the use of a high sensitivity ECL solution for blot development. The predictions were subsequently tested by using the RSK inhibitor BI-D1870 (100 nM) on hippocampal cultures (DIV 14) of wt and Bsn KO mice. Hyperphosphorylation was induced by addition of 50 nM okadaic acid to the culture medium with or without BI-D1870 pretreatment. At this concentration okadaic acid mainly affects protein phosphatase PP2A (Ishihara et al., 1989). In contrast to the previously used Bsn Δ Ex4/5 mice, the mouse line used in this experiment is a gene trap line displaying a complete Bassoon deficiency (Bsn^{gt}) (Frank et al., 2010; Hallermann et al., 2010).

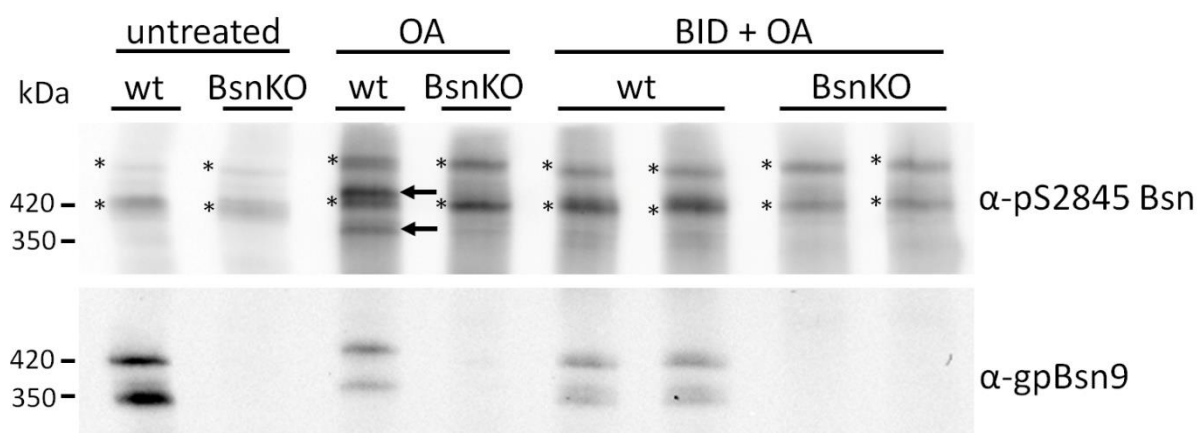


Fig. 19: RSK inhibition prevents Okadaic acid induced phosphorylation of S2845 of Bassoon.

Cultured cortical neurons (DIV14) prepared from wt and Bassoon KO mice were treated with 50 nM okadaic acid for 30 min at 37° C (lanes OA) or preincubated for 15 min with RSK inhibitor 100 nM BI-D1870 before addition of okadaic acid. Cells were harvested and lysates were analysed by immunoblotting. The cross-reactive bands recognised by α -pS2845 Bsn are marked by asterisks, the specific bands for Bassoon (missing in lysates from Bsn KO neurons) are marked by arrows. Note that BI-D1870 treatment interferes with OA-induced phosphorylation of specific Bassoon band in wt lysates. The lower panel shows general Bassoon immunoreactivity of the samples with missing bands in the KO lanes.

With optimised detection conditions the α -pS2845 Bsn antibody indeed revealed a band of the expected 420 kDa even without prior hyperphosphorylation. Unfortunately under these circumstances several additional bands were present in the same size range as well (Fig. 19). Due to these unspecific bands it was not possible to reliably distinguish between the weak signal detected by α -pS2845 Bsn in the untreated wt and KO control samples despite the achieved

improvement of signal strength. Nevertheless the induction of increased phosphorylation levels by OA reproducibly led to the appearance of two bands that could not be identified in the KO samples and therefore must be Bassoon-specific (Fig. 20). Interestingly pretreatment of the cultures with BI-D1870 almost completely inhibited the appearance of these OA-induced Bassoon-specific bands. At the same time the RSK inhibitor had only a mild effect on the intensity of the unspecific bands (Fig. 19). Although this experiment could not reveal if the observed effect was mediated by a direct or an indirect mechanism it clearly showed that RSK family members are necessary for the OA induced phosphorylation of the 14-3-3 binding motif on Bassoon.

To address the question if RSKs can directly phosphorylate Bassoon an *in vitro* phosphorylation experiment was conducted. By this it should be clarified if the mere presence of RSKs is also generally sufficient to induce a direct phosphorylation of the 14-3-3 binding motif. For the experiment a bacterially expressed and affinity-purified His-tagged fusion protein of the Bassoon fragment Bsn11 (His-Bsn11, aa residues 2714-2867, Fig. 14), which included the 14-3-3 binding interface was incubated with commercially available activated RSKs 1, 2, 3 and 4 in the presence of ATP and Mg^{2+} (Fig. 20). Successful phosphorylation of Bassoon S2845 was monitored by immunodetection with the α -pS2845 Bsn antibody. The degree of S2845 phosphorylation increased with the amounts of added kinases, confirming the specificity of the phosphorylation reaction. All tested RSKs directly phosphorylated the Bassoon fragment even at the lowest tested concentration. However, RSK1 and RSK3 were more efficient than RSK2 and RSK4. Both of the conducted experiments confirmed the *in silico* predictions. The first experiment demonstrated that at least under the condition of phosphatase inhibition, kinases from the RSK family are necessary for the phosphorylation of the 14-3-3 binding motif of Bassoon in cultured hippocampal neurons. The second experiment further showed that any member of the RSK family is sufficient to directly phosphorylate Bassoon at the given site in an isolated system. Thus, RSKs appear to be good candidates to control the molecular switch regulating the interaction of Bassoon with 14-3-3.

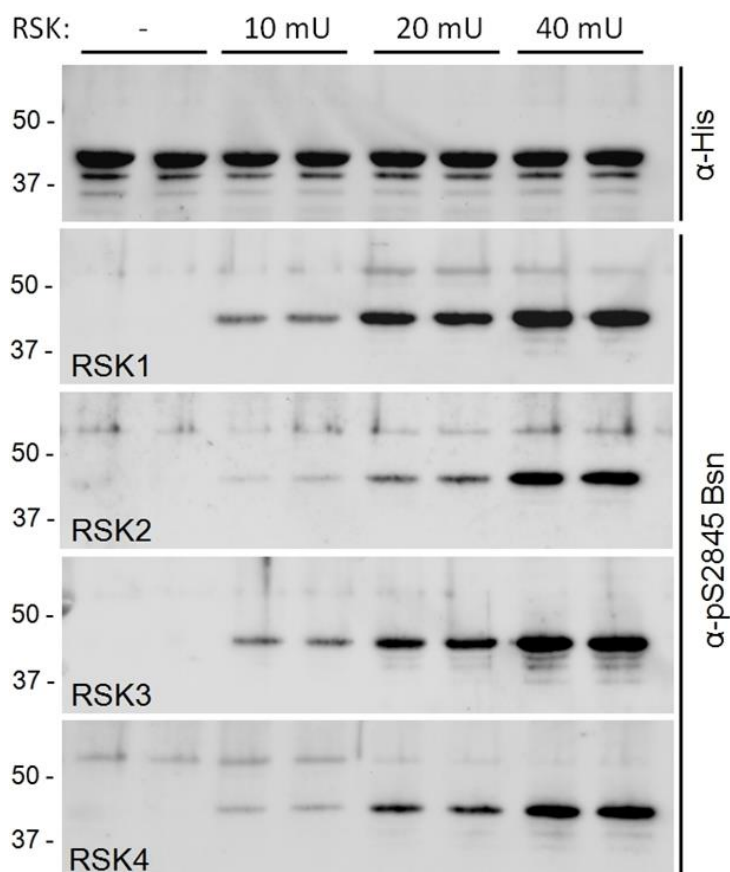


Fig. 20: Protein kinases of the RSK family phosphorylate Bassoon S2845 in vitro.

Bacterially expressed, affinity-purified His-Bsn11 was phosphorylated in vitro by RSK 1, 2, 3 and 4 using ascending amounts (10-40 mU) of active purified kinase. Equal loading of His-Bsn11 in the assay was controlled by immunodetection using α -His in all samples. Phosphorylation of His-Bsn11 was monitored by immunodetection with α -pS2845 Bsn, which revealed increasing phosphorylation depending on the increasing concentrations of kinases. Bars and numbers on the left side of the blots show the sizes and positions of the molecular markers.

3.2.5 Mutation of the 14-3-3 binding site influences molecular dynamics of synaptic Bassoon.

After gathering information about the basic binding characteristics and the regulation of the interaction the most eminent unanswered question that remained was, which physiological function the binding of 14-3-3 to Bassoon could have? It was described in several instances that 14-3-3 induced a spatial redistribution of its binding partners (Dougherty and Morrison, 2004).

Therefore it was next investigated whether the disruption of the interaction may influence the general cellular distribution of Bassoon. For this purpose it was first checked whether the synaptic localisation pattern was altered. GFP-Bsn and its 14-3-3 binding mutant (GFP-Bsn^{S2845A}) were again expressed in cultured hippocampal neurons.

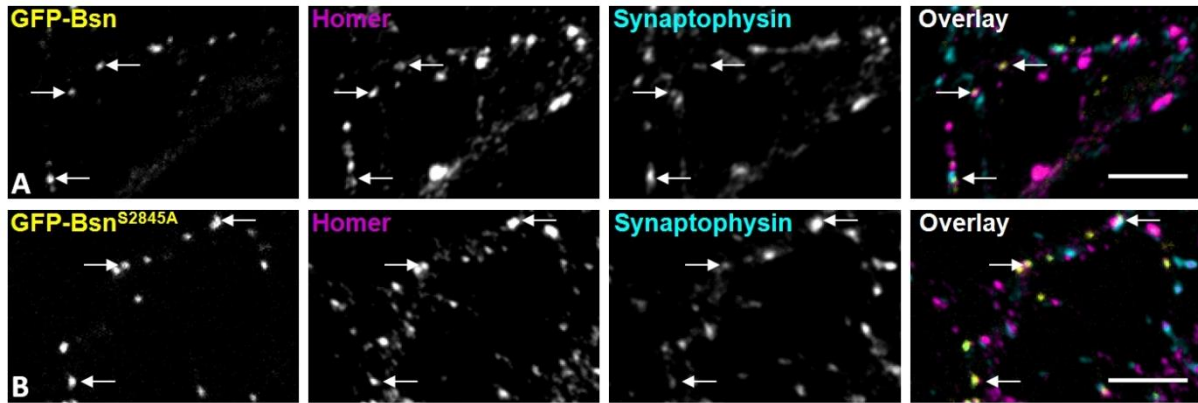


Fig. 21: Co-localisation of GFP-Bsn and GFP-Bsn^{S2845A} with synaptic markers.

Primary hippocampal neurons were transfected with GFP-Bsn (**A**) or GFP-Bsn^{S2845A} (**B**) at DIV3 and analysed at DIV 14-16. Synaptic targeting of both constructs was assessed by co-staining with synaptic markers homer and synaptophysin. The arrows highlight synapses of transfected cells stained for both markers. Scale bar is 20 μ m.

By eye the distribution patterns of expressed wt and mutant constructs could not be distinguished. The degree of synaptic localisation was therefore determined by co-staining of the transfected cells with the two synaptic marker proteins Homer and Synaptophysin (Fig. 21). Co-localisation of the expressed constructs with the synaptic markers was then measured using the software OpenView (Tsurriel et al., 2006). Quantification of the signal overlap in all three channels revealed no significant difference between wt and mutant Bassoon ($86,96 \pm 4,1$ % for GFP-Bsn vs. $88,16 \pm 1,9$ % for GFP-Bsn^{S2845A}; mean \pm SEM; N = 6; P = 0,7977; unpaired t-test) confirming the comparability of their distributions.

Since the static localisation characteristics were not influenced by mutation of the 14-3-3 binding site, the next step was to test whether the interaction influences the dynamic properties of Bassoon. To achieve this goal fluorescence recovery after photobleaching (FRAP) of GFP-Bsn and GFP-Bsn^{S2845A} was measured (Fig. 22). The long half-life and the tight anchoring of Bassoon to the presynaptic active zone (tom Dieck et al., 1998; Phillips et al., 2001; Altrock et al., 2003) led to relatively low fluorescence recovery rates (16 % of initial intensity within 5 min after bleaching for GFP-Bsn), which is in agreement with previously published data (Tsurriel et al., 2009). Our analyses showed that mutation of the 14-3-3 binding site even further

decreased Bassoon recovery significantly by about 20 % compared to wt (Fig. 22B; GFP-Bsn vs. GFP-Bsn^{S2845A}: 100 ± 6 % vs. 79 ± 6 %, mean \pm SEM after 300 s of recovery; normalised to GFP-Bsn, N = 43 vs. 30 videos; P = 0,0136; unpaired t-test).

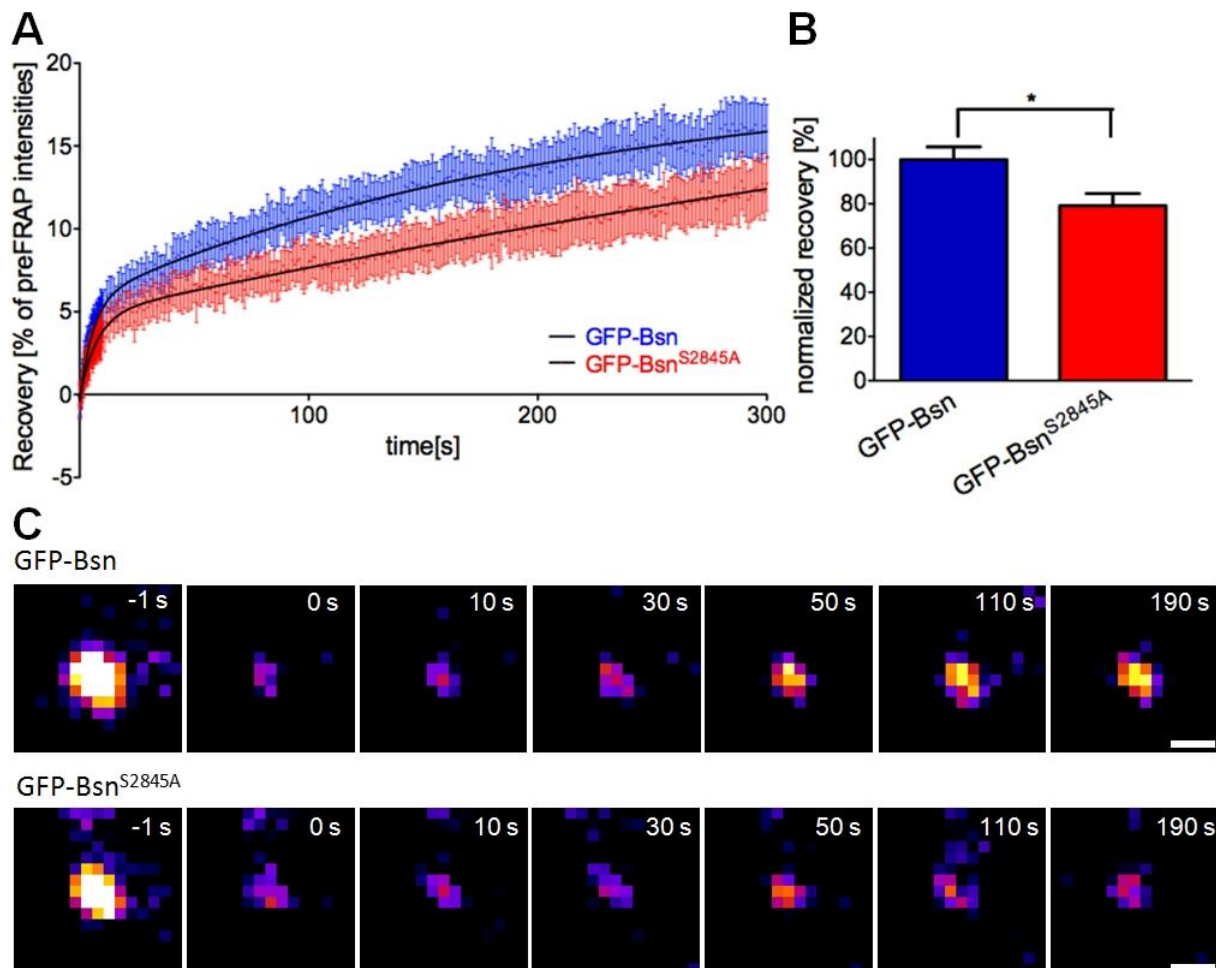


Fig. 22: Analysis of molecular dynamics of GFP-Bsn and GFP-BsnS2845A by FRAP.

Primary hippocampal neurons were transfected with GFP-Bsn or GFP-Bsn^{S2845A} at DIV3 and used for FRAP analysis at DIV 14-16. **(A)** Curves show averaged fluorescence recovery of all analysed puncta plotted as actual spot intensity relative to pre-bleaching intensity. The whiskers show SEM for each value. GFP-Bsn (wt) shows a higher recovery rate compared to GFP-Bsn^{S2845A}. Recovery was significantly lowered for GFP-Bsn^{S2845A} 300 s after photobleaching. **(B)** Columns represent mean value normalised to GFP-Bsn recovery after 300 s of recovery. Whiskers SEM, * indicates P<0.05. All values were obtained from 4 independent imaging sessions. **(C)** Representative example image showing bleaching and recovery of GFP-Bsn and GFP-Bsn^{S2845A} puncta. Scale bar is 1 μ m.

Because variations in recovery rates could theoretically also be caused by differences in the expression levels of the constructs it was necessary to test this possibility. Therefore a quantitative analysis of the fluorescence intensities of GFP-Bsn and GFP-Bsn^{S2845A} puncta was carried out. Additionally the numbers of stationary and moving GFP-positive puncta were counted during a time period of 25 s (100 frames) of the FRAP videos. Comparison between

wt and mutant numbers should reveal if the difference in recovery could be explained by a deviation in the relative amount of moving transport vesicles.

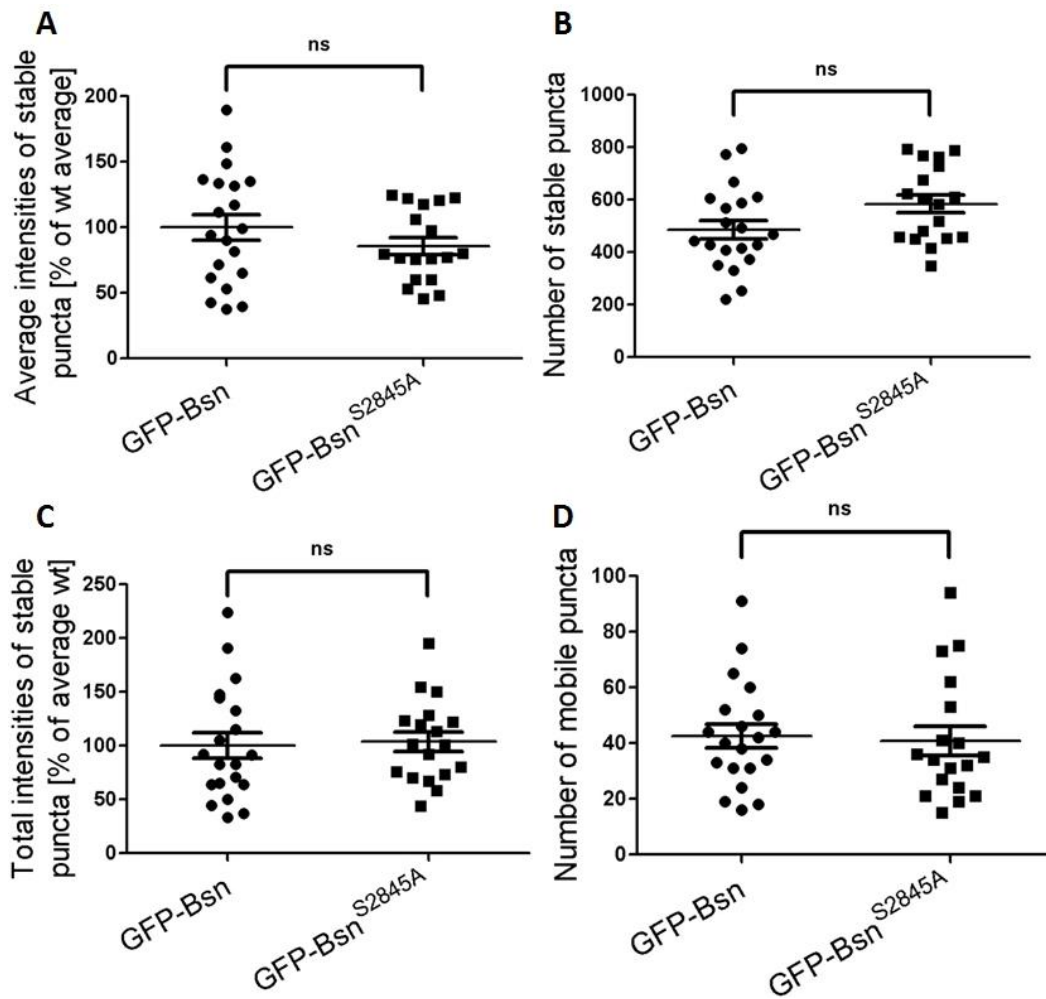


Fig. 23: Expression analysis of GFP-Bsn and GFP-BsnS2845A in the FRAP videos.

Quantification of the expression levels of GFP-Bsn and GFP-Bsn^{S2845A} in the FRAP videos was done by **(A)** measuring the average relative intensities of stable GFP-positive puncta per video, **(B)** counting the number of stable GFP positive puncta per video and **(C)** calculating the total relative intensities of stable GFP-positive puncta per video. **(D)** Additionally the number of mobile GFP-positive puncta was counted. None of the examined parameters differed significantly between wt and mutated Bassoon. Values were obtained from four independent imaging sessions.

Regarding expression levels of the constructs there was a slight but not significant tendency towards lower intensities of stable GFP-Bsn^{S2845A} puncta compared with the wt (Fig. 23A; GFP-Bsn vs. GFP-Bsn^{S2845A}: $100 \pm 9,8$ % vs. $86 \pm 6,5$ %, mean \pm SEM; normalised to GFP-Bsn, N = 20 vs. 18 videos; P = 0,2412; unpaired t-test). Counting of the puncta revealed a notable but also not significant tendency towards a higher number of stable GFP-Bsn^{S2845A} spots. (Fig. 23B; GFP-Bsn vs. GFP-Bsn^{S2845A}: $486 \pm 34,7$ vs. $584 \pm 33,8$ stable puncta; mean \pm SEM; N = 20 vs. 18 videos; P = 0,0529; unpaired t-test). Finally multiplication of the calculated intensities

and numbers yielded the total fluorescence intensity of all stable puncta in each video. For this parameter GFP-Bsn and GFP-Bsn^{S2845A} showed a strong comparability (Fig. 23C; GFP-Bsn vs. GFP-Bsn^{S2845A}: $100 \pm 11,8$ % vs. $104 \pm 9,1$ %; mean \pm SEM; percent of wt average; N = 20 vs. 18 videos; P = 0,8045; unpaired t-test) indicating a similar level of total expression. In accordance with this the numbers of mobile puncta per video also did not differ significantly between the constructs (Fig. 23D; GFP-Bsn vs. GFP-Bsn^{S2845A}: $43 \pm 4,3$ vs. $41 \pm 5,2$; mean \pm SEM; N = 20 vs. 18 videos; P = 0,7807; unpaired t-test). The relative percentage of immobile GFP-Bsn spots was calculated from the total numbers of stable and mobile puncta and, in line with the previous data, confirmed the comparability of GFP-Bsn and GFP-Bsn^{S2845A} ($92 \pm 0,6$ % vs. $93 \pm 0,7$ of total puncta; N = 20 vs. 18 videos; P = 0,1020; unpaired t-test). These results led to the conclusion, that the reduction of FRAP recovery rates by the mutation of the 14-3-3 binding site on Bassoon was not due to differences in the expression levels or the number of moving Bassoon packages.

To check whether the decrease in recovery could be instead mediated by a defect in the supply of mobile GFP-Bsn^{S2845A}, the mobility properties of GFP-labelled mobile puncta were analysed in the next step.

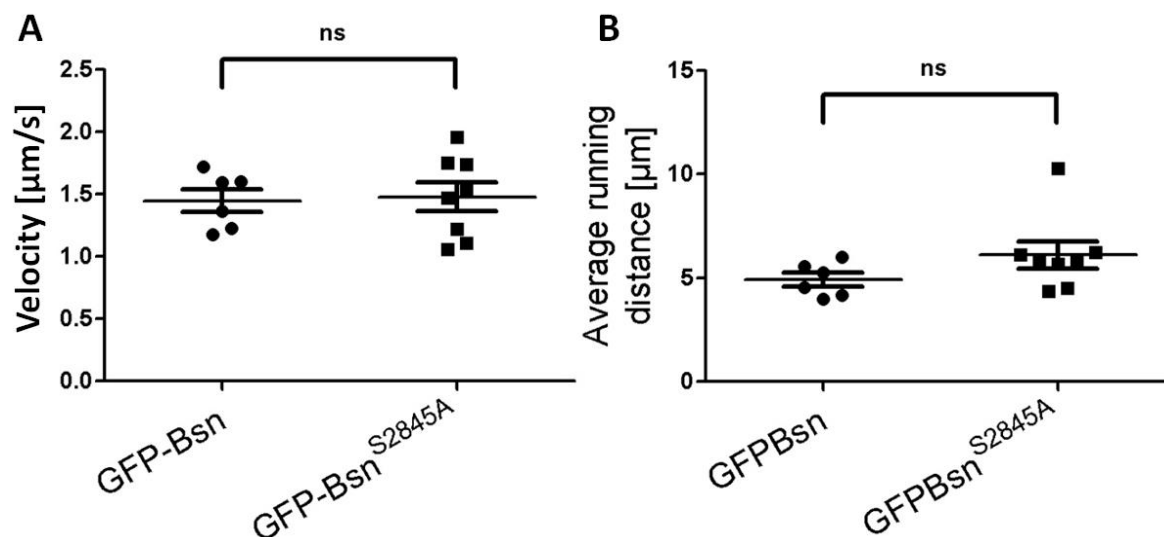


Fig. 24: Analysis of Bassoon transport characteristics.

Kymographs of axonal segments of DIV14-16 neurons transfected with GFP-Bsn or GFP-Bsn^{S2845A} and imaged for 25 s at the rate of 4 Hz were evaluated. Continuous traces of mobile puncta without stop or change of direction were counted as single events and measured for their (A) velocity (µm/s) and (B) average running distance (µm). Averaged results from 6/8 videos respectively were not significantly different between wt and mutant.

To this end the moving velocities and the travelled distances of the mobile puncta were measured. They were analysed by creating kymographs of axonal segments of transfected neurons imaged for 25 s at the rate of 4 Hz. Continuous traces without stop or change of direction were counted as single events and measured for their velocity and average running distance. A slight tendency for an increased travelling distance of GFP-Bsn^{S2845A} compared to the wt was detected. Nevertheless the statistical analysis did not reveal a significant difference between the velocities (Fig. 24A; $1,45 \pm 0,35 \mu\text{m/s}$ for GFP-Bsn vs. $1,48 \pm 0,28 \mu\text{m/s}$ for GFP-Bsn^{S2845A}; mean \pm SEM; N = 6 vs. 8 videos; 539 vs. 304 traces respectively; P = 0,8457; unpaired t-test) or travelling distances (Fig. 24B; $4,91 \pm 2,06 \mu\text{m}$ vs. $6,10 \pm 2,16 \mu\text{m}$; N = 6 vs. 8 videos; 539 vs. 304 traces respectively; P = 0,1660; unpaired t-test) of wt and mutant Bassoon. These results implied that disruption of the 14-3-3 interaction site on Bassoon does not influence the transport properties of potential PTVs. Taken together the lower recovery rate of GFP-Bsn^{S2845A} could not be explained by a defect in the supply of Bassoon from the mobile Bassoon pools to the synapse.

4 Discussion

The general aim of this work was to characterise the physical nature and potential functions of interactions of the presynaptic protein Bassoon with synaptically relevant adaptor proteins. Bassoon is an important scaffolding protein of the CAZ. This protein network harbours essential structural and functional determinants for the mechanism of SV release and recycling and has gained an increasing amount of scientific attention during the past decade (Dresbach et al., 2001; Ziv and Garner, 2004; Schoch and Gundelfinger, 2006; Hida and Ohtsuka, 2010; Gundelfinger and Fejtova, 2012; Sudhof, 2012). Disturbances of the networks integrity can lead to impairments of presynaptic formation, plasticity and signalling capacity and therefore interfere with neuronal function as laid out in the introduction (1.2).

Generally, control of SVC processes by the active zone network can be executed directly by interaction of CAZ proteins with SVs, SNARE complex proteins, voltage-dependent calcium channels or other elements of primary importance for the cycle. Additionally there is the possibility of an indirect regulatory influence via interconnecting adaptor proteins. Pioneering work in the field of signal transduction showed that adaptor proteins are substantial components of many signalling cascades (Flynn, 2001; Schechtman et al., 2001; Kurosaki, 2002). While there are several examples of known synaptically relevant adaptor proteins (1.4) with a well-defined set of binding partners the dynamic regulation of these interactions for the adaption to physiological events is mostly elusive. In this regard the work on the interactions of Bassoon with both of the adaptor proteins was supposed to provide more information about the mechanisms by which CAZ proteins can influence the SVC via accessory molecules. Further it was investigated if these interactions contribute to the synaptic deficiencies, which characterise the phenotype of mice lacking Bassoon. In the following chapter the obtained results will be analysed and discussed subsequentially.

4.1 AP Complexes

The regulation of neurotransmitter release at the active zone is critical for the general process of synaptic signal transmission. It highly depends on the course of the SVC at presynaptic boutons. In regard to the contribution of the CAZ to presynaptic functionality the question to which degree and by which molecular connections cytomatrix elements are involved in various steps of this cycle is therefore of great importance. As outlined previously (1.2) plenty of evidence is available for the role of CAZ proteins in SV release or generally the exocytotic part of the SVC. In contrast information about direct participation of this protein network in endocytotic or recycling processes of the cycle is sparse. The only core CAZ protein that was connected to endocytosis until now is the Bassoon paralogue Piccolo by interactions with GIT1 (Kim et al., 2003) and Abp1 (Fenster et al., 2003). GIT1 regulates CME of several G-protein coupled receptors (Claing et al., 2000) while Abp1 is a direct binding partner of the fission GTPase Dynamin (Kessels et al., 2001). In consideration of this connection it appears interesting that previously mentioned coincidences in the phenotypes emerging from the lack of Bassoon (Hallermann et al., 2010) and the lack of Dynamin (Kawasaki et al., 2000) were proposed to indicate a role for Bassoon in CME. In similarity to neuronal AP3B a direct influence of Bassoon on SV release was also demonstrated under conditions of high frequency stimulation while previous attempts under different conditions missed this detail (Voglmaier et al., 2006; Hallermann et al., 2010). In connection to the working hypothesis this raised the question if not only AP2 but also AP3B could eventually interact with Bassoon and further if this could possibly influence the observed strong stimulation Bassoon phenotype.

In this context the interaction of Bassoon with AP complexes as basic elements of the CME machinery seemed to be a promising target to gain a better understanding of the meaning the CAZ scaffold could hold for endocytosis and vesicle recycling at the presynaptic bouton. For this reason first part of this study deals with description of the interaction of Bassoon with AP μ subunits. It was demonstrated that the association of Bassoon with the AP2 μ subunit depends on a classical Yxx ϕ cargo sorting motif spanning aa 901-904 of Bassoon. Further it was shown that not only the initially identified μ subunit of AP2 but also the corresponding equivalents of the complexes AP1 and AP3A but not AP3B can interact with Bassoon via the same binding site. Co-localisation studies revealed spatial overlap between the distribution patterns of the proteins in growth cones, synapses and at the TGN of neurons. Finally, it was examined if the identified binding site has any influence on general CME, and more specifically on the SV recycling processes. In summary no effect of the interaction on synaptic endocytosis or

recycling processes could be verified. It is proposed that the function of the interaction may instead lie in the classical sorting and targeting of Bassoon.

Interaction of AP complexes with Bassoon is mediated by a typical Yxx ϕ motif

The classical way of AP complexes to bind cargo proteins is via interaction of their μ subunits with tyrosine based Yxx ϕ motifs of the target. In this study it was demonstrated that this mechanism also applies to the interaction with Bassoon. Identification of the responsible binding motif comprising aa 901-904 of Bassoon was achieved by *in silico* prediction and subsequent Y2H experiments. The identified sequence is the only site of Bassoon with these characteristics and evidence for its functionality was gathered by point mutation of the essential aa residues. The site is not conserved in the Bassoon paralogue Piccolo, implicating a functional diversity in the subcellular tasks of the closely related proteins as it was previously suggested for the interaction of the Dynein light chain with Bassoon (Fejtova et al., 2009). Binding of the μ subunit of AP2 to Bassoon was confirmed by a co-clustering assay in COS-7 cells and by Co-IP from transfected HEK-293T cells. Results from the Co-IP further revealed that not only AP2 but also AP1 and AP3A are able to bind Bassoon via the same motif. Since the cargo recognition specificities of the different AP complexes are strongly overlapping (Ohno et al., 1998) a cross-reactivity of Bassoon with multiple AP subtypes was expectable. In contrast to this expectation, the μ subunit of the neuron-specific and synaptically relevant AP3B complex was the only of the tested potential interaction partners that did not bind Bassoon. This result was surprising because AP3B was originally considered as one of the major AP candidates for the Bassoon interaction due to its implication in SV recycling. On the one hand, this led to the conclusion that AP binding to Bassoon is probably not relevant for the endosomal vesicle recycling pathway. On the other hand, this assumption did not necessarily exclude a role for Bassoon in CME and SV recycling from the plasma membrane. The μ subunits of AP2 as well as AP1 can both drive this process (Kim and Ryan, 2009) and were clearly able to interact. From this point of the study the question if the AP-Bassoon interaction is indeed of regulatory nature for the SVC or if it is rather facilitating a classical cargo sorting mechanism for Bassoon became increasingly prominent. It is well documented that during synaptogenesis the transport of Bassoon from the TGN to synapses along the axon is managed by association with special transport vesicles called PTVs (1.3). The complexes AP3A and AP1 are generally supposed to mediate sorting of cargo into transport vesicles derived from the TGN. Due to the positive

interactions of Bassoon with these AP subtypes a corresponding function for the interaction had to be considered additionally to the original working hypothesis of the project (Fig. 25).

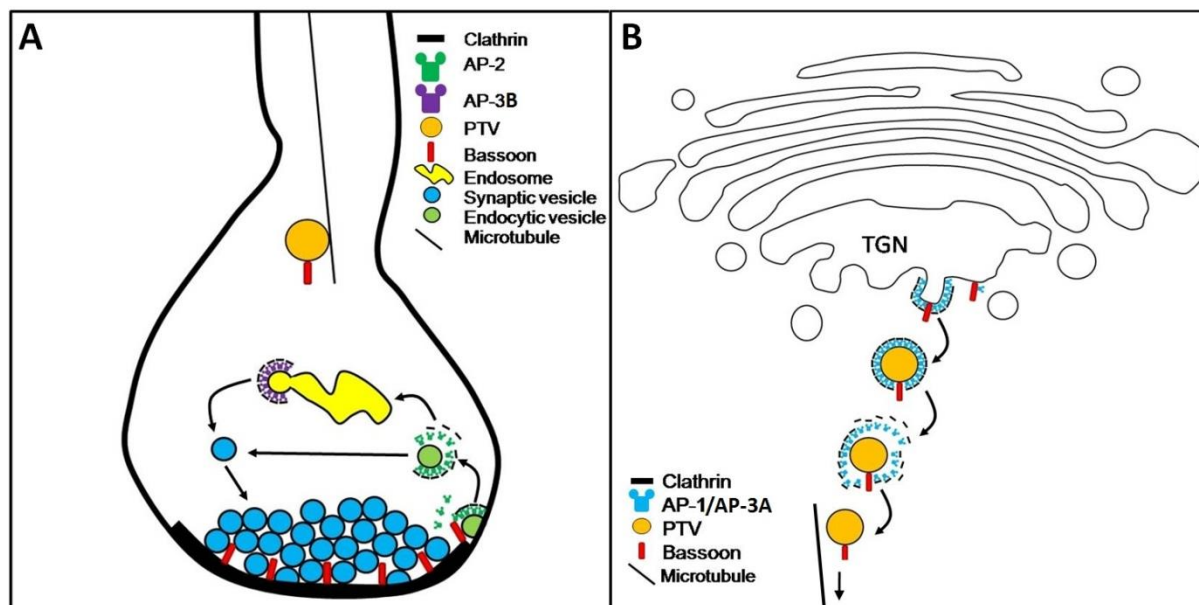


Fig. 25: Hypothetical settings for interaction of Bassoon with AP complexes.

(A) Possible influence of the interaction on SV recycling processes of the SVC at the presynaptic compartment. **(B)** Secondary hypothesis of an involvement of the interaction in the sorting of Bassoon to PTVs at the TGN by AP1 or AP3A.

AP complexes and Bassoon co-localise in developing and mature neurons

To find out where and when Bassoon has the opportunity to interact with different AP subtypes in neurons co-localisation studies in different developmental time windows were carried out. The available AP3 antibodies did not provide the possibility to differentiate between AP3A and AP3B and on top of that didn't yield satisfactory staining. Hence the co-localisation assay was restricted to the comparison of AP2 and AP1. Due to known cellular distribution patterns of the proteins it was expected to find spatial overlaps of Bassoon with AP2 at synapses and with AP1 at the TGN (Traub et al., 1993; Bock et al., 1997; Dresbach et al., 2006; Maas et al., 2012; Spangler et al., 2013). The co-localisation in the peri-nuclear region of young neurons is therefore counted as TGN co-enrichment. Considering Bassoon as well established presynaptic marker protein and AP2 as adaptor for SV recycling the co-enrichment of AP2 at every Bassoon-positive spot was as expected. In turn Bassoon was not present at every AP2 positive spot, which can be explained with the function of AP2 in general CME events from non-synaptic plasma membrane. The fulfilment of both expectations negated the possibility to exclude one of the two functional hypotheses by this assay. Additionally co-localisation between Bassoon and AP2 also occurred at the axonal growth cone during early development.

These findings presented a scenario in which the binding site of Bassoon could have different spatially and temporally distinguishable functions depending on the interacting AP subtype. One function could be to mediate sorting and trafficking via AP1 and possibly AP3A at the TGN especially during early development. Another could be to facilitate an interaction with AP2 at the growth cone in the same time window. In accordance to this the AP2 interaction could influence endocytosis processes at the plasma membrane of growth cones in young neurons or at mature synapses in differentiated neurons.

From a technical view it must be mentioned here that the resolution of a standard light microscopical setup does not allow a completely reliable spatial differentiation between pre- and postsynaptic compartments. Due to this fact the synaptic co-localisation of Bassoon and AP2 at mature synapses could be partly misinterpreted since the synaptic staining of AP2 reflects both pre- and postsynaptic pools of the adaptor complex. Nevertheless AP2 function at the presynaptic compartment was previously shown (Kim and Ryan, 2009). Thus it is appropriate to assume that at least part of the staining is contributed by presynaptic AP2. Since the co-localisation approach can solely provide information about the spatial possibility of an interaction the following experiments were conducted to gather results showing the functional relevance of the binding.

The interaction of Bassoon with AP complexes does not influence endocytosis or SV recycling

This work was generally aimed at presynaptic function and regulation. Thus the hypothesis of an influence on the SVC had a higher priority than the transport hypothesis, which may be looked after in a future study. An example for a possible effect of the interaction in this scenario could be the recruitment of free AP complexes into the vicinity of the active zone. In this way vesicle recycling could be promoted by increasing the spatially available amount of sorting adaptors. The interaction could also influence regulation of the balance of effective AP concentrations between active and periaxonal zone to contribute to the spatial separation of endo- and exocytosis domains. Alternatively Bassoon could theoretically represent a platform for assembly or disassembly of AP complexes at the site of action. The binding could even participate in the uncoating process of recycled vesicles or play a role in the temporal coupling of exocytosis with endocytosis events. Due to the variety of possibilities the aim of the initially performed transferrin uptake assay was to first check whether the interaction had any general influence on the CME machinery. The applied assay was simple and would detect negative as

well as positive deviations in endocytotic performance. In the end the results did not support the hypothesis of a relevance of the interaction for endocytosis. In contrary, neither a simple microscopical approach (data not shown) nor the more sophisticated FACS method detected any deviation in CME of the transferrin receptor upon overexpression of wt or AP binding deficient Bassoon fragments.

Transferrin uptake is rather artificial and functionally relatively far away from the synapse as the system of interest. To control the previous results in a neuronal environment and to exclude the possibility that the negative result was caused by the lack of synaptic endocytosis machinery components an additional assay was used. In the applied synaptotagmin uptake approach the lack of Bassoon produces a phenotype of reduced internalisation of synaptotagmin in synapses of primary hippocampal neurons. Because synaptotagmin is a prominent SV membrane protein this condition indicates a disturbance in the turnover of the SVC and hence indirectly also a lower presynaptic activity in the absence of Bassoon. The rescue approach designed to examine if this perturbation can be attributed to the AP interaction nevertheless demonstrated that this is not the case. Expression of a Bassoon construct with mutated AP binding site replenished the defect in synaptotagmin uptake as efficiently as the wt version. This outcome indirectly confirmed the results of the previous transferrin uptake.

Taken together the attempts to verify the primary working hypothesis of an influence of the Bassoon-AP interaction on the SVC did not yield positive results. There are several potential explanations for this lack of evidence. One possibility is that the interaction initially detected in the Y2H system is an *in vitro* artefact that does not possess any relevance *in vivo*. Nevertheless the confirmation of the interaction in COS and HEK cells speaks against this. The fact that μ subunits of other AP complexes also bind to the same site supports the notion that the interaction is not random but is indeed mediated by a classical and functional Yxx ϕ AP binding motif. Another explanation could be that the functionality of vesicle recycling as a process of major importance is redundantly secured by a mechanistic variety. On the one hand, the previously mentioned substitution of synaptic AP2 function by AP1 as well as the residual endocytotic performance in absence of both AP subtypes strongly points into this direction (Kim and Ryan, 2009; Cheung and Cousin, 2012). On the other hand, even with this in mind at least a minor effect would have been expectable since compensation mechanisms are seldom complete. It is also imaginable that the function of the interaction was missed or has been overlooked due to the nature of the applied methods. Especially considering previously mentioned phenotypes of Bassoon and AP3, which were only detectable under extreme

conditions, a similar scenario is conceivable also here. Last but not least, it is also possible that the assumption of the primary working hypothesis was simply not correct. Especially the kind of interaction strongly argues for this option. While interactions with AP μ subunits are almost exclusively described as cargo related, all relevant accessory proteins or AP modulators bind to other parts of the tetrameric complexes (Fig. 3). The classical interaction via the Yxx ϕ motif therefore rather points into the direction of a sorting and trafficking related function (Fig. 25B) although initial experiments into this direction could not support this hypothesis (data not shown). Even if the study failed to detect any relevance of the binding for the SVC it could be beneficial to keep this possibility in mind for a future study about transport and targeting of Bassoon.

4.2 14-3-3 Proteins

The second part of this study contains the description of a novel interaction of the presynaptic scaffolding protein Bassoon with the small adaptor protein 14-3-3. It is shown that the association of 14-3-3 with Bassoon depends on a specific phosphorylation of Bassoon at aa residue S2845 and kinases of the RSK family are identified as candidates mediating this phosphorylation. Finally, it is demonstrated that the mutation of the functional 14-3-3 interaction motif of Bassoon leads to a decrease in the dynamic exchange rates of synaptic Bassoon in neurons. Taken together, these data provide an exemplary mechanism of a rapid molecular modification inducing a switch of a protein-protein interaction of Bassoon and controlling its dynamic association with the presynaptic cytomatrix.

Phospho-S2845 of Bassoon mediates its interaction with 14-3-3

Protein phosphorylation is a fast and reversible way to modulate protein function and was recognised to induce rearrangements of numerous protein complexes in processes of synaptic plasticity (Sweatt, 2004; Wayman et al., 2008; Hoeffler and Klann, 2010). In recent years, three independent proteomic studies (Collins et al., 2005; Trinidad et al., 2006; Munton et al., 2007) identified 20 to 30 phosphorylation sites on Bassoon constituting it as one of the most highly phosphorylated synaptic proteins. Nevertheless, no functional mechanism mediated by any of the described phosphorylation sites has been established to date. In this study, the phosphorylated S2845 of Bassoon was identified to mediate the interaction of Bassoon with the small adaptor protein 14-3-3. Initially, the interaction with 14-3-3 η was found in an unbiased

Y2H screen for binding partners of Bassoon. The critical dependence on the intact serine residue 2845 of Bassoon and its phosphorylation for its binding to 14-3-3 was demonstrated using interaction studies *in vitro*, in mammalian cell lines and in primary hippocampal neurons. Further it was shown that the ectopic expression of the interaction motif is capable to drive a redistribution of the interaction partner in living cells. Besides the initially found 14-3-3 η isoform also isoforms β , γ and ϵ could interact with Bassoon (Schroder et al., 2013). This is in agreement with the previously reported highly overlapping target motif preferences of 14-3-3 proteins (Yaffe et al., 1997), causing interactions of several 14-3-3 binding partners with multiple 14-3-3 isoforms (Finlin and Andres, 1999; Hausser et al., 2006; Fischer et al., 2009a).

S2845 of Bassoon can be phosphorylated by RSKs

The *in vitro* experiments showed that binding of 14-3-3 to Bassoon critically depends on the phosphorylation of Bassoon S2845. Multiple unbiased proteomic studies previously identified the phosphorylation of Bassoon S2845 (Collins et al., 2005; Trinidad et al., 2006; Munton et al., 2007), which ultimately confirms the physiological occurrence of this modification *in vivo*. In this study, a newly generated phospho-specific antibody against this residue was introduced. This antibody specifically recognised heterologously expressed phosphorylated Bassoon. Unfortunately, it failed to detect the phosphorylated S2845 in mouse or rat brain lysates, probably due to low abundance or transient nature of the phosphoepitope under normal conditions. However, it was possible to detect the phosphorylated S2845 in brain lysates supplemented with Mg^{2+} /ATP upon incubation at 30° C or in lysates of cells treated with the protein phosphatase inhibitor okadaic acid. This demonstrated that the epitope can be phosphorylated by endogenous kinases upon stimulation of kinase activity or inhibition of phosphatase activity. The applied concentration of okadaic acid was previously shown to inhibit the phosphatase PP2A (Ishihara et al., 1989), marking it as a potential candidate enzyme for dephosphorylation of S2845. Interestingly, phosphorylation of S2845 induced by okadaic acid was reverted by pretreatment of the cells with the specific RSK family inhibitor BI-D1870.

The ability of RSK family kinases to target S2845 of Bassoon was subsequently confirmed via *in vitro* phosphorylation assays utilising the α -pS2845 Bsn antibody. RSK1 and 3 were about twice as potent in S2845 phosphorylation as compared to RSK2 and RSK4 *in vitro*. This further supports a role of RSKs in the physiological phosphorylation of Bassoon at this residue. All RSKs genes are expressed in the nervous system, having restricted but overlapping developmental and regional expression patterns (Romeo et al., 2012) and they have been

suggested to share partial functional redundancy (Zeniou et al., 2002). Thus, different RSKs might be involved in the phosphorylation of Bassoon S2845 depending on developmental stage and brain area. RSK1 is expressed during early embryogenesis, whereas RSK3 becomes the most abundant RSK in the fetal and neonatal stages (Zeniou et al., 2002). RSK3 is therefore the best candidate to phosphorylate S2845 of Bassoon in the juvenile stages. In adult brain, RSK1 is most strongly expressed in cerebellar granular cells, whereas RSK2 and RSK3 are abundant in forebrain structures. RSK2 is mutated in the Coffin-Lowry syndrome, a disorder characterised by psychomotor and growth retardation (Trivier et al., 1996). The associated mental disabilities were proposed to be a consequence of a selective defect of RSK2 function in hippocampus and cerebellum (Zeniou et al., 2002). Interestingly, there is a possible convergence with the phenotype of Bassoon mutant mice that show altered short-term plasticity in cerebellar mossy fiber to granule cell synapses and in mossy fiber synapses in the hippocampal CA3 region (Hallermann et al., 2010; Lanore et al., 2010). Additionally, the observed Bassoon KO phenotype of increased BDNF levels could be interesting in connection with RSK kinases. BDNF signalling is not only involved in neuronal development and presynaptic plasticity (Zakharenko et al., 2003; Binder and Scharfman, 2004) but can also lead to activation of RSK kinases (Rakhit et al., 2005; Kharebava et al., 2008).

Role of the 14-3-3 interaction with Bassoon

14-3-3 proteins frequently function as dimers 1) to induce a conformational change of target proteins by interacting with two interaction sites on the same protein and clamping it, 2) to stabilise protein complex formation by bridging two 14-3-3 interaction partners, or 3) to inhibit protein-protein interactions by competing for binding sites (Fig. 4, (Mackintosh, 2004)). The interaction of Bassoon with 14-3-3 was fully disrupted *in vitro* and in cellular context by mutation of S2845. This suggests the existence of only a single 14-3-3 interaction interface on Bassoon. Therefore the first scenario can be considered unlikely. In FRAP experiments lowered recovery rates of GFP-Bsn^{S2845A} were observed, suggesting that 14-3-3 binding favours dissociation of Bassoon from its presynaptic anchor.

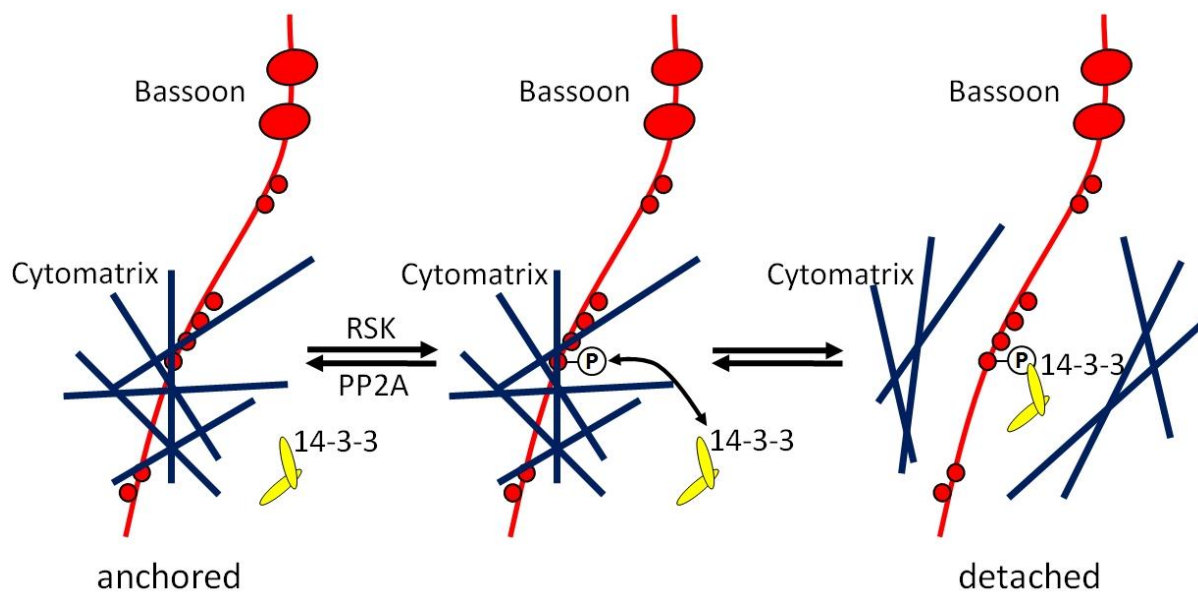


Fig. 26: Proposed mechanism of the Bassoon-14-3-3 interaction.

Bassoon is anchored at the active zone by interaction with cytomatrix proteins. Phosphorylation and dephosphorylation of the 14-3-3 interaction site on Bassoon by RSKs or PP2A phosphatases control the binding of 14-3-3 to Bassoon. Interaction of 14-3-3 with Bassoon disturbs CAZ interactions and favours a detached state of Bassoon.

It is also possible that 14-3-3 associates with free Bassoon and interferes with its association instead. Nevertheless, in either scenario phosphorylation of S2845 and binding of 14-3-3 decreases the attachment of Bassoon to the presynaptic CAZ (Fig. 26).

The complex and tightly interwoven character of the presynaptic protein meshwork is caused by diverse interactions between the single CAZ constituents (Gundelfinger and Fejtova, 2012). Bassoon interacts with CAST/ELKS2 (Takao-Rikitsu et al., 2004), which in turn can interact with Piccolo and RIM (Wang et al., 2002; Takao-Rikitsu et al., 2004). Furthermore, liprin- α also interacts with RIM and CAST (Schoch et al., 2002; Ko et al., 2003). During the period of synaptogenesis membrane-associated Bassoon is transported on PTVs from the cell bodies to the distal axons to be inserted into nascent synapses (Zhai et al., 2001; Shapira et al., 2003; Fejtova et al., 2009). An assembly of a complex protein meshwork at the cytoplasmic surface of transport vesicles could lead to sterical hindrance of the transport process. Therefore, a phosphorylation-induced and 14-3-3-assisted masking of the binding site might be favourable at this stage to facilitate an unhindered distribution. The previously mentioned temporal expression patterns of RSKs during development as well as the negative influence of RSK2 on the number of boutons at the neuromuscular junction of *Drosophila* larvae (Fischer et al., 2009b) support this train of thought. Additionally the role of BDNF in synaptogenesis and neuronal development as well its MAPK activating function (see above) also fit to this line of

argumentation. The observed tendency of an increase in GFP-Bsn^{S2845A} positive spots with a concomitant decrease in spot intensity compared to GFP-Bsn could therefore, despite the missing significance, indicate an impaired redistribution phenotype according to the proposed mechanism.

Activity-dependent synaptic plasticity of mature synapses goes hand in hand with profound rearrangement of the CAZ (Lazarevic et al., 2011; Weyhermuller et al., 2011) but the underlying mechanisms are still unclear. It appears likely that molecular remodelling of complex protein networks, like the presynaptic cytomatrix, requires loosening of intermolecular interactions between its constituents. Therefore it is an appealing hypothesis that rapid and specific phosphorylation of CAZ components might regulate their binding to each other and induce the molecular remodelling during processes of synaptic plasticity. Phosphorylation-dependent dispersion and reclustered of the SV-associated protein Synapsin1 at presynaptic boutons were previously shown and were regulated by synaptic activity (Chi et al., 2001). Connected to this it was further demonstrated that redistribution of Synapsin1 between proximal synapses occurs and can be accelerated by neuronal stimulation (Tsuruel et al., 2006). These findings support a model in which reorganisation and restructuring of presynaptic components are controlled by phosphorylation to facilitate plasticity processes induced by neuronal activity patterns.

Another noteworthy point is that treatment of neurons with the phosphatase inhibitor okadaic acid increases the phosphorylation of the 14-3-3 binding motif on Bassoon in the same way as for RIM1 (Lonart et al., 2003). Particularly this treatment leads to rapid solubilisation and diffusion of the cytomatrix proteins Bassoon, CAST and RIM and to a disruption of the SV pool without affecting the postsynaptic scaffolds (Stefano Romorini, unpublished data), which also supports the presented hypothesis. It is suggested here that phosphorylation of CAZ components and subsequent 14-3-3 binding might support their solubilisation by interfering with the intermolecular interactions among them. RSK activation by signalling of a growth factor like BDNF and the role of this neurotrophin in synaptic plasticity could theoretically represent a physiological pathway for plasticity processes involving the described 14-3-3 interaction with Bassoon. Indeed, the over-expression of a 14-3-3 dominant negative mutant can inhibit LTP induction in the cerebellum, which was discussed in connection with its interaction with the CAZ protein RIM (Simsek-Duran et al., 2004). The interaction of 14-3-3 with RIM was first suggested to be critical for the induction of presynaptic LTP (Lonart et al., 2003). This was controversially discussed later and in contrast to the in vitro data the absence

of the 14-3-3 binding site in RIM did not cause an identifiable phenotype in vivo (Kaesler et al., 2008; Yang and Calakos, 2010). The exact role of the 14-3-3 interaction with RIM is therefore still unclear. In addition to the interactions with Bassoon and RIM, the CAZ components CAST and liprin- α were also found to bind 14-3-3 in two independent proteomic screenings for 14-3-3 interaction partners (Jin et al., 2004; Angrand et al., 2006). The function of these interactions has not been investigated yet and could yield interesting information for comparison with the present hypothesis. What will be the consequence of a specific interference with the interaction between 14-3-3 and Bassoon or other CAZ components in the brain at last remains an exciting question for future studies.

4.3 Conclusions and Outlook

There is no doubt that Bassoon is an important presynaptic scaffold and interaction hub of the CAZ. Nonetheless interactions established by Bassoon do not necessarily also have functions in the regulation of neurotransmitter release from the active zone. In this work two interactions were described which did not show a direct impact on acute synaptic signalling in the applied experimental setups. Still these interactions may influence the functionality of neuronal systems and development independently from direct SV release. While the used methods could not reveal the physiological function of the AP2 binding to Bassoon in the available time, they still showed that the interaction can occur *in vivo*. Even if it is not relevant for the recycling of SVs it would be interesting to find out if it could play a role in Bassoon sorting and trafficking into PTVs at the TGN instead.

The finding that 14-3-3 binding can regulate synaptic exchange and/or attachment of Bassoon indicates an implication in synaptogenesis and possibly also in synaptic plasticity. At the same time it stays unclear how the adaptor 14-3-3 exactly exerts its influence on synaptic Bassoon anchoring. Most scientific approaches in the end yield more new exciting questions than they could answer. The next goal could be to discover more details of the mechanism that facilitates anchoring and detachment of Bassoon especially in regard to activity-dependent cytomatrix reorganisation. Which physiological condition leads to the activation of RSKs and subsequent 14-3-3 binding to Bassoon? And how are the direct and indirect connections of Bassoon to the other CAZ proteins involved in this process? Thinking of the described and potential binding of 14-3-3s to RIM, ELKS and liprin- α , is it conceivable that the described scenario is a common mechanism for CAZ restructuring? These are the questions which are next on the list and which could lead to a better understanding of neuronal function and plasticity in the future.

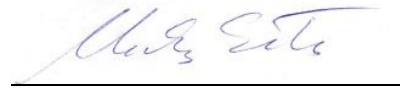
In regard to the two examined proteins and also to the described Bassoon-DLC interaction it is interesting to mention, that none of the identified binding motifs are conserved in the aa sequence of the Bassoon paralogue Piccolo. At this point it all comes back to the fact that adaptor proteins offer the possibility to confer specific attributes and tasks to otherwise similar proteins or complexes. In the end the function of scaffolding proteins with no intrinsic biochemically active capacity is exactly determined only in the patterns of their interaction partners. So to speak, in their world who you are is defined by whom you know...

5 Declaration

Hiermit erkläre ich, dass ich die vorliegende Dissertation selbständig angefertigt habe. Es wurden nur die in der Arbeit ausdrücklich benannten Quellen und Hilfsmittel benutzt. Wörtlich oder sinngemäß übernommenes Gedankengut habe ich als solches kenntlich gemacht.

Hamburg, 11.06.2015

Ort, Datum

A handwritten signature in blue ink, appearing to read 'Andreas Eitel', is written above a horizontal line.

Unterschrift

6 Literature

- Ahmari SE, Buchanan J, Smith SJ (2000) Assembly of presynaptic active zones from cytoplasmic transport packets. *Nat Neurosci* 3:445-451.
- Altrock WD et al. (2003) Functional inactivation of a fraction of excitatory synapses in mice deficient for the active zone protein bassoon. *Neuron* 37:787-800.
- Angrand PO, Segura I, Volkel P, Ghidelli S, Terry R, Brajenovic M, Vintersten K, Klein R, Superti-Furga G, Drewes G, Kuster B, Bouwmeester T, Acker-Palmer A (2006) Transgenic mouse proteomics identifies new 14-3-3-associated proteins involved in cytoskeletal rearrangements and cell signaling. *Mol Cell Proteomics* 5:2211-2227.
- Anjum R, Blenis J (2008) The RSK family of kinases: emerging roles in cellular signalling. *Nat Rev Mol Cell Biol* 9:747-758.
- Aravamudan B, Fergestad T, Davis WS, Rodesch CK, Broadie K (1999) *Drosophila* UNC-13 is essential for synaptic transmission. *Nat Neurosci* 2:965-971.
- Aridor M, Traub LM (2002) Cargo selection in vesicular transport: the making and breaking of a coat. *Traffic* 3:537-546.
- Augustin I, Rosenmund C, Sudhof TC, Brose N (1999) Munc13-1 is essential for fusion competence of glutamatergic synaptic vesicles. *Nature* 400:457-461.
- Balla S, Thapar V, Verma S, Luong T, Faghri T, Huang CH, Rajasekaran S, del Campo JJ, Shinn JH, Mohler WA, Maciejewski MW, Gryk MR, Piccirillo B, Schiller SR, Schiller MR (2006) Minimoto Miner: a tool for investigating protein function. *Nat Methods* 3:175-177.
- Beguin P, Mahalakshmi RN, Nagashima K, Cher DH, Ikeda H, Yamada Y, Seino Y, Hunziker W (2006) Nuclear sequestration of beta-subunits by Rad and Rem is controlled by 14-3-3 and calmodulin and reveals a novel mechanism for Ca²⁺ channel regulation. *J Mol Biol* 355:34-46.
- Betz A, Thakur P, Junge HJ, Ashery U, Rhee JS, Scheuss V, Rosenmund C, Rettig J, Brose N (2001) Functional interaction of the active zone proteins Munc13-1 and RIM1 in synaptic vesicle priming. *Neuron* 30:183-196.
- Betz WJ, Angleson JK (1998) The synaptic vesicle cycle. *Annu Rev Physiol* 60:347-363.
- Binder DK, Scharfman HE (2004) Brain-derived neurotrophic factor. *Growth Factors* 22:123-131.
- Blenis J (1993) Signal transduction via the MAP kinases: proceed at your own RSK. *Proc Natl Acad Sci U S A* 90:5889-5892.
- Blom N, Sicheritz-Ponten T, Gupta R, Gammeltoft S, Brunak S (2004) Prediction of post-translational glycosylation and phosphorylation of proteins from the amino acid sequence. *Proteomics* 4:1633-1649.
- Blumstein J, Faundez V, Nakatsu F, Saito T, Ohno H, Kelly RB (2001) The neuronal form of adaptor protein-3 is required for synaptic vesicle formation from endosomes. *J Neurosci* 21:8034-8042.
- Bock JB, Klumperman J, Davanger S, Scheller RH (1997) Syntaxin 6 functions in trans-Golgi network vesicle trafficking. *Mol Biol Cell* 8:1261-1271.

- Bonni A, Brunet A, West AE, Datta SR, Takasu MA, Greenberg ME (1999) Cell survival promoted by the Ras-MAPK signaling pathway by transcription-dependent and -independent mechanisms. *Science* 286:1358-1362.
- Boston PF, Jackson P, Thompson RJ (1982) Human 14-3-3 protein: radioimmunoassay, tissue distribution, and cerebrospinal fluid levels in patients with neurological disorders. *J Neurochem* 38:1475-1482.
- Bresler T, Shapira M, Boeckers T, Dresbach T, Futter M, Garner CC, Rosenblum K, Gundelfinger ED, Ziv NE (2004) Postsynaptic density assembly is fundamentally different from presynaptic active zone assembly. *J Neurosci* 24:1507-1520.
- Bridges D, Moorhead GB (2004) 14-3-3 proteins: a number of functions for a numbered protein. *Sci STKE* 2004:re10.
- Broadie K, Rushton E, Skoulakis EM, Davis RL (1997) Leonardo, a *Drosophila* 14-3-3 protein involved in learning, regulates presynaptic function. *Neuron* 19:391-402.
- Cai Q, Pan PY, Sheng ZH (2007) Syntabulin-kinesin-1 family member 5B-mediated axonal transport contributes to activity-dependent presynaptic assembly. *J Neurosci* 27:7284-7296.
- Calakos N, Schoch S, Sudhof TC, Malenka RC (2004) Multiple roles for the active zone protein RIM1alpha in late stages of neurotransmitter release. *Neuron* 42:889-896.
- Cardoso C, Leventer RJ, Ward HL, Toyo-Oka K, Chung J, Gross A, Martin CL, Allanson J, Pilz DT, Olney AH, Mutchinick OM, Hirotsune S, Wynshaw-Boris A, Dobyns WB, Ledbetter DH (2003) Refinement of a 400-kb critical region allows genotypic differentiation between isolated lissencephaly, Miller-Dieker syndrome, and other phenotypes secondary to deletions of 17p13.3. *Am J Hum Genet* 72:918-930.
- Carriere A, Ray H, Blenis J, Roux PP (2008) The RSK factors of activating the Ras/MAPK signaling cascade. *Front Biosci* 13:4258-4275.
- Cases-Langhoff C, Voss B, Garner AM, Appeltauer U, Takei K, Kindler S, Veh RW, De Camilli P, Gundelfinger ED, Garner CC (1996) Piccolo, a novel 420 kDa protein associated with the presynaptic cytomatrix. *Eur J Cell Biol* 69:214-223.
- Castillo PE, Schoch S, Schmitz F, Sudhof TC, Malenka RC (2002) RIM1alpha is required for presynaptic long-term potentiation. *Nature* 415:327-330.
- Ceccarelli B, Hurlbut WP, Mauro A (1973) Turnover of transmitter and synaptic vesicles at the frog neuromuscular junction. *J Cell Biol* 57:499-524.
- Chen HK, Fernandez-Funez P, Acevedo SF, Lam YC, Kaytor MD, Fernandez MH, Aitken A, Skoulakis EM, Orr HT, Botas J, Zoghbi HY (2003) Interaction of Akt-phosphorylated ataxin-1 with 14-3-3 mediates neurodegeneration in spinocerebellar ataxia type 1. *Cell* 113:457-468.
- Cheung G, Cousin MA (2012) Adaptor protein complexes 1 and 3 are essential for generation of synaptic vesicles from activity-dependent bulk endosomes. *J Neurosci* 32:6014-6023.
- Chi P, Greengard P, Ryan TA (2001) Synapsin dispersion and recluster during synaptic activity. *Nat Neurosci* 4:1187-1193.
- Chua JJ, Butkevich E, Worseck JM, Kittelmann M, Gronborg M, Behrmann E, Stelzl U, Pavlos NJ, Lalowski MM, Eimer S, Wanker EE, Klopfenstein DR, Jahn R (2012) Phosphorylation-regulated axonal dependent transport of syntaxin 1 is mediated by a Kinesin-1 adapter. *Proc Natl Acad Sci U S A* 109:5862-5867.

- Claing A, Perry SJ, Achiriloaie M, Walker JK, Albanesi JP, Lefkowitz RJ, Premont RT (2000) Multiple endocytic pathways of G protein-coupled receptors delineated by GIT1 sensitivity. *Proc Natl Acad Sci U S A* 97:1119-1124.
- Clayton EL, Evans GJ, Cousin MA (2008) Bulk synaptic vesicle endocytosis is rapidly triggered during strong stimulation. *J Neurosci* 28:6627-6632.
- Collins MO, Yu L, Coba MP, Husi H, Campuzano I, Blackstock WP, Choudhary JS, Grant SG (2005) Proteomic analysis of in vivo phosphorylated synaptic proteins. *J Biol Chem* 280:5972-5982.
- Dick O, tom Dieck S, Altmann WD, Ammermuller J, Weiler R, Garner CC, Gundelfinger ED, Brandstatter JH (2003) The presynaptic active zone protein bassoon is essential for photoreceptor ribbon synapse formation in the retina. *Neuron* 37:775-786.
- Diril MK, Wienisch M, Jung N, Klingauf J, Haucke V (2006) Stonin 2 is an AP-2-dependent endocytic sorting adaptor for synaptotagmin internalization and recycling. *Dev Cell* 10:233-244.
- Dittman JS, Kaplan JM (2006) Factors regulating the abundance and localization of synaptobrevin in the plasma membrane. *Proc Natl Acad Sci U S A* 103:11399-11404.
- Dong H, O'Brien RJ, Fung ET, Lanahan AA, Worley PF, Huganir RL (1997) GRIP: a synaptic PDZ domain-containing protein that interacts with AMPA receptors. *Nature* 386:279-284.
- Dougherty MK, Morrison DK (2004) Unlocking the code of 14-3-3. *J Cell Sci* 117:1875-1884.
- Dresbach T, Qualmann B, Kessels MM, Garner CC, Gundelfinger ED (2001) The presynaptic cytomatrix of brain synapses. *Cell Mol Life Sci* 58:94-116.
- Dresbach T, Hempelmann A, Spilker C, tom Dieck S, Altmann WD, Zuschratter W, Garner CC, Gundelfinger ED (2003) Functional regions of the presynaptic cytomatrix protein bassoon: significance for synaptic targeting and cytomatrix anchoring. *Mol Cell Neurosci* 23:279-291.
- Dresbach T, Torres V, Wittenmayer N, Altmann WD, Zamorano P, Zuschratter W, Nawrothki R, Ziv NE, Garner CC, Gundelfinger ED (2006) Assembly of active zone precursor vesicles: obligatory trafficking of presynaptic cytomatrix proteins Bassoon and Piccolo via a trans-Golgi compartment. *J Biol Chem* 281:6038-6047.
- Dugani CB, Paquin A, Kaplan DR, Miller FD (2010) Coffin-Lowry syndrome: a role for RSK2 in mammalian neurogenesis. *Dev Biol* 347:348-359.
- Dumont J, Umbhauer M, Rassinier P, Hanauer A, Verlhac MH (2005) p90Rsk is not involved in cytoskeletal arrest in mouse oocytes. *J Cell Biol* 169:227-231.
- Ehlers MD (2003) Activity level controls postsynaptic composition and signaling via the ubiquitin-proteasome system. *Nat Neurosci* 6:231-242.
- Emamian ES, Kaytor MD, Duvick LA, Zu T, Tousey SK, Zoghbi HY, Clark HB, Orr HT (2003) Serine 776 of ataxin-1 is critical for polyglutamine-induced disease in SCA1 transgenic mice. *Neuron* 38:375-387.
- Fejtova A, Gundelfinger ED (2006) Molecular organization and assembly of the presynaptic active zone of neurotransmitter release. *Results Probl Cell Differ* 43:49-68.
- Fejtova A, Davydova D, Bischof F, Lazarevic V, Altmann WD, Romorini S, Schone C, Zuschratter W, Kreutz MR, Garner CC, Ziv NE, Gundelfinger ED (2009) Dynein light

- chain regulates axonal trafficking and synaptic levels of Bassoon. *J Cell Biol* 185:341-355.
- Fenster SD, Kessels MM, Qualmann B, Chung WJ, Nash J, Gundelfinger ED, Garner CC (2003) Interactions between Piccolo and the actin/dynamin-binding protein Abp1 link vesicle endocytosis to presynaptic active zones. *J Biol Chem* 278:20268-20277.
- Fenster SD, Chung WJ, Zhai R, Cases-Langhoff C, Voss B, Garner AM, Kaempf U, Kindler S, Gundelfinger ED, Garner CC (2000) Piccolo, a presynaptic zinc finger protein structurally related to bassoon. *Neuron* 25:203-214.
- Ferguson SM, De Camilli P (2012) Dynamin, a membrane-remodelling GTPase. *Nat Rev Mol Cell Biol* 13:75-88.
- Finlin BS, Andres DA (1999) Phosphorylation-dependent association of the Ras-related GTP-binding protein Rem with 14-3-3 proteins. *Arch Biochem Biophys* 368:401-412.
- Fischer A, Baljuls A, Reinders J, Nekhoroshkova E, Sibilski C, Metz R, Albert S, Rajalingam K, Hekman M, Rapp UR (2009a) Regulation of RAF activity by 14-3-3 proteins: RAF kinases associate functionally with both homo- and heterodimeric forms of 14-3-3 proteins. *J Biol Chem* 284:3183-3194.
- Fischer M, Raabe T, Heisenberg M, Sendtner M (2009b) *Drosophila* RSK negatively regulates bouton number at the neuromuscular junction. *Dev Neurobiol* 69:212-220.
- Fischer M, Pereira PM, Holtmann B, Simon CM, Hanauer A, Heisenberg M, Sendtner M (2009c) P90 Ribosomal s6 kinase 2 negatively regulates axon growth in motoneurons. *Mol Cell Neurosci* 42:134-141.
- Flynn DC (2001) Adaptor proteins. *Oncogene* 20:6270-6272.
- Frank T, Rutherford MA, Strenzke N, Neef A, Pangrsic T, Khimich D, Fejtova A, Gundelfinger ED, Liberman MC, Harke B, Bryan KE, Lee A, Egner A, Riedel D, Moser T (2010) Bassoon and the synaptic ribbon organize Ca²⁺ channels and vesicles to add release sites and promote refilling. *Neuron* 68:724-738.
- Frischknecht R, Fejtova A, Viesti M, Stephan A, Sonderegger P (2008) Activity-induced synaptic capture and exocytosis of the neuronal serine protease neurotrypsin. *J Neurosci* 28:1568-1579.
- Frodin M, Gammeltoft S (1999) Role and regulation of 90 kDa ribosomal S6 kinase (RSK) in signal transduction. *Mol Cell Endocrinol* 151:65-77.
- Frodin M, Antal TL, Dummler BA, Jensen CJ, Deak M, Gammeltoft S, Biondi RM (2002) A phosphoserine/threonine-binding pocket in AGC kinases and PDK1 mediates activation by hydrophobic motif phosphorylation. *EMBO J* 21:5396-5407.
- Fujita N, Sato S, Tsuruo T (2003) Phosphorylation of p27Kip1 at threonine 198 by p90 ribosomal protein S6 kinases promotes its binding to 14-3-3 and cytoplasmic localization. *J Biol Chem* 278:49254-49260.
- Geraghty KM, Chen S, Harthill JE, Ibrahim AF, Toth R, Morrice NA, Vandermoere F, Moorhead GB, Hardie DG, MacKintosh C (2007) Regulation of multisite phosphorylation and 14-3-3 binding of AS160 in response to IGF-1, EGF, PMA and AICAR. *Biochem J* 407:231-241.
- Gundelfinger ED, Fejtova A (2012) Molecular organization and plasticity of the cytomatrix at the active zone. *Curr Opin Neurobiol* 22:423-430.

- Gundelfinger ED, Kessels MM, Qualmann B (2003) Temporal and spatial coordination of exocytosis and endocytosis. *Nat Rev Mol Cell Biol* 4:127-139.
- Hallermann S, Fejtova A, Schmidt H, Weyhersmuller A, Silver RA, Gundelfinger ED, Eilers J (2010) Bassoon speeds vesicle reloading at a central excitatory synapse. *Neuron* 68:710-723.
- Harlow ML, Ress D, Stoschek A, Marshall RM, McMahan UJ (2001) The architecture of active zone material at the frog's neuromuscular junction. *Nature* 409:479-484.
- Haucke V, De Camilli P (1999) AP-2 recruitment to synaptotagmin stimulated by tyrosine-based endocytic motifs. *Science* 285:1268-1271.
- Haucke V, Wenk MR, Chapman ER, Farsad K, De Camilli P (2000) Dual interaction of synaptotagmin with mu2- and alpha-adaptin facilitates clathrin-coated pit nucleation. *EMBO J* 19:6011-6019.
- Hausser A, Link G, Hoene M, Russo C, Selchow O, Pfizenmaier K (2006) Phospho-specific binding of 14-3-3 proteins to phosphatidylinositol 4-kinase III beta protects from dephosphorylation and stabilizes lipid kinase activity. *J Cell Sci* 119:3613-3621.
- Heyden A, Ionescu MC, Romorini S, Kracht B, Ghiglieri V, Calabresi P, Seidenbecher C, Angenstein F, Gundelfinger ED (2011) Hippocampal enlargement in Bassoon-mutant mice is associated with enhanced neurogenesis, reduced apoptosis, and abnormal BDNF levels. *Cell Tissue Res* 346:11-26.
- Hida Y, Ohtsuka T (2010) CAST and ELKS proteins: structural and functional determinants of the presynaptic active zone. *J Biochem* 148:131-137.
- Ho A, Morishita W, Atasoy D, Liu X, Tabuchi K, Hammer RE, Malenka RC, Sudhof TC (2006) Genetic analysis of Mint/X11 proteins: essential presynaptic functions of a neuronal adaptor protein family. *J Neurosci* 26:13089-13101.
- Hoeffler CA, Klann E (2010) mTOR signaling: at the crossroads of plasticity, memory and disease. *Trends Neurosci* 33:67-75.
- Ishihara H, Martin BL, Brautigan DL, Karaki H, Ozaki H, Kato Y, Fusetani N, Watabe S, Hashimoto K, Uemura D, et al. (1989) Calyculin A and okadaic acid: inhibitors of protein phosphatase activity. *Biochem Biophys Res Commun* 159:871-877.
- Isobe T, Ichimura T, Sunaya T, Okuyama T, Takahashi N, Kuwano R, Takahashi Y (1991) Distinct forms of the protein kinase-dependent activator of tyrosine and tryptophan hydroxylases. *J Mol Biol* 217:125-132.
- Jakobsson J, Gad H, Andersson F, Low P, Shupliakov O, Brodin L (2008) Role of epsin 1 in synaptic vesicle endocytosis. *Proc Natl Acad Sci U S A* 105:6445-6450.
- Jin J, Smith FD, Stark C, Wells CD, Fawcett JP, Kulkarni S, Metalnikov P, O'Donnell P, Taylor P, Taylor L, Zougman A, Woodgett JR, Langeberg LK, Scott JD, Pawson T (2004) Proteomic, functional, and domain-based analysis of in vivo 14-3-3 binding proteins involved in cytoskeletal regulation and cellular organization. *Curr Biol* 14:1436-1450.
- Johnson C, Crowther S, Stafford MJ, Campbell DG, Toth R, MacKintosh C (2010) Bioinformatic and experimental survey of 14-3-3-binding sites. *Biochem J* 427:69-78.
- Jones DH, Ley S, Aitken A (1995) Isoforms of 14-3-3 protein can form homo- and heterodimers in vivo and in vitro: implications for function as adapter proteins. *FEBS Lett* 368:55-58.

- Jung N, Haucke V (2007) Clathrin-mediated endocytosis at synapses. *Traffic* 8:1129-1136.
- Junge HJ, Rhee JS, Jahn O, Varoqueaux F, Spiess J, Waxham MN, Rosenmund C, Brose N (2004) Calmodulin and Munc13 form a Ca²⁺ sensor/effector complex that controls short-term synaptic plasticity. *Cell* 118:389-401.
- Kaesler PS, Deng L, Chavez AE, Liu X, Castillo PE, Sudhof TC (2009) ELKS2 α /CAST deletion selectively increases neurotransmitter release at inhibitory synapses. *Neuron* 64:227-239.
- Kaesler PS, Kwon HB, Blundell J, Chevaleyre V, Morishita W, Malenka RC, Powell CM, Castillo PE, Sudhof TC (2008) RIM1 α phosphorylation at serine-413 by protein kinase A is not required for presynaptic long-term plasticity or learning. *Proc Natl Acad Sci U S A* 105:14680-14685.
- Kaufmann N, DeProto J, Ranjan R, Wan H, Van Vactor D (2002) Drosophila liprin-alpha and the receptor phosphatase Dlar control synapse morphogenesis. *Neuron* 34:27-38.
- Kawamoto Y, Akiguchi I, Nakamura S, Honjyo Y, Shibasaki H, Budka H (2002) 14-3-3 proteins in Lewy bodies in Parkinson disease and diffuse Lewy body disease brains. *J Neuropathol Exp Neurol* 61:245-253.
- Kawasaki F, Hazen M, Ordway RW (2000) Fast synaptic fatigue in shibire mutants reveals a rapid requirement for dynamin in synaptic vesicle membrane trafficking. *Nat Neurosci* 3:859-860.
- Kessels MM, Engqvist-Goldstein AE, Drubin DG, Qualmann B (2001) Mammalian Abp1, a signal-responsive F-actin-binding protein, links the actin cytoskeleton to endocytosis via the GTPase dynamin. *J Cell Biol* 153:351-366.
- Kharebava G, Makonchuk D, Kalita KB, Zheng JJ, Hetman M (2008) Requirement of 3-phosphoinositide-dependent protein kinase-1 for BDNF-mediated neuronal survival. *J Neurosci* 28:11409-11420.
- Khimich D, Nouvian R, Pujol R, Tom Dieck S, Egner A, Gundelfinger ED, Moser T (2005) Hair cell synaptic ribbons are essential for synchronous auditory signalling. *Nature* 434:889-894.
- Kim S, Ko J, Shin H, Lee JR, Lim C, Han JH, Altroch WD, Garner CC, Gundelfinger ED, Premont RT, Kaang BK, Kim E (2003) The GIT family of proteins forms multimers and associates with the presynaptic cytomatrix protein Piccolo. *J Biol Chem* 278:6291-6300.
- Kim SH, Ryan TA (2009) Synaptic vesicle recycling at CNS synapses without AP-2. *J Neurosci* 29:3865-3874.
- Kirchhausen T (1999) Adaptors for clathrin-mediated traffic. *Annu Rev Cell Dev Biol* 15:705-732.
- Kirsch J, Kuhse J, Betz H (1995) Targeting of glycine receptor subunits to gephyrin-rich domains in transfected human embryonic kidney cells. *Mol Cell Neurosci* 6:450-461.
- Kneussel M, Brandstatter JH, Laube B, Stahl S, Muller U, Betz H (1999) Loss of postsynaptic GABA(A) receptor clustering in gephyrin-deficient mice. *J Neurosci* 19:9289-9297.
- Ko J, Na M, Kim S, Lee JR, Kim E (2003) Interaction of the ERC family of RIM-binding proteins with the liprin-alpha family of multidomain proteins. *J Biol Chem* 278:42377-42385.

- Ko J, Yoon C, Piccoli G, Chung HS, Kim K, Lee JR, Lee HW, Kim H, Sala C, Kim E (2006) Organization of the presynaptic active zone by ERC2/CAST1-dependent clustering of the tandem PDZ protein syntenin-1. *J Neurosci* 26:963-970.
- Kurosaki T (2002) Regulation of B-cell signal transduction by adaptor proteins. *Nat Rev Immunol* 2:354-363.
- Landis DM, Hall AK, Weinstein LA, Reese TS (1988) The organization of cytoplasm at the presynaptic active zone of a central nervous system synapse. *Neuron* 1:201-209.
- Lanore F, Blanchet C, Fejtova A, Pinheiro P, Richter K, Balschun D, Gundelfinger E, Mülle C (2010) Impaired development of hippocampal mossy fibre synapses in mouse mutants for the presynaptic scaffold protein Bassoon. *J Physiol* 588:2133-2145.
- Layfield R, Ferguson J, Aitken A, Lowe J, Landon M, Mayer RJ (1996) Neurofibrillary tangles of Alzheimer's disease brains contain 14-3-3 proteins. *Neurosci Lett* 209:57-60.
- Lazarevic V (2010) Mechanisms of assembly and activity dependent remodelling of the presynaptic cytomatrix at the active zone / von Vesna Lazarevic. In: *Fak. für Naturwiss.*, p 75. Magdeburg: Otto-von-Guericke-Universität.
- Lazarevic V, Schone C, Heine M, Gundelfinger ED, Fejtova A (2011) Extensive Remodeling of the Presynaptic Cytomatrix upon Homeostatic Adaptation to Network Activity Silencing. *J Neurosci* 31:10189-10200.
- Leal-Ortiz S, Waites CL, Terry-Lorenzo R, Zamorano P, Gundelfinger ED, Garner CC (2008) Piccolo modulation of Synapsin1a dynamics regulates synaptic vesicle exocytosis. *J Cell Biol* 181:831-846.
- Lehoux S, Abe J, Florian JA, Berk BC (2001) 14-3-3 Binding to Na⁺/H⁺ exchanger isoform-1 is associated with serum-dependent activation of Na⁺/H⁺ exchange. *J Biol Chem* 276:15794-15800.
- Li Q, Lau A, Morris TJ, Guo L, Fordyce CB, Stanley EF (2004) A syntaxin 1, Galpha(o), and N-type calcium channel complex at a presynaptic nerve terminal: analysis by quantitative immunocolocalization. *J Neurosci* 24:4070-4081.
- Li Y, Wu Y, Zhou Y (2006) Modulation of inactivation properties of CaV2.2 channels by 14-3-3 proteins. *Neuron* 51:755-771.
- Lipstein N, Sakaba T, Cooper BH, Lin KH, Strenzke N, Ashery U, Rhee JS, Taschenberger H, Neher E, Brose N (2013) Dynamic control of synaptic vesicle replenishment and short-term plasticity by ca(2+)-calmodulin-munc13-1 signaling. *Neuron* 79:82-96.
- Lonart G, Schoch S, Kaeser PS, Larkin CJ, Sudhof TC, Linden DJ (2003) Phosphorylation of RIM1alpha by PKA triggers presynaptic long-term potentiation at cerebellar parallel fiber synapses. *Cell* 115:49-60.
- Maas C, Tagnaouti N, Loebrich S, Behrend B, Lappe-Siefke C, Kneussel M (2006) Neuronal cotransport of glycine receptor and the scaffold protein gephyrin. *J Cell Biol* 172:441-451.
- Maas C, Torres VI, Altroock WD, Leal-Ortiz S, Wagh D, Terry-Lorenzo RT, Fejtova A, Gundelfinger ED, Ziv NE, Garner CC (2012) Formation of Golgi-derived active zone precursor vesicles. *J Neurosci* 32:11095-11108.
- MacDonald JI, Dietrich A, Gamble S, Hryciw T, Grant RI, Meakin SO (2012) Nesca, a novel neuronal adapter protein, links the molecular motor kinesin with the pre-synaptic membrane protein, syntaxin-1, in hippocampal neurons. *J Neurochem* 121:861-880.

- Macia E, Ehrlich M, Massol R, Boucrot E, Brunner C, Kirchhausen T (2006) Dynasore, a cell-permeable inhibitor of dynamin. *Dev Cell* 10:839-850.
- Mackintosh C (2004) Dynamic interactions between 14-3-3 proteins and phosphoproteins regulate diverse cellular processes. *Biochem J* 381:329-342.
- Maroun CR, Naujokas MA, Park M (2003) Membrane targeting of Grb2-associated binder-1 (Gab1) scaffolding protein through Src myristoylation sequence substitutes for Gab1 pleckstrin homology domain and switches an epidermal growth factor response to an invasive morphogenic program. *Mol Biol Cell* 14:1691-1708.
- Masters SC, Pederson KJ, Zhang L, Barbieri JT, Fu H (1999) Interaction of 14-3-3 with a nonphosphorylated protein ligand, exoenzyme S of *Pseudomonas aeruginosa*. *Biochemistry* 38:5216-5221.
- Moller DE, Xia CH, Tang W, Zhu AX, Jakubowski M (1994) Human rsk isoforms: cloning and characterization of tissue-specific expression. *Am J Physiol* 266:C351-359.
- Morrison DK (2009) The 14-3-3 proteins: integrators of diverse signaling cues that impact cell fate and cancer development. *Trends Cell Biol* 19:16-23.
- Motley A, Bright NA, Seaman MN, Robinson MS (2003) Clathrin-mediated endocytosis in AP-2-depleted cells. *J Cell Biol* 162:909-918.
- Mukherjee K, Yang X, Gerber SH, Kwon HB, Ho A, Castillo PE, Liu X, Sudhof TC (2010) Piccolo and bassoon maintain synaptic vesicle clustering without directly participating in vesicle exocytosis. *Proc Natl Acad Sci U S A* 107:6504-6509.
- Munton RP, Tweedie-Cullen R, Livingstone-Zatchej M, Weinandy F, Waidelich M, Longo D, Gehrig P, Potthast F, Rutishauser D, Gerrits B, Panse C, Schlapbach R, Mansuy IM (2007) Qualitative and quantitative analyses of protein phosphorylation in naive and stimulated mouse synaptosomal preparations. *Mol Cell Proteomics* 6:283-293.
- Murthy VN, Schikorski T, Stevens CF, Zhu Y (2001) Inactivity produces increases in neurotransmitter release and synapse size. *Neuron* 32:673-682.
- Muslin AJ, Xing H (2000) 14-3-3 proteins: regulation of subcellular localization by molecular interference. *Cell Signal* 12:703-709.
- Muslin AJ, Tanner JW, Allen PM, Shaw AS (1996) Interaction of 14-3-3 with signaling proteins is mediated by the recognition of phosphoserine. *Cell* 84:889-897.
- Nakatsu F, Ohno H (2003) Adaptor protein complexes as the key regulators of protein sorting in the post-Golgi network. *Cell Struct Funct* 28:419-429.
- Newton AJ, Kirchhausen T, Murthy VN (2006) Inhibition of dynamin completely blocks compensatory synaptic vesicle endocytosis. *Proc Natl Acad Sci U S A* 103:17955-17960.
- Niu S, Renfro A, Quattrocchi CC, Sheldon M, D'Arcangelo G (2004) Reelin promotes hippocampal dendrite development through the VLDLR/ApoER2-Dab1 pathway. *Neuron* 41:71-84.
- Ohno H (2006) Clathrin-associated adaptor protein complexes. *J Cell Sci* 119:3719-3721.
- Ohno H, Aguilar RC, Yeh D, Taura D, Saito T, Bonifacino JS (1998) The medium subunits of adaptor complexes recognize distinct but overlapping sets of tyrosine-based sorting signals. *J Biol Chem* 273:25915-25921.

- Ohtsuka T, Takao-Rikitsu E, Inoue E, Inoue M, Takeuchi M, Matsubara K, Deguchi-Tawarada M, Satoh K, Morimoto K, Nakanishi H, Takai Y (2002) Cast: a novel protein of the cytomatrix at the active zone of synapses that forms a ternary complex with RIM1 and munc13-1. *J Cell Biol* 158:577-590.
- Okamoto M, Sudhof TC (1997) Mints, Munc18-interacting proteins in synaptic vesicle exocytosis. *J Biol Chem* 272:31459-31464.
- Owen DJ, Collins BM, Evans PR (2004) Adaptors for clathrin coats: structure and function. *Annu Rev Cell Dev Biol* 20:153-191.
- Patel MR, Lehrman EK, Poon VY, Crump JG, Zhen M, Bargmann CI, Shen K (2006) Hierarchical assembly of presynaptic components in defined *C. elegans* synapses. *Nat Neurosci* 9:1488-1498.
- Petosa C, Masters SC, Bankston LA, Pohl J, Wang B, Fu H, Liddington RC (1998) 14-3-3zeta binds a phosphorylated Raf peptide and an unphosphorylated peptide via its conserved amphipathic groove. *J Biol Chem* 273:16305-16310.
- Phillips GR, Huang JK, Wang Y, Tanaka H, Shapiro L, Zhang W, Shan WS, Arndt K, Frank M, Gordon RE, Gawinowicz MA, Zhao Y, Colman DR (2001) The presynaptic particle web: ultrastructure, composition, dissolution, and reconstitution. *Neuron* 32:63-77.
- Poirier R, Jacquot S, Vaillend C, Southiphong AA, Libbey M, Davis S, Laroche S, Hanauer A, Welzl H, Lipp HP, Wolfer DP (2007) Deletion of the Coffin-Lowry syndrome gene *Rsk2* in mice is associated with impaired spatial learning and reduced control of exploratory behavior. *Behav Genet* 37:31-50.
- Powell CM, Schoch S, Monteggia L, Barrot M, Matos MF, Feldmann N, Sudhof TC, Nestler EJ (2004) The presynaptic active zone protein RIM1alpha is critical for normal learning and memory. *Neuron* 42:143-153.
- Puntervoll P et al. (2003) ELM server: A new resource for investigating short functional sites in modular eukaryotic proteins. *Nucleic Acids Res* 31:3625-3630.
- Putz G, Bertolucci F, Raabe T, Zars T, Heisenberg M (2004) The *S6KII* (*rsk*) gene of *Drosophila melanogaster* differentially affects an operant and a classical learning task. *J Neurosci* 24:9745-9751.
- Qian ZM, Li H, Sun H, Ho K (2002) Targeted drug delivery via the transferrin receptor-mediated endocytosis pathway. *Pharmacol Rev* 54:561-587.
- Rakhit S, Clark CJ, O'Shaughnessy C T, Morris BJ (2005) N-methyl-D-aspartate and brain-derived neurotrophic factor induce distinct profiles of extracellular signal-regulated kinase, mitogen- and stress-activated kinase, and ribosomal s6 kinase phosphorylation in cortical neurons. *Mol Pharmacol* 67:1158-1165.
- Ramm G, Larance M, Guilhaus M, James DE (2006) A role for 14-3-3 in insulin-stimulated GLUT4 translocation through its interaction with the RabGAP AS160. *J Biol Chem* 281:29174-29180.
- Rapp UR, Fischer A, Rennefahrt UE, Hekman M, Albert S (2007) BAD association with membranes is regulated by Raf kinases and association with 14-3-3 proteins. *Adv Enzyme Regul* 47:281-285.
- Richmond JE, Davis WS, Jorgensen EM (1999) UNC-13 is required for synaptic vesicle fusion in *C. elegans*. *Nat Neurosci* 2:959-964.

- Richter K, Langaese K, Kreutz MR, Olias G, Zhai R, Scheich H, Garner CC, Gundelfinger ED (1999) Presynaptic cytomatrix protein bassoon is localized at both excitatory and inhibitory synapses of rat brain. *J Comp Neurol* 408:437-448.
- Rittinger K, Budman J, Xu J, Volinia S, Cantley LC, Smerdon SJ, Gambelin SJ, Yaffe MB (1999) Structural analysis of 14-3-3 phosphopeptide complexes identifies a dual role for the nuclear export signal of 14-3-3 in ligand binding. *Mol Cell* 4:153-166.
- Romeo Y, Zhang X, Roux PP (2012) Regulation and function of the RSK family of protein kinases. *Biochem J* 441:553-569.
- Saheki Y, De Camilli P (2012) Synaptic vesicle endocytosis. *Cold Spring Harb Perspect Biol* 4:a005645.
- Schaefer AW, Kamei Y, Kamiguchi H, Wong EV, Rapoport I, Kirchhausen T, Beach CM, Landreth G, Lemmon SK, Lemmon V (2002) L1 endocytosis is controlled by a phosphorylation-dephosphorylation cycle stimulated by outside-in signaling by L1. *J Cell Biol* 157:1223-1232.
- Schechtman D, Winnen R, Tarrab-Hazdai R, Ram D, Shinder V, Grevelding CG, Kunz W, Arnon R (2001) Expression and immunolocalization of the 14-3-3 protein of *Schistosoma mansoni*. *Parasitology* 123:573-582.
- Schneider CA, Rasband WS, Eliceiri KW (2012) NIH Image to ImageJ: 25 years of image analysis. *Nat Methods* 9:671-675.
- Schoch S, Gundelfinger ED (2006) Molecular organization of the presynaptic active zone. *Cell Tissue Res* 326:379-391.
- Schoch S, Castillo PE, Jo T, Mukherjee K, Geppert M, Wang Y, Schmitz F, Malenka RC, Sudhof TC (2002) RIM1 α forms a protein scaffold for regulating neurotransmitter release at the active zone. *Nature* 415:321-326.
- Schroder MS, Stellmacher A, Romorini S, Marini C, Montenegro-Venegas C, Altrock WD, Gundelfinger ED, Fejtova A (2013) Regulation of presynaptic anchoring of the scaffold protein Bassoon by phosphorylation-dependent interaction with 14-3-3 adaptor proteins. *PLoS One* 8:e58814.
- Setou M, Seog DH, Tanaka Y, Kanai Y, Takei Y, Kawagishi M, Hirokawa N (2002) Glutamate-receptor-interacting protein GRIP1 directly steers kinesin to dendrites. *Nature* 417:83-87.
- Shapira M, Zhai RG, Dresbach T, Bresler T, Torres VI, Gundelfinger ED, Ziv NE, Garner CC (2003) Unitary assembly of presynaptic active zones from Piccolo-Bassoon transport vesicles. *Neuron* 38:237-252.
- Shikano S, Coblitz B, Wu M, Li M (2006) 14-3-3 proteins: regulation of endoplasmic reticulum localization and surface expression of membrane proteins. *Trends Cell Biol* 16:370-375.
- Shimamura A, Ballif BA, Richards SA, Blenis J (2000) Rsk1 mediates a MEK-MAP kinase cell survival signal. *Curr Biol* 10:127-135.
- Shiratori T, Miyatake S, Ohno H, Nakaseko C, Isono K, Bonifacino JS, Saito T (1997) Tyrosine phosphorylation controls internalization of CTLA-4 by regulating its interaction with clathrin-associated adaptor complex AP-2. *Immunity* 6:583-589.
- Siksou L, Rostaing P, Lechaire JP, Boudier T, Ohtsuka T, Fejtova A, Kao HT, Greengard P, Gundelfinger ED, Triller A, Marty S (2007) Three-dimensional architecture of presynaptic terminal cytomatrix. *J Neurosci* 27:6868-6877.

- Simsek-Duran F, Linden DJ, Lonart G (2004) Adapter protein 14-3-3 is required for a presynaptic form of LTP in the cerebellum. *Nat Neurosci* 7:1296-1298.
- Sola M, Bavro VN, Timmins J, Franz T, Ricard-Blum S, Schoehn G, Ruigrok RW, Paarmann I, Saiyed T, O'Sullivan GA, Schmitt B, Betz H, Weissenhorn W (2004) Structural basis of dynamic glycine receptor clustering by gephyrin. *EMBO J* 23:2510-2519.
- Spangler SA, Schmitz SK, Kevenaar JT, de Graaff E, de Wit H, Demmers J, Toonen RF, Hoogenraad CC (2013) Liprin-alpha2 promotes the presynaptic recruitment and turnover of RIM1/CASK to facilitate synaptic transmission. *J Cell Biol* 201:915-928.
- Sproul AA, Xu Z, Wilhelm M, Gire S, Greene LA (2009) Cbl negatively regulates JNK activation and cell death. *Cell Res* 19:950-961.
- Sudhof TC (2004) The synaptic vesicle cycle. *Annu Rev Neurosci* 27:509-547.
- Sudhof TC (2012) The presynaptic active zone. *Neuron* 75:11-25.
- Sweatt JD (2004) Mitogen-activated protein kinases in synaptic plasticity and memory. *Curr Opin Neurobiol* 14:311-317.
- Takahashi E, Abe J, Gallis B, Aebersold R, Spring DJ, Krebs EG, Berk BC (1999) p90(RSK) is a serum-stimulated Na⁺/H⁺ exchanger isoform-1 kinase. Regulatory phosphorylation of serine 703 of Na⁺/H⁺ exchanger isoform-1. *J Biol Chem* 274:20206-20214.
- Takao-Rikitsu E, Mochida S, Inoue E, Deguchi-Tawarada M, Inoue M, Ohtsuka T, Takai Y (2004) Physical and functional interaction of the active zone proteins, CAST, RIM1, and Bassoon, in neurotransmitter release. *J Cell Biol* 164:301-311.
- Takei K, Mundigl O, Daniell L, De Camilli P (1996) The synaptic vesicle cycle: a single vesicle budding step involving clathrin and dynamin. *J Cell Biol* 133:1237-1250.
- Tan DP, Liu QY, Koshiya N, Gu H, Alkon D (2006) Enhancement of long-term memory retention and short-term synaptic plasticity in cbl-b null mice. *Proc Natl Acad Sci U S A* 103:5125-5130.
- Tao-Cheng JH (2007) Ultrastructural localization of active zone and synaptic vesicle proteins in a preassembled multi-vesicle transport aggregate. *Neuroscience* 150:575-584.
- Thorrez L, Van Deun K, Tranchevent LC, Van Lommel L, Engelen K, Marchal K, Moreau Y, Van Mechelen I, Schuit F (2008) Using ribosomal protein genes as reference: a tale of caution. *PLoS One* 3:e1854.
- tom Dieck S, Altmann WD, Kessels MM, Qualmann B, Regus H, Brauner D, Fejtova A, Bracko O, Gundelfinger ED, Brandstätter JH (2005) Molecular dissection of the photoreceptor ribbon synapse: physical interaction of Bassoon and RIBEYE is essential for the assembly of the ribbon complex. *J Cell Biol* 168:825-836.
- tom Dieck S, Sanmarti-Vila L, Langnaese K, Richter K, Kindler S, Soyke A, Wex H, Smalla KH, Kampf U, Franzer JT, Stumm M, Garner CC, Gundelfinger ED (1998) Bassoon, a novel zinc-finger CAG/glutamine-repeat protein selectively localized at the active zone of presynaptic nerve terminals. *J Cell Biol* 142:499-509.
- Toyo-oka K, Shionoya A, Gambello MJ, Cardoso C, Leventer R, Ward HL, Ayala R, Tsai LH, Dobyns W, Ledbetter D, Hirotsume S, Wynshaw-Boris A (2003) 14-3-3epsilon is important for neuronal migration by binding to NUDEL: a molecular explanation for Miller-Dieker syndrome. *Nat Genet* 34:274-285.

- Traub LM (2003) Sorting it out: AP-2 and alternate clathrin adaptors in endocytic cargo selection. *J Cell Biol* 163:203-208.
- Traub LM, Ostrom JA, Kornfeld S (1993) Biochemical dissection of AP-1 recruitment onto Golgi membranes. *J Cell Biol* 123:561-573.
- Trinidad JC, Specht CG, Thalhammer A, Schoepfer R, Burlingame AL (2006) Comprehensive identification of phosphorylation sites in postsynaptic density preparations. *Mol Cell Proteomics*.
- Trivier E, De Cesare D, Jacquot S, Pannetier S, Zackai E, Young I, Mandel JL, Sassone-Corsi P, Hanauer A (1996) Mutations in the kinase Rsk-2 associated with Coffin-Lowry syndrome. *Nature* 384:567-570.
- Trotter J, Lee GH, Kazdoba TM, Crowell B, Domogauer J, Mahoney HM, Franco SJ, Muller U, Weeber EJ, D'Arcangelo G (2013) Dab1 is required for synaptic plasticity and associative learning. *J Neurosci* 33:15652-15668.
- Tsuriel S, Fisher A, Wittenmayer N, Dresbach T, Garner CC, Ziv NE (2009) Exchange and redistribution dynamics of the cytoskeleton of the active zone molecule bassoon. *J Neurosci* 29:351-358.
- Tsuriel S, Geva R, Zamorano P, Dresbach T, Boeckers T, Gundelfinger ED, Garner CC, Ziv NE (2006) Local sharing as a predominant determinant of synaptic matrix molecular dynamics. *PLoS Biol* 4:e271.
- Ubl A, Berg D, Holzmann C, Kruger R, Berger K, Arzberger T, Bornemann A, Riess O (2002) 14-3-3 protein is a component of Lewy bodies in Parkinson's disease-mutation analysis and association studies of 14-3-3 eta. *Brain Res Mol Brain Res* 108:33-39.
- Varoqueaux F, Sigler A, Rhee JS, Brose N, Enk C, Reim K, Rosenmund C (2002) Total arrest of spontaneous and evoked synaptic transmission but normal synaptogenesis in the absence of Munc13-mediated vesicle priming. *Proc Natl Acad Sci U S A* 99:9037-9042.
- Voglmaier SM, Kam K, Yang H, Fortin DL, Hua Z, Nicoll RA, Edwards RH (2006) Distinct endocytic pathways control the rate and extent of synaptic vesicle protein recycling. *Neuron* 51:71-84.
- Wang W, Shakes DC (1996) Molecular evolution of the 14-3-3 protein family. *J Mol Evol* 43:384-398.
- Wang X, Hu B, Zieba A, Neumann NG, Kasper-Sonnenberg M, Honsbein A, Hultqvist G, Conze T, Witt W, Limbach C, Geitmann M, Danielson H, Kolarow R, Niemann G, Lessmann V, Kilimann MW (2009) A protein interaction node at the neurotransmitter release site: domains of Aczonin/Piccolo, Bassoon, CAST, and rim converge on the N-terminal domain of Munc13-1. *J Neurosci* 29:12584-12596.
- Wang Y, Liu X, Biederer T, Sudhof TC (2002) A family of RIM-binding proteins regulated by alternative splicing: Implications for the genesis of synaptic active zones. *Proc Natl Acad Sci U S A* 99:14464-14469.
- Wayman GA, Lee YS, Tokumitsu H, Silva AJ, Soderling TR (2008) Calmodulin-kinases: modulators of neuronal development and plasticity. *Neuron* 59:914-931.
- Wenzel EM, Morton A, Ebert K, Welzel O, Kornhuber J, Cousin MA, Groemer TW (2012) Key physiological parameters dictate triggering of activity-dependent bulk endocytosis in hippocampal synapses. *PLoS One* 7:e38188.

- Weyhersmuller A, Hallermann S, Wagner N, Eilers J (2011) Rapid active zone remodeling during synaptic plasticity. *J Neurosci* 31:6041-6052.
- Wong EV, Schaefer AW, Landreth G, Lemmon V (1996) Involvement of p90rsk in neurite outgrowth mediated by the cell adhesion molecule L1. *J Biol Chem* 271:18217-18223.
- Wu M, Coblitz B, Shikano S, Long S, Cockrell LM, Fu H, Li M (2006) SWTY--a general peptide probe for homogeneous solution binding assay of 14-3-3 proteins. *Anal Biochem* 349:186-196.
- Yaffe MB, Rittinger K, Volinia S, Caron PR, Aitken A, Leffers H, Gamblin SJ, Smerdon SJ, Cantley LC (1997) The structural basis for 14-3-3:phosphopeptide binding specificity. *Cell* 91:961-971.
- Yang Y, Calakos N (2010) Acute in vivo genetic rescue demonstrates that phosphorylation of RIM1alpha serine 413 is not required for mossy fiber long-term potentiation. *J Neurosci* 30:2542-2546.
- Yang Y, Calakos N (2011) Munc13-1 is required for presynaptic long-term potentiation. *J Neurosci* 31:12053-12057.
- Zakharenko SS, Patterson SL, Dragatsis I, Zeitlin SO, Siegelbaum SA, Kandel ER, Morozov A (2003) Presynaptic BDNF required for a presynaptic but not postsynaptic component of LTP at hippocampal CA1-CA3 synapses. *Neuron* 39:975-990.
- Zaru R, Ronkina N, Gaestel M, Arthur JS, Watts C (2007) The MAPK-activated kinase Rsk controls an acute Toll-like receptor signaling response in dendritic cells and is activated through two distinct pathways. *Nat Immunol* 8:1227-1235.
- Zeniou-Meyer M, Gambino F, Ammar MR, Humeau Y, Vitale N (2010) The Coffin-Lowry syndrome-associated protein RSK2 and neurosecretion. *Cell Mol Neurobiol* 30:1401-1406.
- Zeniou-Meyer M, Liu Y, Begle A, Olanich ME, Hanauer A, Becherer U, Rettig J, Bader MF, Vitale N (2008) The Coffin-Lowry syndrome-associated protein RSK2 is implicated in calcium-regulated exocytosis through the regulation of PLD1. *Proc Natl Acad Sci U S A* 105:8434-8439.
- Zeniou M, Ding T, Trivier E, Hanauer A (2002) Expression analysis of RSK gene family members: the RSK2 gene, mutated in Coffin-Lowry syndrome, is prominently expressed in brain structures essential for cognitive function and learning. *Hum Mol Genet* 11:2929-2940.
- Zhai R, Olias G, Chung WJ, Lester RA, tom Dieck S, Langnaese K, Kreutz MR, Kindler S, Gundelfinger ED, Garner CC (2000) Temporal appearance of the presynaptic cytomatrix protein bassoon during synaptogenesis. *Mol Cell Neurosci* 15:417-428.
- Zhai RG, Bellen HJ (2004) The architecture of the active zone in the presynaptic nerve terminal. *Physiology (Bethesda)* 19:262-270.
- Zhai RG, Vardinon-Friedman H, Cases-Langhoff C, Becker B, Gundelfinger ED, Ziv NE, Garner CC (2001) Assembling the presynaptic active zone: a characterization of an active one precursor vesicle. *Neuron* 29:131-143.
- Zhang S, Edelmann L, Liu J, Crandall JE, Morabito MA (2008) Cdk5 regulates the phosphorylation of tyrosine 1472 NR2B and the surface expression of NMDA receptors. *J Neurosci* 28:415-424.

Zhen M, Jin Y (1999) The liprin protein SYD-2 regulates the differentiation of presynaptic termini in *C. elegans*. *Nature* 401:371-375.

Ziv NE, Garner CC (2004) Cellular and molecular mechanisms of presynaptic assembly. *Nat Rev Neurosci* 5:385-399.